Wydział Nauk Geograficznych i Geologicznych

Uniwersytet im. Adama Mickiewicza w Poznaniu

Krzysztof Rymer

Uwarunkowania i zmienność wybranych procesów eolicznych na obszarze środkowego Spitsbergenu (Dolina Ebby)

Conditions and variability of selected aeolian processes in the area of central Spitsbergen (Ebba Valley)

Praca doktorska wykonana w Pracowni Badań Kriosfery pod kierunkiem prof. dr. hab. Grzegorza Rachlewicza

Uniwersytet im. Adama Mickiewicza w Poznaniu

Poznań 2024

Dziękuję wszystkim osobom, które w jakikolwiek sposób pomogły mi w trakcie powstawania niniejszej pracy doktorskiej.

Szczególnie podziękowania kieruję do prof. Grzegorza Rachlewicza za nieustającą motywację do pracy oraz niezmienny optymizm i zapał do działań w obszarach polarnych. Dziękuję za wszystkie dyskusje, wskazówki i ogromną pomoc - szczególnie w terenie.

Za wszelkie sugestie i uwagi merytoryczne dziękuję również profesorom Andrzejowi Kostrzewskiemu oraz Alfredowi Stachowi. Opracowanie i pozyskanie danych nie byłoby możliwe bez pomocy Agaty Buchwał i Jakuba Małeckiego.

Olbrzymie podziękowania należą się osobom, które z niezwykłym zaangażowaniem pomagały mi w pracach terenowych. Mam tu na myśli przede wszystkim Tomasza Kurczabę, Michała Kamińskiego i Mateusza Drożdżyńskiego.

Za pomoc w pracach laboratoryjnych oraz wprowadzenie w świat mikroskopowych badań ziaren kwarcu dziękuję prof. Lucynie Wacheckiej-Kotkowskiej.

Poświęcenie się realizacji pracy doktorskiej nie byłoby również możliwe bez wsparcia moich Rodziców. Dziękuję za możliwość edukacji, cierpliwość i motywację do ukończenia pracy.

Podziękowania składam również wszystkim członkom Wypraw Polarnych UAM na Spitsbergen za każdą udzieloną pomoc, wyrozumiałość i wspaniałą atmosferę w Stacji Polarnej „Petuniabukta".

Badania zostały zrealizowane między innymi dzięki środkom finansowym z projektów badawczych Narodowego Centrum Nauki: „Reakcje kriosfery w kontrastowych warunkach wysokoarktycznych Svalbardu na tle zmian środowiskowych" (NCN 2011/03/B/ST10/06172) oraz „Akumulacja materiału eolicznego i niweoeolicznego w środowisku peryglacjalnym i glacjalnym na obszarze środkowego Spitsbergenu (dolina Ebby)" (NCN 2014/15/N/ST10/00825).

Spis treści

1. Streszczenie

Badania ilościowe i jakościowe procesów eolicznych w wysokich szerokościach geograficznych nie są obecnie prowadzone na szeroką skalę, mimo że stanowią one ważny element funkcjonowania geoekosystemów w regionach polarnych, szczególnie dotkniętych zachodzącymi zmianami klimatycznymi. W niniejszej pracy przedstawiono wyniki pomiarów tempa depozycji eolicznej dla jednej z dolin polodowcowych położonej na środkowym Spitsbergenie (Dolina Ebby). Badania prowadzone były podczas ośmiu sezonów letnich (2012–2018 i 2022), a także opierają się na datowaniach AMS ^{14}C i OSL osadów niweo-eolicznych i eolicznych.

Współczesne średnie tempo depozycji eolicznej w latach 2012–2018 wahało się od 0,1 do 22,9 $g \cdot m^{-2} \cdot dzień^{-1}$ w wybranych częściach doliny i wynosiło średnio od 2,1 do 12,3 $g \cdot m^{-2} \cdot dzień^{-1}$ w ciągu pierwszych siedmiu analizowanych sezonów letnich. Stosunkowo silne zależności ($r^2 = 0,71$, $p = 0,017$) zaobserwowano pomiędzy średnią temperaturą powietrza a wartością średniej depozycji eolicznej, co może wskazywać na kluczowe znaczenie materiału fluwioglacjalnego jako materiału źródłowego. Pomiary wykonane w sezonie letnim 2022 wykazały, że tempo depozycji eolicznej było niskie na początku sezonu, wahając się od 0,3 do 0,6 $g \cdot m^{-2} \cdot dzień^{-1}$. Mogło jednak dochodzić do poziomu 25,4 $g \cdot m^{-2} \cdot dzień^{-1}$ pod koniec sezonu.

Tempo depozycji niweo-eolicznej oszacowano dla okresu od XI wieku, poprzez małą epokę lodową, do drugiej połowy XX wieku i wykazano, że ma ono dość stałą wartość 0,05 cm rocznie. Od tego czasu tempo depozycji niweo-eolicznej wzrosło do 0,3 cm rocznie, co może być związane ze wzrostem temperatury powietrza i spowodowanymi tym panarktycznymi zmianami środowiskowymi.

Dodatkowo przeprowadzono analizę obtoczenia i zmatowienia ziaren kwarcu zebranych z pułapek eolicznych. Ta część prac opierała się na czterech letnich sezonach badawczych (2015–2018). Wybrano ziarna kwarcu o średnicy 0,8–1,0 mm i poddano je dalszej analizie pod mikroskopem, co pozwoliło na podzielenie ich na sześć klas. Charakter ziaren może w dużej mierze wskazywać na warunki środowiskowe, w których materiał był transportowany. W zebranym materiale dominowały ziarna o niskim stopniu obtoczenia, co może wskazywać na stosunkowo krótki transport rzeczny lub eoliczny. Niewielkie ilości typowo zmatowionych ziaren kwarcu mogą wskazywać na niską dynamikę środowiskową i krótki transport, a także na fakt, że duże ilości materiału mogą być wywiewane z wnętrza doliny do pobliskiej zatoki i fiordu. Na podstawie uzyskanych wyników można wywnioskować, że świeży materiał jest włączany w obieg z dwóch głównych źródeł – osadów morenowych i rzecznych,

a następnie ulega on redystrybucji eolicznej, szczególnie biorąc pod uwagę tunelowy charakter dolin poglacjalnych.

W pracy podkreślono złożone interakcje między procesami eolicznymi a warunkami środowiskowymi w rejonach zimnych. Postępujące zmiany klimatu mogą znacząco wpłynąć na aktywność procesów eolicznych w przyszłości.

Słowa kluczowe: depozycja eoliczna, pułapka eoliczna, datowanie osadów, warunki peryglacjalne, środowiska sedymentacyjne, Arktyka

2. Abstract

Quantitative and qualitative measurements of aeolian activity at high latitudes are not currently carried out on a large scale, even though these processes are important elements of the geomorphic system of polar regions, which are particularly affected by climate change. This study presents the results of aeolian deposition rates measured and calculated for one of the central Spitsbergen postglacial valleys (Ebba Valley). The results are based on eight summer season field campaigns (2012–2018 and 2022), as well as on AMS ^{14}C and OSL dating of niveo-aeolian and aeolian sediments.

Contemporary mean aeolian deposition rates in the years 2012-2018 ranged from 0.1 to 22.9 $g \cdot m^{-2} \cdot day^{-1}$ over selected parts of the valley and averaged from 2.1 to 12.3 $g \cdot m^{-2} \cdot day^{-1}$ over the studied first seven summer seasons. Interestingly strong relationships (r^2 = 0.71, p = 0.017) between mean air temperature and mean aeolian deposition were observed, possibly indicating the importance of the source material delivered to the valley by glaciofluvial processes. Measurements performed in the summer season 2022 revealed that aeolian deposition rates were low at the start of the season, ranging from 0.3 to 0.6 $g \cdot m^{-2} \cdot day^{-1}$, but peaked at 25.4 $g \cdot m^{-2} \cdot day^{-1}$ towards the end of the season.

Niveo-aeolian deposition rates were estimated for the period since the 11th century, through the Little Ice Age, till the second half of the 20th century and revealed a rather constant value of 0.05 cm per year. Since then, the niveo-aeolian deposition rate has significantly increased and equalled 0.3 cm per year, which may be related to rising air temperatures and associated pan-Arctic environmental changes.

Additionally, analysis of rounding and matting of quartz grains collected from aeolian deposition traps was performed. This part of the study was based on four summer field campaigns (2015–2018). Quartz grains with a diameter of 0.8–1.0 mm were selected and subjected to further analysis under a microscope, which allowed them to be divided into six individual classes. The nature of the grains can largely indicate the environmental conditions in which the material was transported. The collected material was dominated by grains with a low degree of roundness, which may indicate relatively short fluvial or aeolian transport. The small amounts of typically matted quartz grains may indicate low environmental dynamics and short transport, as well as the fact that large amounts of material are blown from the valley interior to the nearby bay and fjord. This results highlights the importance of a fresh sediment supply from two main sources, moraines and rivers, and their subsequent aeolian redistribution, particularly in a wind-channelled valley environment.

The study underscore the complex interactions between aeolian processes and environmental conditions in cold regions. Climate change may significantly affect the magnitude of aeolian processes in the future.

Keywords: aeolian deposition, aeolian trap, sediment dating, periglacial conditions, sedimentary environments, Arctic

3. Publikacje wchodzące w skład rozprawy doktorskiej

Rozprawa doktorska składa się z trzech artykułów naukowych stanowiących spójny tematycznie zbiór publikacji.

Artykuł nr 1

Rymer K.G., Rachlewicz G., Buchwal A., Temme A.J.A.M., Reimann T., van der Meij W.M., 2022: Contemporary and past aeolian deposition rates in periglacial conditions (Ebba Valley, central Spitsbergen). CATENA, 211. DOI: 10.1016/j.catena.2021.105974

Artykuł nr 2

Rymer K.G., 2024: Intraseasonal changes in aeolian deposition rates in Ebba Valley, central Spitsbergen. Landform Analysis, 43: 41-46. DOI: 10.12657/landfana-043-004

Artykuł nr 3

Rymer K.G., Wachecka-Kotkowska L., 2024: Sources of the aeolian material in periglacial conditions based on quartz grain analysis, Ebba Valley, Svalbard. Quaestiones Geographicae, 43(4): 17–29. DOI: 10.14746/quageo-2024-0034

4. Wstęp

Procesy i zjawiska środowiskowe w regionach polarnych cechują się jedną z najwyższych na świecie wrażliwością na globalne zmiany klimatyczne. Istotne zmiany obserwuje się nie tylko pod względem ocieplenia klimatu i cofania się czół lodowców, ale również w kontekście zmian w sukcesji roślinnej, wysokości opadów, wilgotności powietrza i gleby oraz warunków anemometrycznych (IPCC 2021). Wszystkie te czynniki są niezwykle istotne dla rozwoju procesów eolicznych i związanych z nimi form terenu. Jednak rola i znaczenie aktywności wiatru w systemie peryglacjalnym są jednymi z najmniej rozpoznanych oraz najtrudniejszych do oceny, zwłaszcza w kontekście ilościowym. Już Troll (1948) zasugerował, że procesy eoliczne są jednymi z najważniejszych czynników morfogenetycznych w środowiskach peryglacjalnych. Niemniej jednak, procesy te są często pomijane w analizach obiegu energii i materii w geoekosystemach arktycznych. Na przykład Beylich i in. (2016) wskazują, że wciąż istnieje stosunkowo ograniczona ilość danych, które można wykorzystać do stworzenia kompleksowych modeli koncepcyjnych i matematycznych dotyczących zlewni zlodowaconych.

Znaczący przegląd współczesnej wiedzy dotyczącej rozwoju procesów i form eolicznych w wysokich szerokościach geograficznych przedstawili m.in. McKenna Neuman (1993), Seppälä (2004), Brookfield (2011), Bullard (2012) i Bateman (2013). Najczęściej jednak szczegółowe pomiary terenowe procesów eolicznych ograniczały się do zaledwie kilku wybranych miejsc w wysokiej Arktyce (zob. Maher 2011). Między innymi niewielka liczba badań obejmowała Spitsbergen, lub inne części archipelagu Svalbard. Ponadto, większość badań dotyczących problematyki eolicznej w tej części Arktyki przeprowadzono w latach 70. i 80. XX wieku. Nawet wtedy bezpośrednie pomiary terenowe były zazwyczaj ograniczone do krótkoterminowych obserwacji. Co więcej, większość badań eolicznych prowadzono na zachodnim wybrzeżu Spitsbergenu, które charakteryzuje się większą wilgotnością niż wewnętrzne części wyspy (Dahlke i in. 2020). W rejonie Hornsundu oszacowano średnie roczne wartości akumulacji eolicznej na 29 $g \cdot m^{-2}$, a w przypadku nunataków wyniosły one nawet 117 $g \cdot m^{-2}$ (Pękala 1980, Baranowski i Pękala 1982). Depozycja eoliczna była szczególnie zauważalna podczas burz pyłowych, osiągając wartości 1,398 $g \cdot m^{-2}$ na sezon letni (Piotrowski 1983), a w niektórych przypadkach 105 $g \cdot m^{-2}$ na 10 s (Szczypek 1982). Dla regionu Arktyki oszacowano również, że w wyniku aktywności eolicznej, średnio rocznie może być gromadzone 0,5–2,0 mm materiału (Wojtanowicz 1976). Czeppe (1966, 1968), który prowadził obserwacje deflacji i akumulacji eolicznej zimą 1957/58 w otoczeniu Hornsundu, zauważył, że na południowym Spitsbergenie procesy eoliczne osiągają największą

intensywność w okresie między październikiem a marcem. Na podstawie jego badań oszacowano, że roczna wielkość akumulacji eolicznej w regionie Hornsundu wynosiła około 300–400 $g \cdot m^{-2}$. Inne prace opisujące procesy eoliczne na Svalbardzie opublikowali między innymi Åkerman (1980, 1983), Gębica i Szczęsny (1988), Kida (1981, 1986, 1995) oraz Migała i Sobik (1984). Większość z tych badań stosowała różne metody pomiarowe w różnych skalach czasowych, co uniemożliwia bezpośrednie porównanie wyników.

Jeśli chodzi o centralny Spitsbergen, kompleksowe badania geologiczne i geograficzne obszaru Doliny Ebby są prowadzone od ponad 40 lat, jednak kwestie eoliczne były poruszane w tym rejonie wyjątkowo rzadko. Należy wspomnieć, że w Dolinie Ebby w trakcie lata 2002 roku prowadzone były pomiary efektywności transportu i akumulacji materiału eolicznego (Paluszkiewicz 2003). Wykazano, że deflacja i akumulacja dotyczy głównie frakcji pyłowej. Największą efektywność transportu eolicznego zaobserwowano, gdy prędkość wiatru przekraczała 5-6 $m \cdot s^{-1}$. Największy wpływ na intensywność procesów eolicznych miały wilgotność powietrza i gleby, morfologia terenu oraz pokrycie roślinnością. Ze względu na brak stałych i silnych wiatrów latem 2002 roku efektywność transportu i akumulacji eolicznej była stosunkowo mała. Badania procesów eolicznych w Dolinie Ebby przeprowadzono również latem 2005 roku, ale ograniczały się one do identyfikacji form akumulacji i erozji eolicznej (Górska-Zabielska 2007). Ponadto, depozycja eoliczna została oszacowana i uwzględniona jako istotny czynnik formowania gleby w dolinie (van der Meij i in. 2016). Wpływ działalności wiatru na pokrywę roślinną był również analizowany przez Borysiak i in. (2020). W ostatnim czasie Kavan i in. (2020) oszacowali całkowitą zawartość osadów (pyłu) w próbkach śniegu podczas sezonu śnieżnego w otoczeniu Zatoki Petunia na 2,66–24,56 $g \cdot m^{-2}$.

Pomimo wieloletniego rozwoju metod dotyczących analiz charakteru i cech osadów eolicznych, fluwialnych i fluwioglacjalnych (Folk 1980, Pye i Tsoar 2009, Wachecka-Kotkowska i in. 2014, Woronko i in. 2015, Zieliński i in. 2015) tego typu wyniki pochodzące ze współczesnych środowisk peryglacjalnych wciąż należą do rzadkości.

Niezbędne wydaje się więc prowadzenie dalszych ilościowych badań dotyczących depozycji eolicznej dla wciąż mało zbadanej środkowej części Spitsbergenu, przede wszystkim w celu określenia warunków środowiskowych wysokiej Arktyki, zarówno w dłuższych, jak i krótszych skalach czasowych. Jest to szczególnie ważne w świetle ostatnio obserwowanego w centralnej części Spitsbergenu rosnącego kontynentalizmu klimatu (Przybylak i in. 2014, Dahlke i in. 2020, Ivanov i in. 2020), co może być potencjalnie związane z większą intensywnością procesów eolicznych i/lub wyższymi wskaźnikami depozycji eolicznej w przyszłości.

Praca zakładała realizację pięciu najważniejszych celów badawczych:

a) określenie tempa depozycji eolicznej w warunkach peryglacjalnych wysokiej Arktyki w długiej skali czasu (tj. kilku sezonów badawczych) oraz w skali sezonowej (w obrębie jednego sezonu letniego);

b) zbadanie występowania zależności pomiędzy depozycją eoliczną oraz cechami zdeponowanego materiału, a wybranymi czynnikami meteorologicznymi i środowiskowymi;

c) obliczenie tempa depozycji niweo-eolicznej i eolicznej od początku małej epoki lodowej

d) przeprowadzenie analizy ilościowej i jakościowej ziarn kwarcu zdeponowanych w pułapkach eolicznych;

e) określenie źródeł pochodzenia materiału transportowanego przez wiatr.

Badania prowadzone były w Dolinie Ebby zlokalizowanej na Spitsbergenie (Ryc. 1), największej wyspie archipelagu Svalbard. Dolina położona jest nad Zatoką Petunia – północnym krańcem fiordu Bille. Pod względem geologicznym jest to bardzo zróżnicowany region o złożonych strukturach skał metamorficznych i osadowych i urozmaiconych formach terenu (Dallmann i in. 2004, Rachlewicz 2009). Seria sześciu podniesionych teras morskich tworzy część ujściową doliny. Najstarsza terasa została wydatowana metodą luminescencji na 13,3 tys. lat temu, a najmłodsza na 1,5 tys. lat temu (van der Meij i in., 2016). Dawne podniesione plaże zbudowane są głównie z piasku i żwiru, zawierającego muszle mięczaków. Osady polodowcowe, znajdują się pod warstwami osadów terasowych i lokalnie na zboczach doliny. Obszar ten współcześnie kształtowany jest przez procesy fluwioglacjalne oraz aktywne ruchy masowe na stokach otaczających dolinę masywów górskich (Kłysz i in. 1989, Karczewski i in. 1990, Pleskot 2015).

Średnia roczna temperatura powietrza w regionie Zatoki Petunia, na podstawie obserwacji dla lat 2000-2003, wynosi około −6,5 °C (Rachlewicz i Szczuciński 2008). Temperatury powyżej 0 °C są zwykle rejestrowane między połową maja/początkiem czerwca a początkiem września (Rymer i Rachlewicz 2014). Lipiec i sierpień to najcieplejsze miesiące ze średnią temperaturą 5–6 °C. Obszar badań charakteryzuje się relatywnie wyższymi temperaturami powietrza w lecie niż pobliska stacja meteorologiczna w Svalbard Lufthavn (Rachlewicz 2003, Rachlewicz i Styszyńska 2007). Ponadto obszar ten charakteryzuje się silniejszą kontynentalnością niż południowa i zachodnia część Svalbardu (Przybylak i in. 2014).

Obszar badań można zaliczyć do typu tak zwanych zimnych pustyń (cold deserts) (Brookfield 2011) z sumą rocznych opadów poniżej 200 mm. Opady latem są zwykle niższe

niż 50 mm, a maksymalne opady dzienne rzadko przekraczają 10 mm. Wilgotność powietrza jest stosunkowo wysoka ze względu na niewielką odległość od fiordu. Pokrywa śnieżna zwykle nie jest gruba i rzadko przekracza 0,5 m (Rachlewicz 2003, Przybylak i in. 2006, Rachlewicz i Szczuciński 2008).

Wiatry południowe i północno-wschodnie są typowe dla Doliny Ebby (Przybylak i in. 2006). Jednak maksymalną prędkość wiatru i najsilniejsze porywy wiatru, przekraczające 20 $m \cdot s^{-1}$, obserwuje się głównie ze wschodu, północy i północnego zachodu (Rachlewicz 2003, Małecki 2015).

Obszar badań znajduje się w strefie tundry arktycznej, porośniętej głównie mchem, porostami i nieciągłą roślinnością karłowatych krzewinek. W regionie zatoki Petunia występuje sześć głównych typów zbiorowisk roślinnych: *Dryas octopetala*, *Saxifraga oppositifolia*, *Carex*, *Deschampsia borealis*, *Papaver dahlianum* oraz *Festuca baffinensis* (Klimešová i in. 2012). Najbardziej zwartą pokrywę roślinną można znaleźć w zachodniej części Doliny Ebby, tj. blisko ujścia rzeki Ebba. Najczęstszymi gatunkami karłowatych krzewinek w dolinie są *Salix polaris* (Buchwal i in. 2013) i *Dryas octopetala* (Borysiak i in. 2020).

Pomiary depozycji eolicznej prowadzono przez siedem sezonów letnich (2012-2018). Ze względu na ograniczenia logistyczne wynikające z prowadzenia badań w Arktyce pomiary wykonywano w przedziałach czasu różniących się liczbą dni. Najdłużej badania prowadzono w roku 2015 (64 dni), natomiast najkrócej w roku 2016 (44 dni).

Tempo depozycji eolicznej mierzone było przy użyciu zmodyfikowanych pułapek Marble Dust Collector. Projekt pułapki został zaproponowany przez Ganora w 1975 roku, udoskonalony przez Halla i Uptona (1988). Testy wykazały występowanie wysokiej zależności między wydajnością zbierania materiału w warunkach laboratoryjnych i terenowych. Skuteczność wychwytywania materiału przez pułapki malała jednak stopniowo wraz ze zmniejszaniem się wielkości cząstek do 100 µm. Poniżej tej wartości ponownie obserwowany był wzrost wydajności. Wzrost prędkości wiatru był kolejnym czynnikiem zmniejszającym skuteczność pułapek (Hall i Upton 1988). Goossens i Offer (2000) udowodnili, że wyniki uzyskane przy użyciu pułapek Marble Dust Collector można wykorzystać do pomiaru depozycji osadów eolicznych.

W badaniach zastosowano dwa rodzaje pułapek o średnicy 195 i 210 mm. Każda pułapka została umieszczona bezpośrednio na powierzchni gruntu. Wysokość krawędzi pułapki wynosiła około 2,5 cm, co zapobiegało gromadzeniu się wewnątrz pułapki materiału nieeolicznego (tj. pochodzącego ze spływu powierzchniowego lub materiału wzbijanego w powietrze przez uderzające krople deszczu). Taka konstrukcja pułapki pozwalała na wychwytywanie zarówno grubszego materiału przemieszczającego się w wyniku saltacji

eolicznej, jak i drobniejszego materiału przemieszczającego się w zawieszeniu. W latach 2012–2015 pułapki były wypełnione przepłukanymi, w celu usunięcia drobniejszych ziaren, osadami lokalnego żwiru plażowego (o wielkości cząstek > 4 mm). Materiał ten w dużej mierze odzwierciedlał warunki powierzchniowe występujące w otoczeniu pułapek eolicznych. Od roku 2016 osady żwirowe w niektórych pułapkach były częściowo zastępowane szklanymi kulkami (*marbles*), aby ułatwić późniejszy zbiór materiału eolicznego z pułapek. Pod koniec każdego sezonu pomiarowego pułapki były czyszczone poprzez mycie filtrowaną wodą żwiru lub szklanych kulek wraz z wewnętrzną częścią pułapki. Po dekantacji materiał był suszony w temperaturze pokojowej i wysyłany do laboratorium w celu dokładnego zważenia. Aby zapewnić porównywalność otrzymanych wyników pomiędzy pułapkami o różnych średnicach, a także w różnych sezonach badawczych (o różnej długości), dokonano przeliczenia na jednostki wyrażone w $g \cdot m^{-2} \cdot dzień^{-1}$.

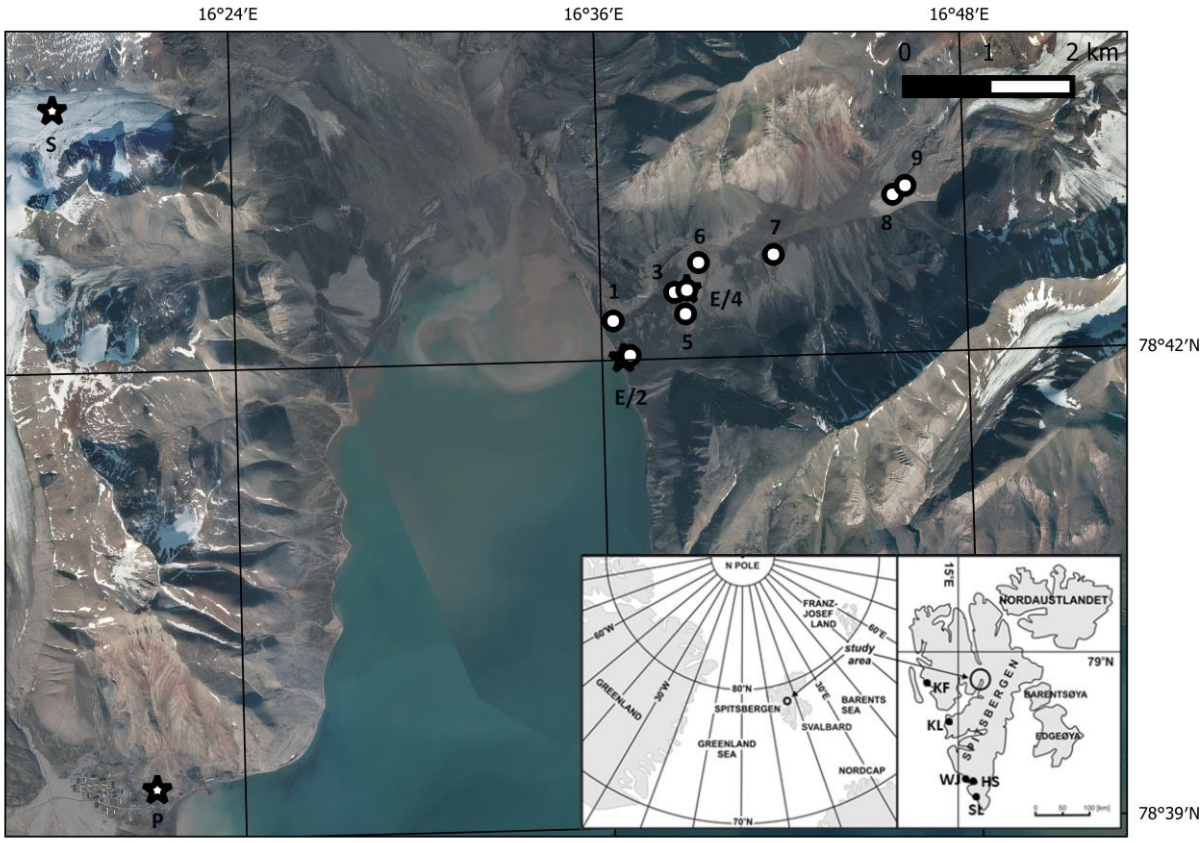

Ryc. 1. Ortofotomapa obszaru badań z dziewięcioma stanowiskami testowymi depozycji eolicznej (1–9) w dolinie Ebba. Stacje meteorologiczne (E – dolina Ebba, S – lodowiec Sven, P – miasto Pyramiden) są oznaczone czarnymi gwiazdkami. Źródło ortofotomapy – Norweski Instytut Polarny. Wewnętrzna mapa przedstawia lokalizację obszaru badań (czarne strzałki i okrąg) na Spitsbergenie.

Depozycję eoliczną mierzono w dziewięciu lokalizacjach (stanowiskach testowych), odzwierciedlających różne warunki geomorfologiczne i wegetacyjne wzdłuż osi Doliny Ebby (Ryc. 1): stanowiska tundrowe położone najbliżej fiordu z gęstą pokrywą roślinną: wilgotne (1) i suche (2); stanowiska w obrębie najwyższej dawnej terasy morskiej z mało lub rzadko występującą roślinnością tundrową: stok zawietrzny (3), szczyt (4) i stok dowietrzny (5); stanowisko na pokrywie piaszczystej (6) porośnięte jedynie pojedynczymi kępami trawy; oraz trzy stanowiska testowe niemal bez roślinności położone w centralnej części doliny (7), na sandrze (8) i na morenie (9). Łącznie zebrano materiał z 132 pułapek eolicznych podczas siedmiu sezonów badawczych (w latach 2012-2014 na każdym stanowisku testowym znajdowało się po jednej pułapce, natomiast w latach 2015-2018 wykorzystano po trzy pułapki na każdym stanowisku). Liczba pułapek została zwiększona po przeprowadzeniu eksperymentu terenowego w 2014 r., który wykazał, że pomiary depozycji eolicznej mogą różnić się znacząco nawet pomiędzy pułapkami zlokalizowanymi w obrębie tego samego stanowiska testowego (umieszczonymi w odległości 1–2 m). Ponadto, z powodu aktywności zwierząt w dolinie, trzy pułapki zostały uszkodzone, dlatego część wyników nie została uwzględniona w analizie. Było to po jednej pułapce ze stanowisk: (5) stok dowietrzny (rok 2012), (6) pokrywa piaszczysta (rok 2015) oraz (7) centrum doliny (rok 2016). Ponadto, z powodu uszkodzenia przez człowieka, pomiary w 2014 roku na stanowisku dowietrznym (5) przeprowadzono tylko w drugiej połowie sezonu pomiarowego.

Aby obliczyć tempo depozycji eolicznej w dłuższej skali czasu, pobrano dwie próbki osadów do datowania metodą OSL i siedem próbek do datowania metodą AMS ^{14}C. Osady do datowania metodą OSL pobrano 14 sierpnia 2014 roku z wkopów wykonanych w osadach niweoeolicznych i eolicznych, z głębokości 38 cm i 57 cm. Wszystkie próbki pobrano w warunkach zapewniających ochronę przed światłem słonecznym. Osady do datowania metodą AMS ^{14}C pobrano z wkopu wykonanego w osadach niweoeolicznych 9 września 2018 roku. Były to trzy próbki z głębokości 60 cm (w miejscu kontaktu piasku eolicznego z dawną powierzchnią terasy morskiej), dwie próbki z głębokości 58 cm, jedną próbkę z głębokości 17 cm i jedną próbkę z głębokości 12 cm. Na głębokości 58–60 cm materiał organiczny użyty do datowania metodą AMS ^{14}C składał się z bardzo dobrze zachowanych fragmentów i całych liści roślinności tundrowej. W dwóch płytszych warstwach pobrany materiał zawierał pozostałości wymieszanej materii organicznej.

Dodatkowo, na podstawie wniosków wyciągniętych z badań z lat 2012-2018, w roku 2022 przeprowadzono pomiary uzupełniające na jednym ze stanowisk testowych – w centralnej części doliny (7). Na stanowisku tym notowane były wartości depozycji eolicznej

zbliżone do średniej depozycji obliczonej dla całej doliny na podstawie porównania wszystkich dziewięciu stanowisk testowych. Podobnie jak w latach poprzednich pozostawiono w terenie trzy pułapki na okres całego sezonu pomiarowego (który trwał 41 dni). Ponadto, trzykrotnie podczas sezonu na tym samym stanowisku rozmieszczono po trzy dodatkowe pułapki na krótsze okresy (od 11 do 17 dni).

Większość danych meteorologicznych zebrana została za pomocą urządzeń ONSET HOBO zlokalizowanych w pobliżu stanowiska na szczycie najwyższej dawnej terasy morskiej (E/4, Ryc. 1). Prędkość i kierunek wiatru (na wysokości 2 m) rejestrowano w następujących odstępach czasu: 5 min (w latach 2012, w 1. połowie roku 2013 i w roku 2014) i 15 min (w latach 2016, 2017 i 2018). Niestety, w wyniku pracy w trudnych warunkach, niektóre urządzenia pomiarowe ulegały częstym awariom. Dlatego część wykorzystanych danych dotyczących prędkości i kierunku wiatru pochodziła z automatycznej stacji meteorologicznej (rejestrującej w odstępach jednogodzinnych), zlokalizowanej w pobliżu stanowiska testowego tundra sucha (E/2, Ryc. 1). Dane te zostały wykorzystane do uzupełnienia luk w drugiej połowie roku 2013 (od 5 sierpnia) i za rok 2015. Z powodu awarii czujnika w roku 2015 zapis informacji dotyczącej kierunku wiatru rozpoczął się dopiero 17 sierpnia.

W celu weryfikacji dokładności uzyskanych danych meteorologicznych, jak również w celu przeprowadzenia korelacji z wynikami depozycji eolicznej w roku 2022 użyto także wyników uzyskanych z innych pobliskich automatycznych stacji meteorologicznych (P, S, Ryc. 1). Wykorzystano między innymi automatyczną stację meteorologiczną (rejestrującą w odstępach czasowych co 10 minut) zlokalizowaną na lodowcu Sven od 2011 roku (Małecki 2019). Ponadto pozyskano dane meteorologiczne z pobliskiej miejscowości Pyramiden, których rejestracja rozpoczęła się od końca 2012 roku oraz stacji meteorologicznej znajdującej się w stolicy Spitsbergenu - Longyearbyen, położonej ok. 60 km na południowy zachód od obszaru badań. Dane zostały pozyskane za pośrednictwem bazy Seklima (Norweski Instytut Meteorologiczny, https://seklima.met.no/).

Dane dotyczące wilgotności gleby dla Doliny Ebby zostały zebrane za pomocą czujnika Decagon umieszczonego na głębokości 10 cm na stanowisku znajdującym się w pobliżu najwyższej terasy morskiej. Czujnik ten został zamontowany w kępach karłowatych krzewinek arktycznych i działa od 2012 r. Dodatkowy czujnik wilgotności gleby (ONSET HOBO) został umieszczony na głębokości 5 cm w pobliżu stanowiska testowego na tundrze wilgotnej. Czujnik ten został umieszczony w zwartej pokrywie roślinnej i działał od 2014 r. Dane dotyczące temperatury powietrza i wilgotności powietrza zostały pozyskane z czujników Decagon umieszczonych na wysokości 10 cm nad powierzchnią gleby na stanowisku znajdującym się w pobliżu najwyższej terasy morskiej. Wszystkie pozyskane dane zostały

zagregowane (średnia arytmetyczna) do odpowiadających im okresów pomiaru depozycji eolicznej.

Aby dokonać charakterystyki materiału zdeponowanego w pułapkach, przeprowadzono analizę wielkości ziaren przy użyciu standardowej metody sitowej. W tym celu użyto zestawu sit o odstępach połowy fi. Ze względu na niewielką ilość materiału zdeponowanego w większości pułapek (tj. mniejszą niż 100 g) do dalszej analizy użyto tylko materiału pochodzącego z trzech losowych pułapek (o wadze materiału > 30 g). Analizy statystyczne wyników wielkości ziaren przeprowadzono przy użyciu oprogramowania Gradistat 9.1 (Blott i Pye 2001). Obliczenia parametrów statystycznych oparte były na założeniach Folka i Warda (1957) oraz Folka (1954). Tę samą metodę zastosowano do analizy osadów pochodzących z wkopów wykonanych w celu wykonania datowań (próbki reprezentowały osady z różnych głębokości: 6–13 cm, 14–21 cm, 38–44 cm i poniżej 60 cm).

Materiał eoliczny pochodzący z pomiarów depozycji eolicznej w latach 2015-2018 został przesiany w celu wyizolowania ziaren o średnicy 0,8–1,0 mm, co jest typowe dla analiz obtoczenia i zmatowienia ziaren (Goździk 1980, 1995, Mycielska-Dowgiałło i Woronko 1998). Do dalszych analiz wybrano wyłącznie ziarna kwarcu. Za względu na brak zanieczyszczenia ziaren węglanami nie zastosowano przemywania kwasem solnym. Ziarna kwarcu zaklasyfikowano następnie, przy użyciu binokularu, do sześciu grup na podstawie metody obtoczenia według Krumbeina (1941) oraz klasyfikacji stopnia obtoczenia i zmodyfikowanej metody zmatowienia powierzchni ziaren kwarcu według Cailleux (1942), wraz z modyfikacjami zaproponowanymi przez Goździka (1980, 1995) oraz Mycielską-Dowgiałło i Woronko (1998): nieobrobione (NU), matowe okrągłe (RM), błyszczące zaokrąglone (EL), matowe pośrednie (EM-RM), błyszczące pośrednie (EM-EL) i pęknięte (C). Wybrano łącznie 106 próbek depozycji eolicznej, co pozwoliło na analizę 1974 ziaren kwarcu pod kątem stopnia obtoczenia i zmatowienia.

Datowania dwóch próbek metodą OSL zostały przeprowadzone przez Netherlands Centre for Luminescence na Uniwersytecie w Wageningen w Holandii zgodnie z przyjętą metodologią wykonywania tego typu analiz. Natomiast materiał organiczny pozyskany z osadów niweo-eolicznych został wydatowany metodą AMS ^{14}C. Analizy te przeprowadzono w poznańskim laboratorium ^{14}C. Wszystkie otrzymane metodą AMS ^{14}C daty zostały skalibrowane do lat kalendarzowych przy użyciu oprogramowania kalibracyjnego OxCal, wersja 4.4 (Bronk Ramsey 2009). Obliczenia dla próbek 58–60 cm oparto na krzywej kalibracyjnej IntCal 20 (Reimer i in. 2013, Reimer i in. 2020). Dla próbek 12–17 cm zastosowano krzywą kalibracyjną Bomb 13 NH1 (Hua i in. 2013).

Analizy statystyczne dotyczyły w największym stopniu sprawdzenia wpływu parametrów meteorologicznych na wielkość depozycji eolicznej oraz charakter deponowanego materiału. W badaniach stosowano metody oparte na prostej regresji liniowej (r Pearsona, współczynnik determinacji r^2 oraz współczynnik korelacji rang Spearmana). Każda zmienna meteorologiczna została uśredniona do okresu odpowiadającemu czasowi prowadzenia pomiarów w danym sezonie badawczym. Dane weryfikowano pod kątem rozkładu normalnego poprzez wizualny przegląd histogramów i test Shapiro-Wilka.

Uzyskane metodami AMS ^{14}C i OSL daty zostały wykorzystane do obliczenia tempa depozycji eolicznej w długiej skali czasu. Wykorzystano tutaj model zaproponowany przez van der Meij i in. (2019).

5. Najważniejsze wnioski

Artykuł nr 1

Ocena ilościowa dynamiki i aktywności procesów eolicznych w Wysokiej Arktyce w ostatnich latach nie była prowadzona na szeroką skalę. Wyniki dotyczące tempa letniej depozycji eolicznej uzyskane dla siedmiu okresów badawczych, uzupełnione o oszacowanie tempa depozycji eolicznej i niweo-eolicznej w przeszłości, są jedynymi z pierwszych tego rodzaju i wnoszą cenny wkład do obecnej wiedzy na temat funkcjonowania geoekosystemów peryglacjalnych i ich przemian. W szczególności możliwe było obliczenie średniej wielkości depozycji eolicznej w Dolinie Ebby wynoszącej 5,6 $g \cdot m^{-2} \cdot dzień^{-1}$. Na tej podstawie można wskazać, że dno doliny może być pokrywane do ok. 500–600 $g \cdot m^{-2}$ materiału eolicznego podczas każdego sezonu letniego. Wielkość średniej depozycji eolicznej była pozytywnie skorelowana ze średnią temperaturą powietrza, a zależności te były bardziej zauważalne na stanowiskach testowych położonych bliżej obszaru występowania fluwioglacjalnego materiału źródłowego. Wykazano również, że wartości średniej depozycji eolicznej są lokalnie ograniczane przez obecność pokrywy roślinnej. Współczesne procesy eoliczne w tej części centralnego Spitsbergenu wydają się mieć raczej lokalny charakter, a transportowi ulega materiał dostarczany do doliny przez strumienie i rzeki wypływające z lodowców. Materiał transportowany na duże odległości prawdopodobnie jest deponowany w wodach fiordu.

Obliczone wartości depozycji niweo-eolicznej i eolicznej od XI wieku wykazały, że następujące zmiany klimatyczne, a zwłaszcza ocieplenie, mają wpływ na aktywność eoliczną. Wzrost wielkości depozycji eolicznej z 0,05 do 0,3 cm rocznie, zaznaczający się od początku lat 60. XX wieku, jest znaczącym indykatorem zachodzących zmiany środowiska na badanym obszarze. Można się spodziewać, że dalszy wzrost temperatury powietrza, prognozowany dla Arktyki, może powodować w przyszłości dalsze zwiększanie wartości deponowanego materiału. Będzie to miało istotny wpływ na funkcjonowanie pokrywy roślinnej, zmiany albedo lodowców, dostarczanie osadów do fiordów, a także na życie ludzi i zwierząt w tym regionie.

Artykuł nr 2

Podjęte badania były jednymi z pierwszych, w których celem była szczegółowa ocena ilościowa wielkości depozycji eolicznej w ciągu jednego sezonu letniego.

Pomimo, że rok 2022 różnił się pod względem warunków meteorologicznych od lat poprzednich, zmierzone wartości depozycji eolicznej znajdowały się w podobnym zakresie, choć były wyższe od tych uzyskanych w latach 2012-2018.

Co ważne, wyniki wskazują, że depozycja materiału niesionego przez wiatr rozpoczyna się dopiero pod koniec sezonu letniego. Wynika to z faktu, że z reguły pod koniec lata obserwuje się silniejsze wiatry, większe sumy opadów i niższe temperatury powietrza. To właśnie niższe temperatury powietrza powodują obniżenie poziomu wody w rzekach, co z kolei powoduje odsłanianie osadów naniesionych przez rzeki lodowcowe w pełni lata. Świeży materiał fluwioglacjalny może być wówczas włączany do transportu przez wiatr i osadzany w dnie doliny.

Badania wykazały, że różnice w tempie depozycji eolicznej w ciągu sezonu mogą być znaczne. Przez większą część lata dobowe wartości depozycji eolicznej osiągają 0,3-0,6 $g \cdot m^{-2}$. Pod koniec sezonu letniego mogą one wzrosnąć nawet do 25,4 $g \cdot m^{-2}$ na dobę.

Artykuł nr 3

Na podstawie analizy danych pochodzących z materiału zebranego w pułapkach eolicznych w latach 2015-2018 udało się ustalić zależności pomiędzy występowaniem ziaren należących do określonych klas morfologicznych, a zmiennymi środowiskowymi (parametrami meteorologicznymi i geomorfologicznymi).

Co istotne zidentyfikowano dwa główne źródła pochodzenia materiału eolicznego deponowanego w pułapkach. Pierwszym z nich był świeży materiał nieobrobiony (ziarna NU) pochodzący najprawdopodobniej z osadów z morenowych, gdzie występuje silne wietrzenie mrozowe osadów. Materiał ten jest rozprowadzany przez wiatr na krótkich odcinkach wewnątrz doliny (zgodnie z osią doliny) i podczas tego transportu może nabierać cech ziaren przejściowych, których udział procentowy był zazwyczaj najwyższy. Drugim był osad fluwioglacjalny (ziarna EL i EM-EL) pochodzący z aluwiów rzecznych. Wielkość dostarczanego materiału jest najczęściej uzależniona od poziomu rzeki, czyli pośrednio od ilości niesionego osadu. Poziom ten z kolei zależy przede wszystkim od temperatury i ilości opadów w danym roku. Zaobserwowano, że dystrybucję tego materiału mogą ograniczać silniejsze wiatry z kierunków przeciwnych do wylotu osi doliny. Zarówno transport eoliczny, jak i fluwialny, w stosunkowo krótkich dolinach Spitsbergenu, nie trwa zwykle długo, co przekłada się na największy udział ziaren należących do klas pośrednich EM-EL i EM-RM. Ziarna te mogą

również mieć cechy nabyte w pierwotnych środowiskach sedymentacyjnych - lodowcowym i fluwioglacjalnym.

Stosunkowo niewielka liczba ziaren należących do klasy RM, czyli tych o typowych cechach eolicznych, może wskazywać na bardzo krótki transport lub niską dynamikę środowiskową w tego typu dolinach peryglacjalnych. Większość materiału przed nabraniem cech danego typu jest prawdopodobnie wywiewana i osadzana w pobliskiej zatoce i fiordzie. Może to potwierdzać stosunkowo wysoki udział ziaren RM w pobliżu zatoki na suchym stanowisku tundrowym. Drugim powodem tak małej eolizacji może być zbyt krótki okres, w którym panują warunki pozwalające na zmatowienie powierzchni pojedynczych ziaren lub brak objęcia badaniami okresu jesieni.

Ze względu na swoją orientację i morfologię Dolina Ebby może odzwierciedlać warunki panujące w tunelu aerodynamicznym, w którym świeże osady w środowisku peryglacjalnym przechodzą początkową fazę eolizacji.

W warunkach zachodzących zmian klimatu dynamika środowiska będzie ulegała dalszym zmianom. Może to również wpłynąć na zmianę dotychczasowych proporcji dostawy materiału wietrzejącego z moren i tego dostarczanego przez rzeki proglacjalne. To drugie źródło materiału uczestniczącego w aktywności eolicznej na Spitsbergenie może zyskać na znaczeniu ze względu na rosnące wartości opadów oraz wzrost temperatury powietrza w Arktyce. Zmiany te mogą znacząco wpłynąć na funkcjonowanie geoekosystemów peryglacjalnych zarówno w skali lokalnej, jak i regionalnej.

6. Bibliografia

Åkerman J., 1980. Studies on periglacial geomorphology in West Spitsbergen (PhD. thesis). Lunds Universitets Geografiska Inst. Ser. Avh., LXXXIX: 297 pp.

Åkerman J., 1983. Notes concerning the vegetation on deflation surfaces, Knapp Linné, Spitsbergen. Polar Research, 1: 161–169.

Baranowski S., Pękala K., 1982. Nival-eolian processes in the tundra area in the nunatak zone of the Hans and Werenskiold Glaciers (SW Spitsbergen). Results of investigations of the Polish Scientific Spitsbergen Expeditions, 4. Acta Universitatis Wratislaviensis, 525: 11–27.

Bateman M.D., 2013. Aeolian processes in periglacial environments. W: Shroder J., Giardino R., Harbor J. (red.), Treatise on Geomorphology. Academic Press, San Diego, vol. 8, Glacial and Periglacial Geomorphology: 416–429.

Beylich A.A., Dickson J.C., Zwolinski Z., 2016. Source-To-Sink Fluxes in Undisturbed Cold Environments. Cambridge University Press.

Blott S.J., Pye K., 2001. Grain Size Distribution and Statistics of Unconsolidated Sediments. Earth Surface Processes and Landforms, 26: 1237–1248.

Borysiak J., Pleskot K., Rachlewicz G., 2020. Dryas aeolian landforms in Arctic deflationary tundra, central Spitsbergen. Polish Polar Research, 41(1): 41–68.

Bronk Ramsey C., 2009. Bayesian analysis of radiocarbon dates. Radiocarbon, 51(1): 337–360.

Brookfield M.E., 2011. Aeolian processes and features in cool climates. W: Martini I.P, French H.M., Pérez Alberti A. (red.), Ice-marginal and Periglacial Processes and Sediments. Geological Society, London: 241–258.

Buchwal A., Rachlewicz G., Fonti P., Cherubini P., Gaertner H., 2013. Temperature modulates intra-plant growth of Salix polaris from a high Arctic site (Svalbard). Polar Biology, 36(9): 1305-1318.

Bullard J.E., 2012. Contemporary glacigenic inputs to the dust cycle. Earth Surface Processes and Landforms, 38: 71–89.

Cailleux A., 1942. Les action eoliennes periglaciaires en Europe. Mémoires de la Société géologique de France, 41: 1-176.

Czeppe Z., 1966. Przebieg głównych procesów morfogenetycznych w południowozachodnim Spitsbergenie. Zeszyty Naukowe UJ, Prace Geograficzne, 13: 96–102.

Czeppe Z., 1968. The annual rhythm of morphogenetic processes in Spitsbergen. Geographia Polonica, 14: 57–65.

Dahlke S., Hughes N.E., Wagner P.M., Gerland S., Wawrzyniak T., Ivanov B., Maturilli M., 2020. The observed recent surface air temperature development across Svalbard and concurring footprints in local sea ice cover. International Journal of Climatology, 40: 5246–5265.

Dallmann W.K., Pipejohn K., Blomeier D., 2004. Geological Map of Billefjorden, Central Spitsbergen, Svalbard with geological excursion guide 1:50 000. Norsk Polarinstitutt Tematkart 36.

Folk R.L., 1954. The distinction between grain size and mineral composition in sedimentary-rock nomenclature. Journal of Geology, 62: 344–359.

Folk R.L., 1980. Petrology of Sedimentary Rocks. Hemphill Publishing Company.

Folk R.L., Ward W.C., 1957. Brazos River bar: a study in the significance of grain size parameters. Journal of Sedimentary Petrology, 27: 3–26.

Gębica P., Szczęsny R., 1988. Symptoms of aeolian accumulation in western Sorkapp Land. Spitsbergen. Polish Polar Research, 9(4): 447–460.

Goossens D., Offer Z.Y., 2000. Wind tunnel and field calibration of six aeolian dust samplers. Atmospheric Environment, 34: 1043–1057.

Goździk J., 1980. Zastosowanie morfoskopii i graniformametrii do badań osadów w kopalni węgla brunatnego "Bełchatów". Studia Regionalne, IV(IX): 101-104.

Goździk J.S., 1995. Wybrane metody kształtu ziarn piasków do celów paleogeograficznych i stratygraficznych. In: Mycielska-Dowgiałło E., Rutkowski J. (eds), Badania osadów czwartorzędowych. Wybrane metody i interpretacja wyników. WGiSR, UW, Warszawa: 115-132.

Górska-Zabielska M., 2007. Formy eoliczne na przedpolu lodowca Ebba, środkowy Spitsbergen. W: Smolska, E., Giriat, D. (red.), Rekonstrukcja dynamiki i procesów geomorfologicznych – formy rzeźby i osady. Uniwersytet Warszawski, Wydział Geografii i Studiów Regionalnych, Komitet Badań Czwartorzędu Polskiej Akademii Nauk: pp. 199- 204.

Hall D.J., Upton S.L., 1988. A wind tunnel study of the particle collection efficiency of an inverted Frisbee used as a dust deposition gauge. Atmospheric Environment, 22(7): 1383–1394.

Hua Q., Barbetti,M., Rakowski A.J., 2013. Atmospheric Radiocarbon for the Period 1950–2010. Radiocarbon, 55(4): 2059–2072.

IPCC, 2021. Summary for Policymakers. W: Masson-Delmotte, V., Zhai, P., Pirani, A., Connors, S.L., Péan, C., Berger, S., Caud, N., Chen, Y., Goldfarb, L., Gomis, M.I., Huang, M., Leitzell, K., Lonnoy, E., Matthews, J.B.R., Maycock, T.K., Waterfield, T., Yelekçi, O., Yu, R., Zhou, B. (red.), Climate Change 2021: The Physical Science Basis. Contribution of Working Group I to the Sixth Assessment Report of the Intergovernmental Panel on Climate Change. Cambridge University Press: 3-32.

Ivanov B.V., Prokhorova U.V., Sviashchennikov P.N., 2020. Analysis of continentality and anomality of Svalbard climate according to observations of surface air temperature in the second half of the XX century. IOP Conf. Series: Earth and Environmental Science, 606: 012021.

Karczewski A. (red.), Borówka M., Gonera P., Kasprzak L., Kłysz P., Kostrzewski A., Lindner L., Marks L., Rygielski W., Stankowski W., Wojciechowski A., Wysokiński L., 1990. Petuniabukta, Billefjorden, Spitsbergen. Geomorphology. 1:40 000. Adam Mickiewicz University, Poznan.

Kavan J., Láska K., Nawrot A., Wawrzyniak T., 2020. High Latitude Dust Transport Altitude Pattern Revealed from Deposition on Snow. Svalbard. Atmosphere, 11: 1318.

Kida J., 1981. Badania procesów i form eolicznych na Ziemi Wedel-Jarlsberga (Spitsbergen). W: VII Sympozjum Polarne w Sosnowcu, Materiały cz. II, IG UŚl., Katowice: 36-37.

Kida J., 1986. Eolian Processes in the Werenskiold, Nann and Torell glacier forefields (Wedel-Jarlsberg Land, SW Spitsbergen). Results of Investigation of the Polish Scientific Spitsbergen Expeditions, 6. Acta Universitatis Wratislaviensis, 966: 25–43.

Kida J., 1995. Procesy eoliczne na wybrzeżach SW Spitsbergenu. W: Pereyma J., Piasecki J., XXII Sympozjum Polarne, Wrocław – Książ, 27-28 października 1995: 41-47.

Klimešová J., Doležal J., Prach K., Košnar J., 2012. Clonal growth forms in Arctic plants and their habitat preferences: a study from Petuniabukta, Spitsbergen. Polish Polar Research, 33: 421–442.

Kłysz P., Lindner L., Marks L., Wysokiński L., 1989. Late Pleistocene and Holocene relief remodeling in the Ebbadalen-Nordenskiöldbreen region in Olav V Land, central Spitsbergen. Polish Polar Research, 10(3): 277–301.

Krumbein W.C., 1941. Measurement and geological significance of shape and roundness of sedimentary particles. Journal of Sedimentary Petrology, 11(2): 64-72.

Maher B.A., 2011. The magnetic properties of Quaternary aeolian dusts and sediments, and their palaeoclimatic significance. Aeolian Research 3(2): 87–144.

Małecki J., 2015. Glacio–meteorology of Ebbabreen, Dickson Land, central Svalbard, during 2008–2010 melt seasons. Polish Polar Research, 36(2): 145–161.

Małecki J., 2019. Meteorology and summer net radiation of an Arctic alpine glacier: Svenbreen. Svalbard. International Journal of Meteorology, 39(10): 4107–4124.

McKenna Neuman, C., 1993. A review of aeolian transport processes in cold environments. Progress in Physical Geography 17(2): 137–155.

Migała K., Sobik M., 1984. Deflation and nival eolian phenomena observed under conditions of congelation in the forefield of the Werenskiold Glacier (SW Spitsbergen). Zeitschrift fur Gletscherkunde und Glazialgeologie, 20: 197–206.

Mycielska-Dowgiałło E., Woronko B., 1998. Analiza obtoczenia i zmatowienia powierzchni ziarn kwarcowych frakcji piaszczystej i jej wartość interpretacyjna. Przegląd Geologiczny, 46(12): 1275-1281.

Paluszkiewicz R., 2003. Zróżnicowanie natężenia transportu eolicznego w warunkach polarnych jako efekt zmienności czynników meteorologicznych na przykładzie doliny Ebby (Petuniabukta, Billefjorden, Spitsbergen Środkowy). W: Olech M.A. (red.), XXIX Międzynarodowe Sympozjum Polarne. Funkcjonowanie ekosystemów polarnych na tle globalnych zmian środowiska. Instytut Botaniki Uniwersytetu Jagiellońskiego, Kraków: pp. 235- 237.

Pękala K., 1980. Morphogenetic processes and cover deposits of nunataks in the Hornsund area (SW Spitsbergen). Polish Polar Research, 1(2–3): 9–44.

Piotrowski A., 1983. Results of investigations over a magnitude of aeolian transport in the western part of Oscar II Land (NW Spitsbergen) during summer 1979. Acta Universitatis Nicolai Copernici, Geografia, XVII, 56: 63–67.

Pleskot K., 2015. Sedimentological characteristics of debris flow deposits within ice− cored moraine of Ebbabreen, central Spitsbergen. Polish Polar Research, 36(2): 125–144.

Przybylak R., Araźny A., Gluza A., Hojan M., Migała K., Sikora S., Siwek K., Zwoliński Z., 2006. Porównanie warunków meteorologicznych na zachodnim wybrzeżu Spitsbergenu w sezonie letnim 2005 r. Problemy Klimatologii Polarnej, 16: 125–138.

Przybylak R., Araźny A., Nordli Ø., Finkelnburg R., Kejna M., Budzik T., Migała K., Sikora S., Puczko D., Rymer K., Rachlewicz G., 2014. Spatial distribution of air temperature on Svalbard during 1 year with campaign measurements. International Journal of Climatology, 34: 3702–3719.

Pye K., Tsoar H., 2009. Aeolian Sand and Sand Dunes. Springer.

Rachlewicz G., 2003. Warunki meteorologiczne w Zatoce Petunia (Spitsbergen środkowy) w sezonach letnich 2000 i 2001. Problemy Klimatologii Polarnej, 13: 127–138.

Rachlewicz G., 2009. Contemporary sediment fluxes and relief changes in high Arctic glacierized valley systems (Billefjorden, Central Spitsbergen). Wydawnictwo Naukowe UAM, Poznań.

Rachlewicz G., Styszyńska A., 2007. Porównanie przebiegu temperatury powietrza w Petuniabukta i Svalbard-Lufthavn (Isfjord, Spitsbergen) w latach 2001-2003. Problemy Klimatologii Polarnej, 17: 121-134.

Rachlewicz G., Szczuciński W., 2008. Changes in thermal structure of permafrost active layer in a dry polar climate, Petuniabukta, Svalbard. Polish Polar Research, 29: 261–278.

Reimer P.J., Bard E., Bayliss A., Beck J.W., Blackwell P.G., Bronk Ramsey C., Grootes P.M., Guilderson T.P., Haflidason H., Hajdas I., Hatt'e C., Heaton T.J., Hoffmann D.L., Hogg A.G., Hughen K.A., Kaiser K.F., Kromer B., Manning S.W., Niu M., Reimer R.W., Richards D.A., Scott E.M., Southon J.R., Staff R.A., Turney C.S.M., van der Plicht J., 2013. IntCal13 and Marine13 Radiocarbon Age Calibration Curves 0–50,000 Years cal BP. Radiocarbon, 55(4): 1869–1887.

Reimer P., Austin W., Bard E., Bayliss A., Blackwell P., Bronk Ramsey C., Butzin M., Cheng H., Edwards R., Friedrich M., Grootes P., Guilderson T., Hajdas I., Heaton T., Hogg A., Hughen K., Kromer B., Manning S., Muscheler R., Palmer J., Pearson C., van der Plicht J., Reimer R., Richards D., Scott E., Southon J., Turney C., Wacker L., Adolphi F., Büntgen U., Capano M., Fahrni S., Fogtmann-Schulz A., Friedrich R., Köhler P., Kudsk S., Miyake F., Olsen J., Reinig F., Sakamoto M., Sookdeo A., Talamo S., 2020. The IntCal20 Northern Hemisphere radiocarbon age calibration curve (0–55 cal kBP). Radiocarbon, 62(1): 821–863.

Rymer K., Rachlewicz G., 2014. Thermal dynamics of the permafrost active layer in Ebba valley (Central Spitsbergen) in the years 2009–2012. International Journal of Applied and Natural Sciences, 3: 79–86.

Seppälä M., 2004. Wind as a Geomorphic Agent in Cold Climates. Cambridge University Press.

Szczypek T., 1982. Działalność eoliczna w rejonie Zatoki Gas (południowy Spitsbergen). Wyprawy polarne Uniwersytetu Śląskiego 1977–1980, t. I. Prace Naukowe U. Śl., 543: 87–108.

Troll C., 1948. Der subnivale oder periglaziale Zyklus der Denudation. Erdkunde, 2: 1–21.

van der Meij W.M., Temme A.J.A.M., de Kleijn C.M.F.J.J., Reimann T., Heuvelink G.B.M., Zwoliński Z., Rachlewicz G., Rymer K., Sommer M., 2016. Arctic soil development on a series of marine terraces on Central Spitsbergen, Svalbard: a combined geochronology, fieldwork and modelling approach. SOIL, 2: 221–240.

van der Meij W.M., Reimann T., Vornehm V.K., Temme A.J.A.M., Wallinga J., Van Beek R., Sommer M., 2019. Reconstructing rates and patterns of colluvial soil redistribution in agrarian (hummocky) landscapes. Earth Surface Processes and Landforms, 44(12): 2408–2422.

Wachecka-Kotkowska L., Krzyszkowski D., Król E., Klaczak K., 2014. Middle Weichselian Pleniglacial fluvial erosion and sedimentation in the Krasówka river valley, Szczerców field, Bełchatów open cast mine, central Poland. Annales Societatis Geologorum Poloniae, 84, 4: 323–340.

Wojtanowicz J., 1976. Occurrence and intensity of the recent deflation and accumulation of aeolian dust. Biul. Inst. Geol., 297: 93–99.

Woronko B., Zieliński P., Sokołowski R.J., 2015. Climate evolution during the Pleniglacial and Late Glacial as recorded in quartz grain morphoscopy of fluvial to aeolian successions of the European Sand Belt. Geologos, 21(2): 89-103.

Zieliński P., Sokołowski R.J., Woronko B., Jankowski M., Fedorowicz S., 2015. The depositional conditions of the fluvio-aeolian succession during the last climate minimum based on the examples from Poland and NW Ukraine. Quaternary International, 386: 30-41.

7. Załącznik nr 1

Artykuł nr 1

Rymer K.G., Rachlewicz G., Buchwal A., Temme A.J.A.M., Reimann T., van der Meij W.M., 2022: Contemporary and past aeolian deposition rates in periglacial conditions (Ebba Valley, central Spitsbergen). CATENA, 211. DOI: 10.1016/j.catena.2021.105974

Errata do Artykułu nr 1

W nagłówku tabeli nr 6 prezentującej wyniki datowań metodą OSL prawidłową jednostką dla pozycji „OSL age” powinno być „ka” a nie „Gy”.

Catena 211 (2022) 105974

Contents lists available at ScienceDirect

Catena

journal homepage: www.elsevier.com/locate/catena

Contemporary and past aeolian deposition rates in periglacial conditions (Ebba Valley, central Spitsbergen)

Krzysztof G. Rymer [a,*], Grzegorz Rachlewicz [a], Agata Buchwal [a], Arnaud J.A.M. Temme [b], Tony Reimann [c], W. Marijn van der Meij [c]

[a] Institute of Geoecology and Geoinformation, Adam Mickiewicz University in Poznań, ul. Bogumiła Krygowskiego 10, 61-680 Poznań, Poland
[b] Department of Geography and Geospatial Sciences, Kansas State University, 920 N17th Street, Manhattan, KS 66506, USA
[c] Institute of Geography, University of Cologne, Zülpicher Str. 45, 50674 Köln, Germany

ARTICLE INFO

Keywords:
Aeolian deposition
Aeolian trap
Sediment dating
Periglacial conditions
Arctic
Svalbard

ABSTRACT

Quantitative measurements of aeolian activity at high latitudes are not currently carried out on a large scale, even though these processes are important elements of the geomorphic system of polar regions, which are particularly affected by climate change. This study presents the results of aeolian deposition rates measured and calculated for one of the central Spitsbergen postglacial valleys (Ebba Valley). The results are based on seven summer season field campaigns (2012–2018), as well as on AMS ^{14}C and OSL dating of niveo-aeolian and aeolian sediments. Contemporary mean aeolian deposition rates ranged from 0.1 to 22.9 g·m^{-2}·day^{-1} over selected parts of the valley and averaged from 2.1 to 12.3 g·m^{-2}·day^{-1} over the studied summer seasons. Interestingly strong relationships ($r^2 = 0.71$, $p = 0.017$) between mean air temperature and mean aeolian deposition were observed, possibly indicating the importance of the source material delivered to the valley by fluvioglacial processes. Moreover, aeolian deposition dependence on the source material reflected in the local nature of the process was observed. Niveo-aeolian deposition rates were estimated for the period since the 11th century, through the Little Ice Age, till the second half of the 20th century and revealed a rather constant value of 0.05 cm per year. Since then, the niveo-aeolian deposition rate has significantly increased and equalled 0.3 cm per year, which may be related to rising air temperatures and associated pan-Arctic environmental changes.

1. Introduction

Environmental processes in polar regions are some of the most sensitive indicators of global climate change. This is observed not only in terms of climate warming and glacier retreat but also in changes of plant succession, precipitation, air humidity and soil moisture, as well as wind conditions (IPCC, 2021). All these factors are extremely important for developing aeolian processes and landforms. However, the role and significance of wind activity in the periglacial system is one of the most difficult to assess and so far, the least recognized especially in quantitative terms. Troll (1948) suggested that aeolian processes are some of the most important morphogenetic factors in periglacial environments. However, these processes are often overlooked in analyses of energy and matter circulation of Arctic ecosystems. For example, Beylich et al. (2016) points out that there is still a relatively limited amount of data that can be used to create comprehensive conceptual and mathematical models of geomorphic system in glacierized catchments.

A significant overview of contemporary development of aeolian processes and landforms at high latitudes was presented by i.a. McKenna Neuman (1993), Seppälä (2004), Brookfield (2011), Bullard (2012) and Bateman (2013). However, detailed field measurements of aeolian processes were limited to only few sites located in the High Arctic (see Maher, 2011). For example, many worldwide studies of aeolian processes do not include Spitsbergen or other parts of the Svalbard archipelago. Furthermore, most of the aeolian research in this part of the Arctic was conducted in the 1970 s and 1980 s. Even then, direct field measurements were usually limited to a short-term observations. Moreover, the majority of the aeolian studies were conducted on the western coast of Spitsbergen, which is more humid than its interior (Dahlke et al., 2020). In the Hornsund area, the estimated mean niveo-

Abbreviations: AMUPS, Adam Mickiewicz University Polar Station; EBB, Ebba Valley; LYR, Longyearbyen (town); PYR, Pyramiden (town); SD, Standard deviation; SVE, Sven Glacier.

* Corresponding author.
E-mail address: krym@amu.edu.pl (K.G. Rymer).

https://doi.org/10.1016/j.catena.2021.105974
Received 10 June 2021; Received in revised form 15 November 2021; Accepted 20 December 2021
Available online 3 January 2022

aeolian deposition totalled 29 g·m^{-2} per year and specifically for nunataks it equalled 117 g·m^{-2} per year (Pękala, 1980; Baranowski and Pękala, 1982) (Fig. 1, site HS). Aeolian deposition was especially noticeable during dust storms with values of 1,398 g·m^{-2} per summer season (Piotrowski, 1983) (Fig. 1, site KF) and 105 g·m^{-2} per 10 s (Szczypek, 1982) (Fig. 1, site HS). For the Arctic region, it has also been estimated that, as a result of aeolian activity, 0.5–2.0 mm per year of material on average can be accumulated (Wojtanowicz, 1976). Also, Czeppe (1966, 1968) who ran observations of deflation and aeolian accumulation during the winter 1957/58 in the Hornsund area (Fig. 1, site HS), noted that on southern Spitsbergen aeolian processes achieve the largest intensity in the period between October and March. Based on his study, the estimated rate of aeolian accumulation in the Hornsund region was ca. 300–400 g·m^{-2} per year. Other work describing the aeolian processes on Svalbard was performed by Åkerman (1980, 1983) (Fig. 1, site KL), Gębica and Szczęsny (1988) (Fig. 1, site SL), Kida (1981, 1986, 1995) (Fig. 1, site WJ) and Migała and Sobik (1984) (Fig. 1, site WJ). Most of these studies have used different measurement methods at various time scales, which makes direct comparison impossible. In contrast to southern Spitsbergen, the only recent study from central Svalbard (Petunia Bay) by Kavan et al. (2020) estimated High Latitude Dust deposition at 2.66–24.56 g·m^{-2} per snow season, i.e., total sediment concentration in snow samples. Therefore, it is essential to fill the existing knowledge gap and to conduct quantitative study on aeolian deposition in the continental, i.e. largely understudied part of the Svalbard archipelago, over a longer time scale than one season. This is especially important in the light of an increasing continentality recently observed in the interior of Spitsbergen (Przybylak et al., 2014; Dahlke et al., 2020; Ivanov et al., 2020), which, in terms of both warmer and drier climate, might be potentially coupled with greater intensity of aeolian processes and/or higher aeolian deposition rates.

The main goal of the study was i) to quantify aeolian deposition rates in High Arctic periglacial conditions over a long time-scale (i.e. across two and more seasons), and ii) to investigate relationships between aeolian deposition and selected meteorological settings in order to determine which weather variables induce high aeolian deposition rates. Beforehand, meteorological conditions of the Ebba Valley were characterised. In addition, we aimed to calculate the niveo-aeolian and aeolian deposition rates since the beginning of the Little Ice Age and discuss possible links or discrepancies between centennial and annual time scales.

2. Study area

The Ebba Valley is located on Spitsbergen, the Svalbard archipelago's largest island. The valley is almost perpendicular to the axis of Billefjord, in its northern tip called Petunia Bay (Fig. 2). Geologically it is a very diverse region with complex sediment structures and landforms (Dallmann et al., 2004; Rachlewicz, 2009). A series of six raised marine terraces form the mouth section of the valley. The oldest terrace has been luminescence dated to 13.3 ka, and the youngest to 1.5 ka ago (van der Meij et al., 2016). The raised beaches are mainly built of sand and gravel, with some mollusc shells. Past glacial processes are recorded as glacial sediments present underneath terraces sediments layers and locally on valley slopes. The area is being shaped by fluvioglacial processes, as well as active mass movements on the surrounding mountain massifs (Kłysz et al., 1989; Karczewski et al., 1990; Pleskot, 2015).

The mean annual temperature in the Petunia Bay region is about −6.5 °C, as assessed for the period 2000–2003 (Rachlewicz and Szczuciński, 2008). Temperatures above 0 °C are usually registered between mid-May/early June and early September (Rymer and Rachlewicz, 2014). July and August are the warmest months with average temperatures of 5–6 °C. The study area is characterised by higher air temperatures during summers than the nearby meteorological station in Svalbard Lufthavn (LYR) (Rachlewicz, 2003; Rachlewicz and Styszyńska, 2007). Also, the area is characterised by stronger continentality than the southern and western parts of Svalbard (Przybylak et al., 2014).

The study area is located in a semi-arid cold desert (Brookfield, 2011) with annual precipitation less than 200 mm. Summer precipitation is usually less than 50 mm and maximum daily precipitation rarely exceeds 10 mm. Air humidity is relatively high due to close distance to the fjord. The snow cover is usually not thick (Rachlewicz, 2003; Przybylak et al., 2006; Rachlewicz and Szczuciński, 2008).

Southern and north-eastern winds are typical for the Ebba Valley region (Przybylak et al., 2006). However, maximum wind speed and strongest wind gusts are mostly observed from the east, north and northwest (Rachlewicz, 2003; Małecki, 2015).

The study area is located in the Arctic tundra zone, covered mostly with moss, lichens and discontinuous dwarf shrubs vegetation. There are six main plant community types in the Petunia Bay region: *Dryas octopetala*, *Saxifraga oppositifolia*, *Carex* – moss, *Deschampsia borealis*, *Papaver dahlianum*, *Festuca baffinensis* (Klimešová et al., 2012). The highest vegetation can be found in the western section of the Ebba Valley, i.e., close to the mouth of the Ebba River. The most common shrub species in the valley are *Salix polaris* (Buchwal et al., 2013) and

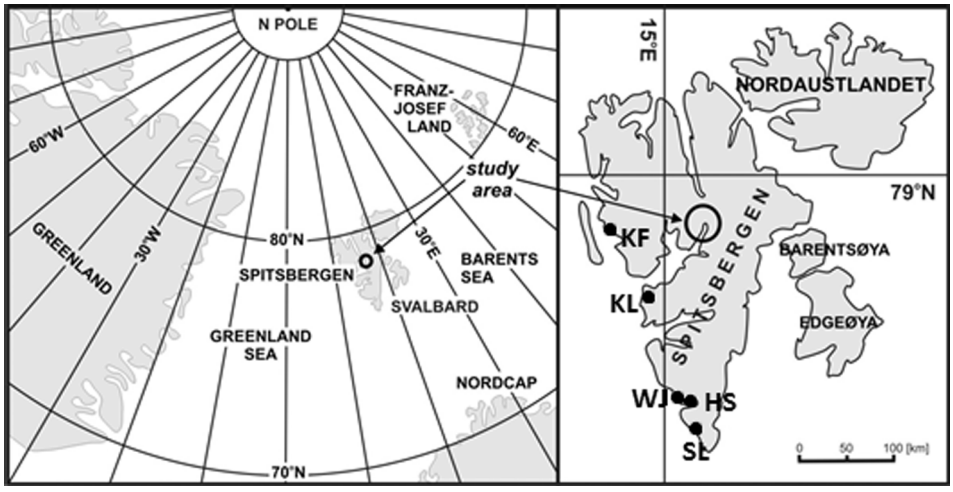

Fig. 1. The location of the study area (black arrows and circle) in the central Spitsbergen, High Arctic. Black dots mark the location of the sites where the previous aeolian studies were conducted on Svalbard (see Introduction): Kaffiøyra, Oscar II Land (KF), Kapp Linné Region (KL), Wedel Jarlsberg Land (WJ), Hornsund Fjord Region (HS), Sørkapp Land Region (SL).

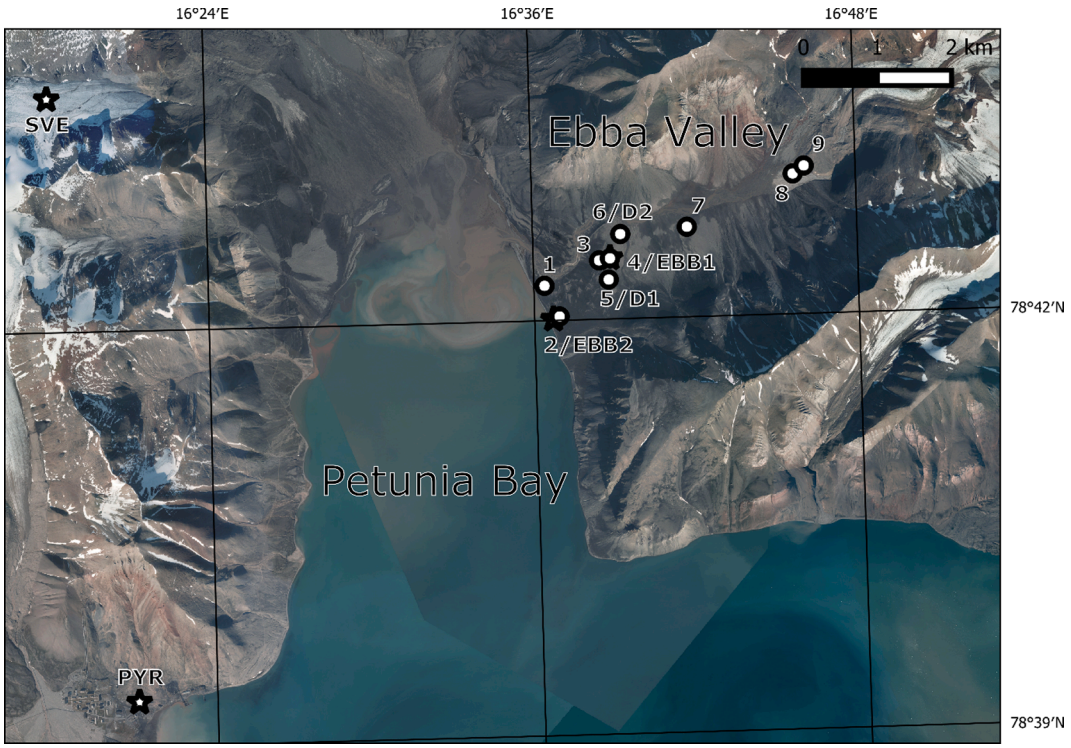

Fig. 2. Orthophotomap of the study area with nine aeolian deposition test sites (1–9) and two sediments dating sites (D1, D2) locations in the Ebba Valley. Four weather stations (EBB1, EBB2, SVE, PYR) are marked with black stars. Orthophotomap source - Norwegian Polar Institute.

Dryas octopetala (Borysiak et al., 2020).

3. Methods

3.1. Current and past aeolian deposition

Measurements of aeolian deposition were conducted across seven summer seasons. During the study any mineral material deposited in the traps, regardless of grain size, was considered as aeolian deposition. Due to logistic constraints in this remote area, the aeolian deposition measurements were performed in various time windows over the subsequent summer periods (Table 1). The longest study season was in 2015 (64 days), whereas the shortest in 2016 (44 days).

Aeolian deposition rates were obtained using modified Marble Dust Collector traps. This trap design was proposed by Ganor in 1975 (later developed by Hall and Upton, 1988) and measures vertical dust flux. It was revealed that this type of trap shows high coherence between dust collection efficiency between laboratory and field tests. However, collection effectiveness of such traps decreased gradually with decreasing particle size up to 100 μm but increased below this value. Wind speed increases were another factor reducing collection effectiveness (Hall and Upton, 1988). Goossens and Offer (2000) proved that results obtained using Marble Dust Collector traps can be used to measure aeolian sediment concentration and deposition. Two types of sedimentary traps i.e., with the diameter of 195 and 210 mm, were used. Each trap was placed directly on the ground surface. Trap rim height was 2.5 cm, which prevent the non-aeolian material (i.e., from surface runoff or rainfall splash) to be accumulated within the trap. Such trap design allowed to capture both coarser material travelling by aeolian saltation and also finer material travelling by suspension. In the period 2012–2015 the traps were filled with pre-rinsed local beach gravel sediments (with particle size > 4 mm, in order to remove finer grains). This material largely reflected the surface conditions next to the aeolian traps. From 2016, the gravel sediments in some traps were partially replaced by glass marbles to facilitate the subsequent collection of aeolian material from the traps. At the end of each sampling season (Table 1), the traps were cleaned by washing the gravel or glass marbles, together with the inside part of the trap, with filtered water. After decantation, material was dried at room temperature, and sent to a laboratory for accurate weighing. To ensure the comparability of the obtained results between different trap diameters as well across field seasons of various lengths, conversion into units expressed in $g{\cdot}m^{-2}{\cdot}day^{-1}$ was made.

Aeolian deposition was measured at nine field test sites reflecting different geomorphological and vegetation settings along the Ebba Valley axis (Fig. 2): wet (1) and dry (2) tundra sites located closest to the fjord with dense tundra vegetation; leeward (3), top (4) and windward (5) sites located at the highest marine terrace with less or sparse tundra vegetation; sandy surface (6) site covered only with individual tufts of grass; and three test sites with almost no vegetation located in the central part of the valley (7), sandur (8) and moraine (9). In total 132 sedimentary traps were collected during seven sampling seasons, i.e., with one or three traps per test site in the period 2012–2014 and 2015–2018, respectively. The number of sedimentary traps per test site was increased after field experiment conducted in 2014 showing that aeolian deposition measurements differ significantly between traps located within the same test site (placed at a distances of 1–2 m). Also,

Table 1
Time periods for aeolian deposition measurements during summer seasons 2012–2018.

Year	Start date of measurements	End date of measurements	Number of days	Number of traps per test site
2012	July 18	September 14	58	1
2013	July 18	September 5	49	1
2014	July 13	September 9	58	1
2015	July 6	September 8	64	3
2016	July 19	September 1	44	3
2017	July 22	September 17	57	3
2018	July 20	September 12	54	3

due to wild animal encounters three traps were damaged, thus were not included in the analysis, i.e., one trap from the windward, sandy surface and central part of the valley test site from the year 2012, 2015 and 2016, respectively. Further, due to unintentional human activity, measurements in 2014 at the windward test site were carried out only in the second half of the measurement season.

To calculate long-term past aeolian deposition rates, two sediment samples for OSL and seven samples for AMS ^{14}C dating were collected. Sediments for OSL dating were gathered on August 14, 2014 from pits dug in aeolian deposits, from a depth of 38 cm at site D1 (78.7N, 16.6E) and from a depth of 57 cm at site D2 (78.7N, 16.6E) (Fig. 2). All samples were taken under light-protected conditions. Sediments for AMS ^{14}C dating were collected from the excavation at site D1 on September 9, 2018 (Fig. 3): three samples from a depth of 60 cm (i.e., at a contact of the aeolian sand with an old marine terrace surface), two samples from a depth of 58 cm, one sample from a depth of 17 cm and one sample from a depth of 12 cm. At the depth of 58–60 cm the organic material used for AMS ^{14}C dating consisted of very well-preserved fragments and entire tundra shrubs leafs. In the two shallower layers, the sampled material contained more dispersed remains of organic matter.

3.2. Meteorological and soil moisture data

Most of the meteorological data were collected using ONSET HOBO devices located close to the highest marine terrace test site (EBB1, Fig. 2). Wind speed and direction (at 2 m height) were recorded at the following intervals: 5 min (in the years 2012, 1st half of 2013 and 2014) and 15 min (in the years 2016, 2017 and 2018). Unfortunately, some of the recording devices left in the area were occasionally damaged and left defective. Therefore, wind speed and direction data from the automatic weather station (recorded at one-hour intervals) located close to the dry tundra test site (EBB2, Fig. 2) were used to fill data gaps for the second half of the year 2013 (since August 5) and for year 2015. Due to sensor failure in the year 2015, wind direction recording started only on August 17.

Meteorological data obtained from other nearby automatic weather stations were used to verify data accuracy. For this purpose an automatic weather station (recording at 10-minutes interval) installed on Sven Glacier (SVE, Fig. 2) since year 2011 was used (Małecki, 2019). Moreover, daily meteorological data for Pyramiden, operating since the end of 2012, (PYR, Fig. 2) and the Longyearbyen meteorological station, located ca. 60 km south-west from the study area, were acquired via the Seklima database (Norwegian Meteorological Institute, https://seklima.met.no/).

Soil moisture data for the Ebba Valley, represented by a volumetric water content, were collected using a Decagon sensor placed at a 10 cm depth, located close to the EBB1 station. This sensor was mounted in sparse tundra vegetation and has been operating since 2012. An additional soil moisture sensor (ONSET HOBO) was placed at 5 cm depth near the EBB2 station. This sensor was positioned in dense tundra vegetation and has been operating since 2014. Air temperature and air humidity data were acquired from Decagon sensors located at a 10 cm height above the soil surface next to EBB1 (Fig. 2). Mean daily meteorological and soil moisture data were aggregated (arithmetic mean) to corresponding aeolian deposition measurement periods (Table 1).

3.3. Laboratory analyses and dating

To characterise the material deposited in the traps, grain size analysis was performed using the standard dry sieve method. For this purpose, a set of sieves with an interval of half phi was used. Due to the small amount of material found in some traps (i.e., less than 100 g) only three random traps (with the amount of the material $>$ 30 g) were used for subsequent analysis. Statistical analyses on grain size results were performed using Gradistat 9.1 software (Blott and Pye, 2001). Statistical parameter calculations were based on Folk and Ward (1957) and Folk (1954). The same approach was then used for the analysis of the sediments at the D1 dating site (samples represented sediment from different depths: 6–13 cm, 14–21 cm, 38–44 cm and below 60 cm).

OSL and radiocarbon dating methods are widely used in the geosciences and archaeology. Previous analyses of other samples taken in the year 2014 showed the usefulness of the OSL method in the dating of sandy sediments in the Ebba Valley (van der Meij et al., 2016) and in this study the same procedures were maintained. The two samples used for OSL dating (SPI-D with lab ID: NCL-2114069 and SPI-E with lab ID: NCL-2114070) were opened and prepared under subdued orange light conditions. After sieving to the 180–250 μm fraction, purified quartz-rich extracts were retrieved through mineral separation and HF etching. Blue OSL equivalent dose (D_e) measurements were performed using small aliquots (~40–70 grains) and a single aliquot regenerative dose protocol (Murray and Wintle, 2003) combined with an early background subtraction approach (Cunningham and Wallinga, 2010). The measurements were repeated on at least 96 replicates per sample to obtain meaningful D_e distributions. The Central Age Model (CAM; Galbraith et al. 1999) was applied to establish the palaeodose of each sample, which is the best estimate of the radiation dose received by the samples since burial. To calculate the burial age for the samples, the sample palaeodose was divided by the corresponding dose rate; the latter established based on the radionuclide concentrations of the sample (through gamma spectrometry) considering water attenuation effects (Aitken, 1998) and the contribution from the cosmic dose rate (Prescott and Hutton, 1994). More details on the experimental set-up, data analyses, and performance tests are provided in van der Meij et al. (2016). OSL dating was carried out at the Netherlands Centre for Luminescence

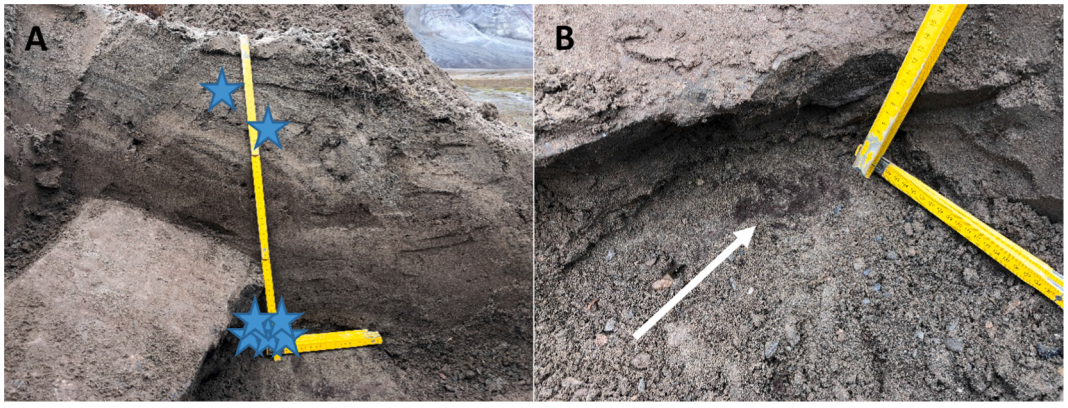

Fig. 3. Overview of A) the profile D1 from which sediments samples for AMS ^{14}C dating were acquired. Blue stars represent sampling points. B) Indication of organic material, i.e., tundra shrub leafs (white arrow), found at the depth of 60 cm.

at Wageningen University in the Netherlands.

The macrofossil organic material (i.e., tundra shrub leafs) found in the sediments was used for the AMS 14C dating. AMS ^{14}C dating was performed at the Poznań ^{14}C Laboratory. Goslar et al. (2004) showed high precision of AMS ^{14}C results obtained using a Compact Carbon AMS system installed at the Laboratory. All AMS ^{14}C ages were calibrated to calendar years using OxCal calibration software, version 4.4 (Bronk Ramsey, 2009). Calculations for the 58–60 cm samples were based on the IntCal 20 calibration curve (Reimer et al., 2013; Reimer et al., 2020). For the 12–17 cm (post-bomb) samples, a Bomb 13 NH1 calibration curve was applied (Hua et al., 2013).

3.4. Climate and aeolian deposition relationship analyses

In order to explore which climatic parameters impact aeolian deposition in the Ebba Valley, seasonal values of aeolian deposition were compared with available meteorological data. For this reason, both mean seasonal aeolian deposition for the Ebba Valley as well mean seasonal aeolian deposition for each test site were regressed against: i) air temperature, ii) air humidity (both measured at a 10 cm height from the soil surface), and iii) wind speed measured for the Ebba Valley (at 2 m height, EBB1). Each meteorological variable was represented by a seasonal mean value computed for each calendar year and study period length (Table 1). For simple linear regression at test sites level all values were standardized using a z-score. The data were checked for normality by a visual review of histograms and the Shapiro test.

3.5. Age modelling and calculation of past deposition rates

AMS ^{14}C and OSL dates were used to calculate past aeolian deposition rates. To calculate meaningful deposition rates from multimodal age distributions, several steps were taken, similar to the calculation of deposition rates in van der Meij et al. (2019). First, weighted averages of the uncalibrated ages were calculated for samples at 60 cm and 58 cm depth using the errors as weights (Maybeck, 1979). The averaged ages were calibrated using an IntCal 20 calibration curve (Reimer et al., 2020) and combined with the modern ^{14}C ages and an OSL sample SPI-D in a Bayesian deposition model in OxCal 4.4 (Bronk Ramsey, 2008; Bronk Ramsey, 2009). The deposition models in OxCal use stratigraphic positions of samples and dynamics of the deposition process to constrain age distributions and reduce the uncertainty of the ages obtained and resulting deposition rates. The Sequence-deposition model was selected, which only uses the relative stratigraphic order of the samples. OxCal also offers other, more complex, deposition models, where information on the dynamics of the deposition process can be used to further constrain the ages, but it was not possible to determine this information for the study site. Next to the age uncertainty of the samples, also the sampling depth has an uncertainty caused by the size of the samples taken. A uniform probability distribution of sample depths for a 2 cm vertical range for the AMS ^{14}C samples and 4 cm vertical range for the OSL samples was used.

The aeolian deposition rates between two samples were calculated using the age distributions resulting from the deposition model and depth distributions that represent the uncertainty of sampling depth. These data were not normally distributed, so the Markov Chain Monte Carlo approach to repeatedly sample ages from the age distributions and depths from the depth distributions was used (n = 10,000). When the sampled ages and depths were in correct chronological and stratigraphic order, these ages and depths were used to calculate deposition rates by dividing the depth difference by the age difference between two samples. This resulted in probability distributions for the deposition rates.

4. Results

4.1. Meteorological and soil moisture conditions in summer seasons 2012–2018

Mean wind speed values observed in Petunia Bay area were relatively low compared to the more open fjord system in the vicinity of Longyearbyen (Table 2, Fig. 4). The bay in the interior of the fjord is mostly surrounded by high mountain ranges which inhibit higher wind speeds. Wind speeds in the Ebba Valley were half as high as in Longyearbyen. In the years 2013, 2017 and 2018 average wind speeds in the Ebba Valley were the lowest and did not exceed 2.33 m·s^{-1}. At the same time, it is worth noting that the mean wind speed values obtained in the year 2013 and 2018 were the lowest at all four stations analysed. In contrast, in 2012, 2014 and 2015, the mean wind speeds in the Ebba Valley exceeded 3 m·s^{-1} and reached a maximum of 3.73 m·s^{-1} in the year 2012. However, data from the other stations indicated that higher wind speeds were more frequently noted in 2015, 2016 and 2017. Similar trends were observed for average wind gust speeds. This was especially noticeable when it comes to the occurrence of the weakest winds in 2018 and the strongest in 2016. Therefore, it should be considered that the most favourable winds for the aeolian activity occurred in the Ebba Valley in the summer seasons 2012, 2014, 2015 and 2016. The anemometric conditions in the years 2013, 2017 and 2018 were the least favourable for these processes. Maximum registered wind gusts in the Ebba Valley exceeded 14.9 m·s^{-1} (year 2012) and 13.1 m·s^{-1} (years 2015 and 2017, 2018).

The percentage of days with mean wind speeds higher than 5 m·s^{-1} ranged from 0% (in the year 2013) to only 18% (years 2012 and 2015). However, the percentage of days with average wind gusts above 5 m·s^{-2} ranged from 26% (in the year 2017) to 57% (year 2016). Thus, although the mean wind speed conditions were less favourable for aeolian activity, wind gusts were adequate to allowed redeposition of sediments within the valley.

The dominant wind directions for the Ebba Valley were convergent with the axis of the valley and the fjord. Therefore, most of the winds came from the north-east, north and south, and south-west. This shows that the wind conditions in the Ebba Valley are not as coherent as in the rest of the Petunia Bay region, where one main wind direction is dominant (Fig. 4).

Taking into account all weather stations, the highest air humidity was observed in 2013 and 2018. The summer season 2015 was relatively the driest, with air humidity reaching 78.8% in the Ebba Valley, 71.6% in Pyramiden and 82.1% on Sven glacier (Table 2). Also, air humidity showed a good correlation with total precipitation noted for Longyearbyen. Thus, it should be assumed that a similar precipitation amounts occurred in the Petunia Bay as in Longyearbyen. Soil moisture was the lowest in the years 2014, 2015 and 2016 and the highest in 2018, which overlaps with the lowest and the highest precipitation sums for Longyearbyen (Table 2).

The highest mean air temperature of 7.4 °C was measured in the Ebba Valley during the study season in 2015, whereas the lowest mean temperature was noted in 2012 (5.7 °C) and 2017 (5.6 °C) (Table 2).

4.2. Aeolian deposition rates in summer seasons 2012–2018

Mean aeolian deposition for the Ebba Valley equalled 5.6 g·m^{-2}·day^{-1} and was highly heterogeneous between both study seasons and test sites (Table 3). The highest mean aeolian deposition equalled 12.3 and 9.5 g·m^{-2}·day^{-1} and was observed in year 2015 and 2018, respectively. In the summer 2016 and 2017, mean aeolian deposition was the lowest and reached around 2 g·m^{-2}·day^{-1}, i.e., less than 40% of the mean aeolian deposition calculated for seven summer seasons.

At the test sites level, the highest mean aeolian deposition was found on the sandy surface and reached 74.4 g·m^{-2}·day^{-1}. At the test sites covered with dense tundra vegetation, the mean aeolian deposition did

Table 2
Selected weather and soil variables measured at the Ebba Valley (EBB1 + 2), Sven Glacier (SVE), Pyramiden (PYR) and Longyearbyen (LYR) weather stations for the summer seasons (2012–2018).

Variable	Station	2012	2013	2014	2015	2016	2017	2018	Average
		($m \cdot s^{-1}$)							
average wind speed	EBB 1 + 2	3.73	2.20	3.13	3.17	2.94	2.33	2.27	2.82
	SVE	1.88	1.68	1.73	1.90	1.91	1.79	1.69	1.80
	PYR	NA	2.02	2.37	2.23	2.43	2.48	1.75	2.21
	LYR	4.76	4.15	4.28	4.50	4.72	5.14	4.12	4.52
		(%)							
average air humidity	EBB 1	82.0	85.6	80.7	78.8	82.7	82.5	86.1	82.6
	SVE	84.9	87.0	85.6	82.1	86.0	84.8	86.4	85.3
	PYR	NA	80.7	81.5	71.6	73.5	75.0	76.7	76.5
	LYR	73.9	76.7	73.9	75.9	75.6	75.7	78.0	75.7
		($m^3 \cdot m^{-3}$)							
average soil volumetric water content	EBB1	NA	0.18	0.16	0.16	0.17	0.16	0.18	0.17
	EBB2	NA	NA	0.30	0.28	0.33	0.31	0.35	0.31
		(mm)							
total precipitation	LYR	52.1	71.2	31.8	42.7	38.0	22.2	64.9	46.1
		(°C)							
average air temperature	EBB 1	5.7	6.8	5.6	7.4	6.1	5.7	6.4	6.3
	PYR	NA	6.9	6.0	7.2	6.3	5.7	6.6	6.5
	LYR	5.8	7.0	6.2	6.5	6.4	5.9	6.6	6.3

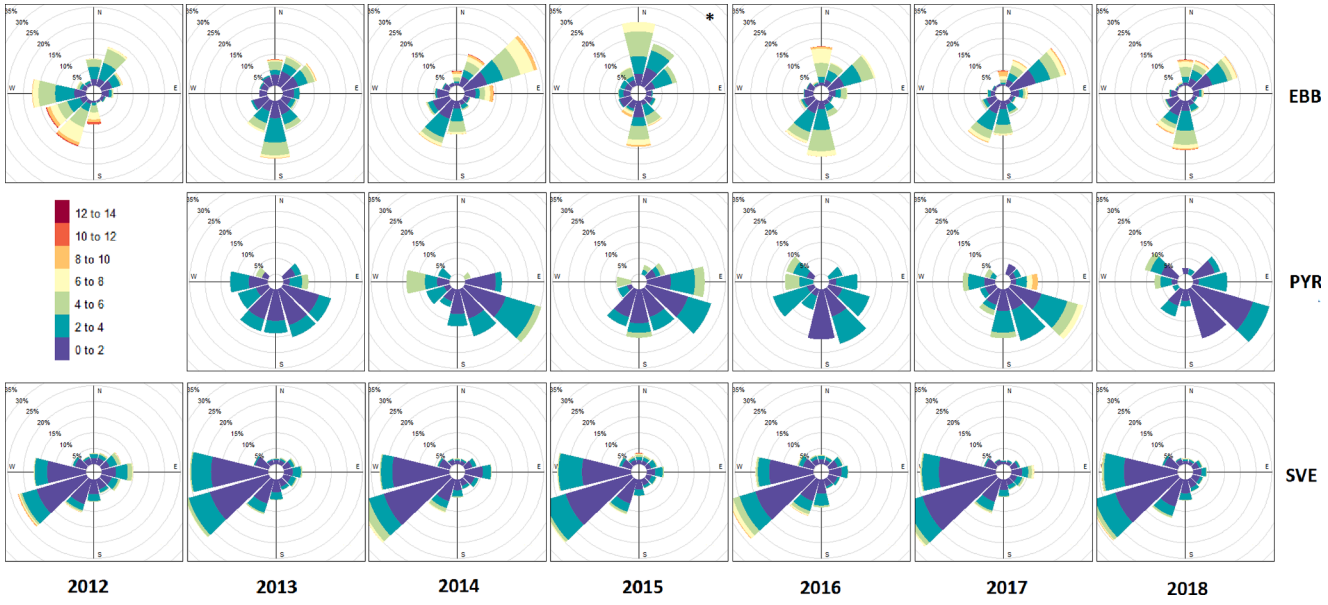

Fig. 4. Wind roses presenting absolute frequencies and directions of wind in Petunia Bay area for the summer seasons (2012–2018) measured in three meteorological stations: Ebba Valley (EBB, top row), Pyramiden (PYR, middle row) and Sven glacier (SVE, bottom row). Wind speed scale is presented in $m \cdot s^{-1}$. The 2015 chart for EBB applies only to the second half of the measurement season (i.e., from August 17).

Table 3
Mean daily aeolian deposition rates with standard deviations (italic font) calculated for nine test sites in the Ebba Valley during summer seasons (2012–2018). *) The result applies only to the second half of the summer season 2014. **) The results are based only on the mean of two traps (see section 3.1.).

Test site	2012	2013	2014	2015	2016	2017	2018	Mean
	($g \cdot m^{-2} \cdot day^{-1}$)							
Wet tundra	0.1	0.1	0.0	0.0 *(0.0)*	0.2 *(0.1)*	0.1 *(0.0)*	0.1 *(0.0)*	0.1 *(0.0)*
Dry tundra	0.0	0.1	0.0	0.1 *(0.0)*	0.1 *(0.1)*	0.2 *(0.0)*	0.1 *(0.0)*	0.1 *(0.0)*
Leeward slope	3.2	5.9	1.2	0.8 *(0.6)*	0.5 *(0.3)*	0.3 *(0.2)*	15.3 *(4.0)*	3.9 *(1.3)*
Highest marine terrace top	5.1	5.5	1.7	2.3 *(0.2)*	0.9 *(0.3)*	1.4 *(0.1)*	8.5 *(0.1)*	3.6 *(0.2)*
Windward slope	NA	9.2	20.2*	9.2 *(2.1)*	9.3 *(6.5)*	2.2 *(1.3)*	13.6 *(6.2)*	10.6 *(4.0)*
Sandy surface	9.4	17.3	8.8	74.4** *(0.3)*	3.8 *(0.6)*	7.5 *(2.5)*	39.3 *(13.1)*	22.9 *(4.1)*
Central part	2.9	7.1	2.0	16.4 *(5.6)*	2.7** *(0.2)*	3.1 *(0.9)*	7.0 *(0.5)*	5.9 *(1.8)*
Sandur	1.7	7.2	0.7	5.6 *(3.3)*	1.0 *(0.5)*	1.2 *(0.4)*	0.9 *(0.1)*	2.6 *(1.1)*
Moraine	2.1	2.8	0.5	1.6 *(0.7)*	0.8 *(0.4)*	0.6 *(0.0)*	1.0 *(0.2)*	1.4 *(0.3)*
Mean	3.1	6.1	3.9	12.3 *(1.4)*	2.1 *(1.0)*	1.8 *(0.6)*	9.5 *(2.7)*	5.6 *(1.4)*

not exceed 0.2 g·m^{-2}·day^{-1}. Overall, deposition rates exceeding 10 g·m^{-2}·day^{-1} were rare. The standard deviation (SD) values for the years 2015–2018, i.e., with three traps used per test site, were relatively high. On average, SD exceeds 25% of mean aeolian deposition, but in many cases, SD equalled up to 50% of the mean. The largest SD values were noted in 2016 (SD = 48% of the mean) and 2017 (SD = 33% of the mean). The lowest SD was obtained for 2015 (SD = 11% of the mean). Among nine test sites the largest SD was revealed for windward slope (SD = 51% of the mean) and sandur (SD = 42% of the mean) sites. The lowest SD (i.e., ca. 6% of the mean) was found for the following test sites: wet tundra, dry tundra and highest marine terrace.

4.3. Aeolian and niveo-aeolian material characteristics in the Ebba Valley

Analysis of material collected from the three aeolian deposition traps (i.e., two traps from sandy surface test sites from years 2015 and 2018; one trap from a leeward slope test site from 2018) showed that the material mainly consisted of unimodal, moderately sorted (sorting 1.664–1.901 μm) fine sands, with a mean grain size (Mz) around 157.3–223.3 μm (AD, Fig. 5). The sediments were characterised by symmetrical skewness and meso- and platykurtic kurtosis.

Characteristics and grain size composition of the sediment samples collected at D1 are shown on Fig. 5 (D1 A-D) and in Table 4. The niveo-aeolian sands were deposited on the well visible old raised marine beach sediments base. All niveo-aeolian deposits at D1 were characterised by coarse skewness and mesokurtic kurtosis. Among these sediments only the material from 14 to 21 cm depth (D1 B) layer stand out for its slightly finer grain size and better sorting.

4.4. Relationship between meteorological factors and aeolian deposition

A positive relationship between seasonal mean aeolian deposition and mean air temperature ($r^2 = 0.71$, $p = 0.017$) was found for the Ebba Valley (Fig. 6A). However, relationships between mean aeolian deposition and average air humidity (Fig. 6B) and wind speed (Fig. 6C) were not significant. Also, relationships between mean aeolian deposition and both, total precipitation values for Longyearbyen and soil moisture for the Ebba Valley, were not significant.

Table 4
Sediment characteristics for the D1 profile.

Sample ID	Depth	Mean grain size	Sorting	Skewness	Kurtosis	Sediment type
	(cm)	μm				
D1 A	6–13	169.5	1.830	0.134	1.000	unimodal moderately sorted slightly very fine gravelly fine sand
D1 B	14–21	128.6	1.556	0.144	1.032	unimodal moderately well sorted slightly very fine gravelly very fine sand
D1 C	38–44	156.7	1.806	0.166	0.947	unimodal, moderately sorted, slightly very fine gravelly fine sand
D1 D	60–65	910.2	6.689	−0.053	0.549	trimodal, very poorly sorted, sandy fine gravel

At the test sites level, the strongest relationship between aeolian deposition and air temperature was found for test sites located closer to the glacier and in the central part of the Ebba Valley (Fig. 7). Significant positive relationships between air temperature and the mean aeolian deposition rates were obtained for the central part ($p = 0.003$), sandy surface ($p = 0.022$) and sandur ($p = 0.029$).

4.5. Past aeolian deposition rates

All five AMS ^{14}C samples collected at the contact of the old marine terrace and aeolian sand cover (58–60 cm depth) were dated from the 11th to the 13th centuries with a considerable overlap in datings (Fig. 8, Table 5). The average date at 60 cm ranged from 1169 to 1260 cal CE,

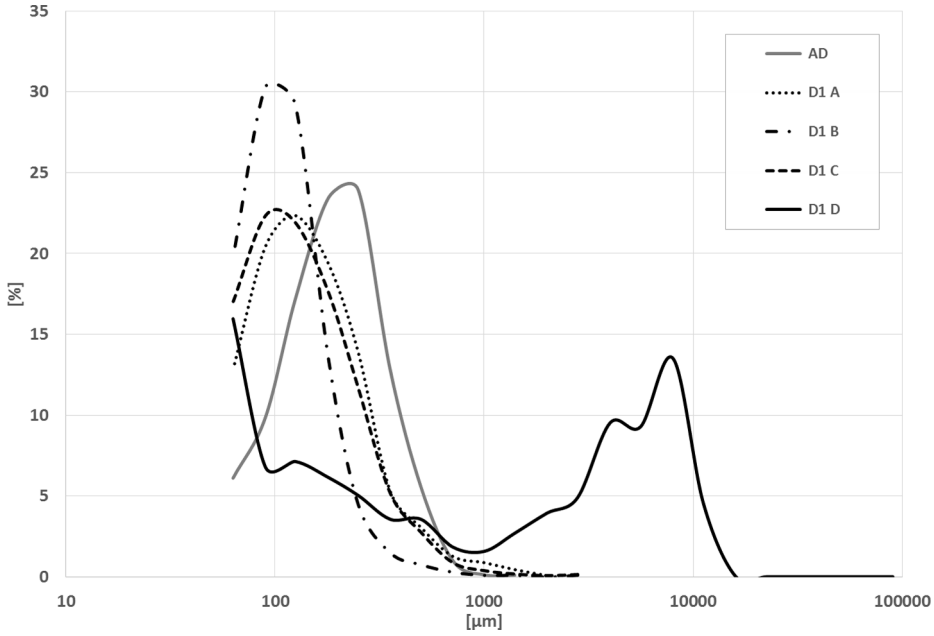

Fig. 5. Grain size distributions for the Ebba Valley sediments. AD (grey solid line) represents sediments collected from the trap located in the sandy surface test site in the year 2015. Grain size distributions for D1 (A - D) represent sediment dating profile D1 with different depths: D1 A (depth of 6–13 cm), D1 B (14–21 cm), D1 C (38–44 cm), D1 D (less than60 cm).

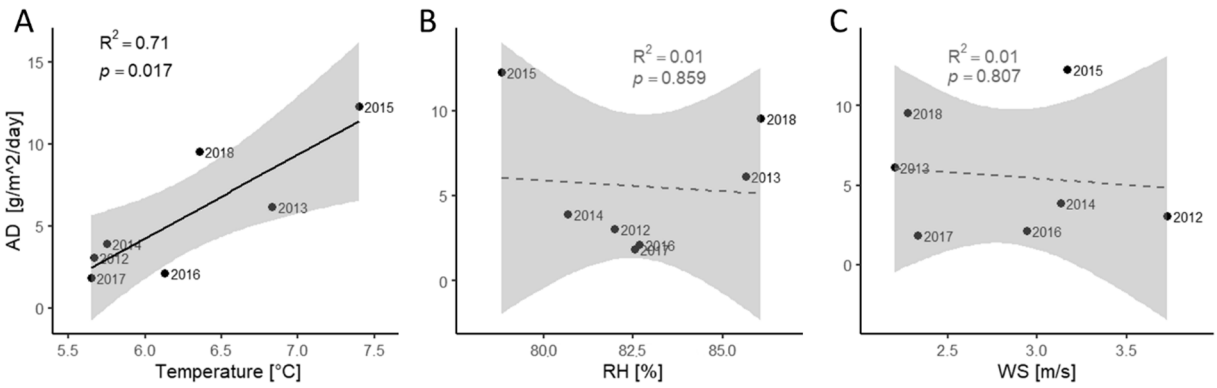

Fig. 6. Relationships between mean aeolian deposition rates (AD) in the Ebba Valley and (A) seasonal mean air temperatures measured at 0.1 m height, (B) seasonal mean air humidity measured at 0.1 m height, (C) seasonal mean wind speed in the Ebba Valley measured at height 2 m. Seasonal means for meteorological values were calculated using summer seasons lengths for each calendar year (Table 1). Grey shades represent 95% confidence levels. Grey font indicates non-significant values.

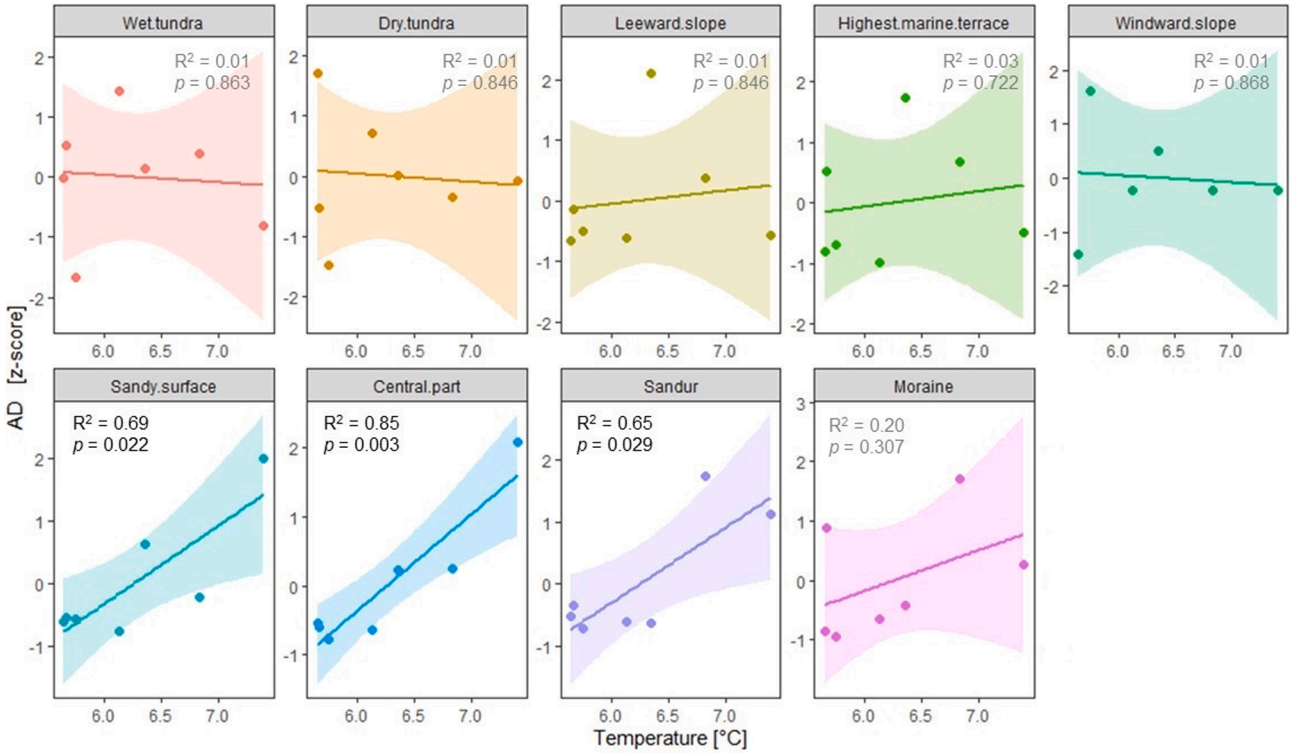

Fig. 7. Relationships between mean aeolian deposition rates (AD, scaled) acquired from nine test sites located in the Ebba Valley and seasonal mean air temperature measured at 0.1 m height (C) in the Ebba Valley (EBB1). Seasonal means for meteorological values were calculated using summer seasons lengths for each calendar year (Table 1). Shades represent 95% confidence levels. Grey font indicates non-significant values.

while the average date at 58 cm ranged from 1161 to 1264 cal CE. This indicates that aeolian deposition in this part of the study area started at the end of the Medieval Warm Period. Because of the lack of organic material in the studied aeolian sediments, an OSL date at a depth of 38 cm was included to support the chronology (Sample SPI-D, NCL-2114069, Table 6). The age of this sample was 1570 ± 40 CE. For most of this first analysed period, deposition took place under conditions of the turn between the Medieval Warm Period and Little Ice Age, which started on Svalbard in the 14th century (Svendsen and Mangerud, 1997; Mann, 2002; Grove, 2004). A second period of aeolian deposition was associated with further development and the end of the Little Ice Age. A sample taken from a depth of 17 cm was dated to 1963–1970 cal CE.

In addition, one OSL sample (SPI-E, NCL-2114070) was taken from the contact between glacial till and aeolian sands at a depth of 57 cm at the sandy surface test site (Table 6). The calculated OSL age of the sample was 1740 ± 30 CE, which coincides with the phase of the greatest development of the Little Ice Age. The calculated deposition rates since that time reached 0.20–0.25 cm·a^{-1}.

The deposition model employed in the study shows a good fit between original and modelled data, with a model agreement index of 87.8%. An index above 60% indicates a good fit (Bronk Ramsey, 1995). The model provided narrower age ranges for the AMS ^{14}C samples (Table 7). The OSL sample was unaffected by the deposition model, because there was no overlap in the chronology of this sample with samples located above and below. When age distributions of two given samples overlapped, the age distribution of the older sample moved to the older ages, and the age distribution of the younger sample moved to the younger ages – as expected and appropriate.

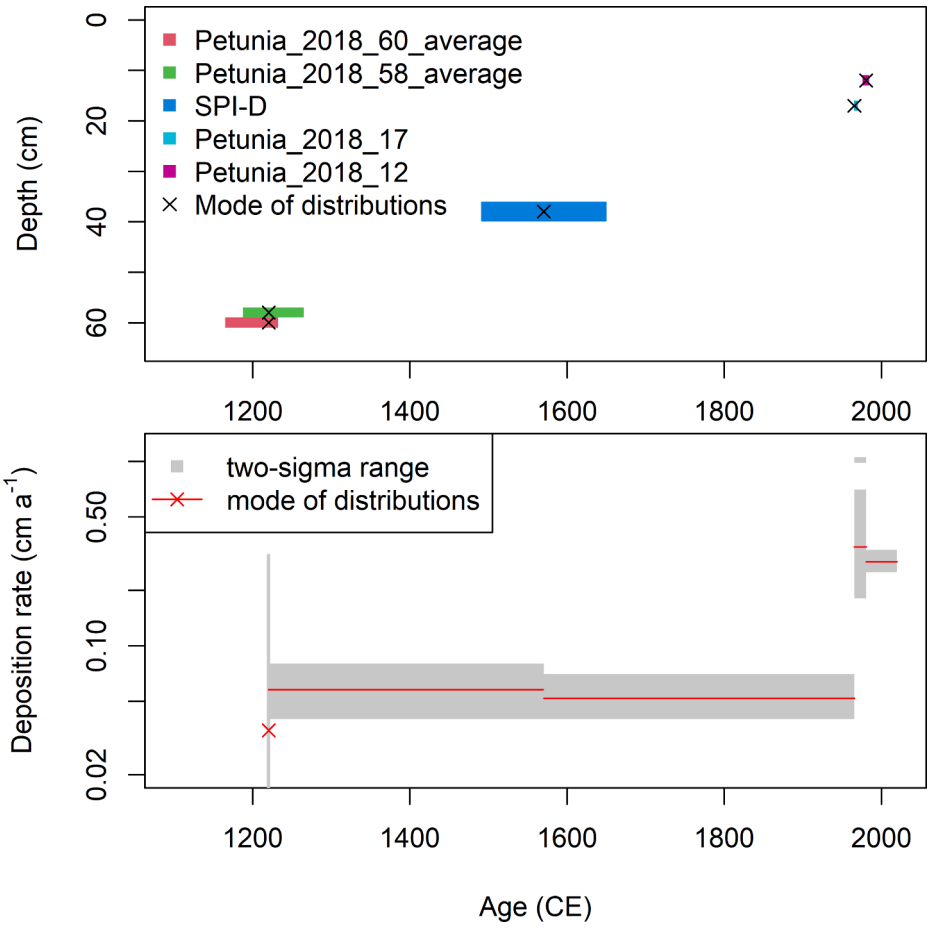

Fig. 8. Plot of age-depth distributions resulting from the deposition model (top) and distributions of deposition rate (bottom). The ranges represent two-sigma intervals for the ages, depths and rates. The crosses and red lines indicate the modes of the distributions. Note that the y-axis of the bottom graph shows a logarithmic scale.

Table 5
Dating results from the AMS ^{14}C samples taken at D1 sediment profile. The calibrated ages are provided in two sigma ranges (95.4%). The duplicate samples at 58 and 60 cm depths were aggregated to a weighted average age and error. The calibrated ages in bold were used in the subsequent age modelling (Table 7).

Laboratory code	Field code	Depth (cm)	Calibration curve	Age (uncalibrated BP, *pMC)	Age (cal CE)
Poz-111515	Petunia_2018_60_A	60	Intcal20	815 ± 30	1175–1275
Poz-111516	Petunia_2018_60_B	60	Intcal20	860 ± 30	1052–1077 & 1156–1263
Poz-111517	Petunia_2018_60_C	60	Intcal20	850 ± 30	1054–1060 & 1157–1267
	Petunia_2018_60_average	60	Intcal20	842 ± 17	**1169–1234 & 1239–1260**
Poz-111494	Petunia_2018_58_A	58	Intcal20	860 ± 30	1052–1077 & 1156–1263
Poz-111518	Petunia_2018_58_B	58	Intcal20	790 ± 60	1050–1081 & 1152–1304 & 1367–1381
	Petunia_2018_58_average	58	Intcal20	846 ± 27	**1161–1264**
Poz-111495	Petunia_2018_17	17	Bomb13NH1	159.69 ± 0.42*	**1963 & 1968–1970**
Poz-111519	Petunia_2018_12	12	Bomb13NH1	128.77 ± 0.64*	**1959 & 1961 & 1979–1980**

Table 6
OSL dating results. Note: OSL ages refer to the year of sampling and sample preparation, which was 2014 CE. SPI-D sample was taken at D1 dating site and SPI-E sample was taken at D2 dating site.

NCL Lab. code	Field code	Depth (cm)	Palaeodose (Gy)	Dose rate (Gy·ka^{-1})	OSL age (Gy)	Systematic	Random	Calendar year (CE)
NCL-2114069	SPI-D	38	1.08 ± 0.10	2.46±0.08	0.44±0.04	0.02	0.04	1570 ± 40
NCL-2114070	SPI-E	57	0.57 ± 0.05	2.14±0.08	0.27±0.03	0.01	0.02	1740 ± 30

The modelled ages were used to calculate deposition rates between two samples or between the sample Petunia_2018_12 and the soil surface (Table 7, Fig. 8). The deposition rates show an increase with time. Until around 1950 CE, rates were on the order of 0.05 cm a^{-1}. For later periods rates increased substantially to around 0.3 cm a^{-1}. The rates calculated between samples located at 60 and 58 cm of depth and between samples at 17 and 12 cm of depth showed a fairly large degree of uncertainty. This problem was caused by partly overlapping age distributions and small distance between the samples. The modes of these distributions, representing the rate with the highest probability, were at the lower end

Table 7
Results from the age modelling and calculation of deposition rates. The unmodelled ages are the same as mentioned in Table 5. The modelled ages result from the deposition model. The deposition rates were calculated between the sample of the row they are located on and the sample located above or the soil surface respectively. The ranges represent two-sigma intervals.

Sample	Method	Unmodelled age (CE)	Modelled age (CE)	Deposition rate ($cm \cdot a^{-1}$)	
				Mode	Range
Petunia_2018_60_average	AMS ^{14}C	1169–1234 & 1239–1260	1165–1233	0.04	0.00–0.32 & 0.34–0.37
Petunia_2018_58_average	AMS ^{14}C	1161–1264	1186–1266	0.06	0.04–0.08
SPI-D	OSL	1490–1650	1490–1650	0.05	0.04–0.07
Petunia_2018_17	AMS ^{14}C	1963 & 1968–1970	1962–1974	0.34	0.18–0.71 & 0.92–1.00
Petunia_2018_12	AMS ^{14}C	1959 & 1961 & 1979–1980	1973–1985	0.28	0.25–0.33

of the studied ranges.

5. Discussion

The assessment of mean aeolian deposition rates in the Ebba Valley across seven summer seasons is the first example of such comparative study conducted on aeolian activity in the High Arctic. Moreover, the study of modern aeolian deposition rates were supplemented with results on past aeolian and niveo-aeolian deposition, starting from the Medieval Warm Period. The climate and aeolian deposition analyses indicated a significant relationship between air temperature and mean aeolian deposition, which highlights a need for a relatively new approach in aeolian activity studies in the polar regions under warming climate.

5.1. Current aeolian deposition rates

To ensure comparability of individual summer seasons, the total seasonal aeolian deposition measures were converted into daily values. It should be assumed that the period of summer aeolian activity in the Ebba Valley, when transportable material is not frozen to the ground or too moist, is ca. 90 to 100 days long. Therefore, multiplication of mean daily aeolian deposition values by 100 should be appropriate to estimate mean annual values of aeolian deposition rates for the study area. This assumption is potentially highly biased and further research should determine the adequate length of aeolian activity in the Ebba Valley. However, the importance of summer seasons in aeolian deposition was also shown by sediments collected for the purpose of OSL dating: the well-bleached sand grains suggest that aeolian transport of material during polar nights in the Ebba Valley is unlikely. Accepting for the moment a 100-day summer aeolian activity, the total mean aeolian deposition can be estimated at 560 $g \cdot m^{-2}$ per year for the whole valley. This aeolian deposition value is comparable with the dust deposition results obtained for sites in Iceland (Arnalds, 2010; Bullard, 2012), but higher than those obtained for the Hornsund area in southern Spitsbergen where in mid-60 s aeolian deposition was estimated at 300 to 400 $g \cdot m^{-2}$ per year (Czeppe, 1966). The highest aeolian deposition rate of 7,440 $g \cdot m^{-2}$ per year was calculated for the sandy surface test site in 2015. This high aeolian deposition value, that relates to entire aeolian deposition including material transported through saltation and suspension, is five times higher than the ones recorded previously during dust storms on north-western Spitsbergen by Piotrowski (1983).

To some extent, the high aeolian deposition value obtained in this study may be due to the sediment trap type used, which tends to overestimate the deposition. This is primarily related to the inability to drain rainwater from the trap, causing the water to capture the material carried by ambient wind activity especially during rainy summer seasons. Moreover, the gravel material used in the traps may have provided a greater frictional force than ambient surface. Even without rainwater, the trapped material had a limited opportunity for redeposition, especially at the beginning of the season or at sites where deposition values were generally lower. Therefore, it should be noted that the obtained results estimate potentially the highest aeolian deposition rates that could be achieved under the given set of conditions. Additionally, the mean grain size of the material collected in the aeolian traps was coarser than the aeolian covers found in the valley (Fig. 5), which highlights the drawbacks of the method used (see Section 3.1). The further drawback of the sampling method may also be indicated by statistically significant positive relationship between mean seasonal aeolian deposition rates and mean soil volumetric water content obtained for the last three days of each 2012–2018 study period ($r^2 = 0.73$). However, this relationship may be coincidental and future research should aim to study aeolian deposition and weather conditions relationships at finer temporal scales (i.e., at weekly or daily basis).

The spatial variation in aeolian deposition within Ebba Valley was related to the vegetation cover. For example, local source material was not accessible where dense tundra cover occurred, i.e., particularly within the dry and wet tundra test sites. The proximity of easily available material for aeolian transport near sites appears to be an important factor. This was best observed in the sandy surface test site that has mean aeolian deposition rates four times higher than the mean for all test sites. The local nature of the source material for the aeolian processes in the Ebba Valley may also be indicated by relatively high values of SD obtained for most of the test sites. Large discrepancies in mean aeolian deposition values among the traps placed within one test site suggest high turbulence in the material displacement over short distances.

Numerous previous studies have suggested that strong winds and low humidity are the most important conditions for aeolian activity (e.g., Seppälä, 2004). Temperature, on the other hand, is practically never taken into account as an significant factor. Our results suggest greater complexity in the aeolian deposition and weather conditions relationship on-going in the periglacial environments. Aeolian transport and deposition of transported material should not be confounded. Both processes have different characteristics, and it should especially be noted that aeolian deposits can form under relatively calm wind conditions. Considering the impact of meteorological conditions on mean aeolian deposition, surprisingly, relationships with wind properties were statistically not significant. We hypothesise, that since strong winds occurred mostly from the northern and north-eastern directions, most source material on windy days was possibly carried to the fjord, and thus had low chance to be deposited in the Ebba Valley. Strong winds are more important in calculating the amount of aeolian transport than deposition. Additionally, grain size analysis of the sediments deposited in the traps suggests that most of the finer material was transported over greater distances and probably accumulated in the fjord. Unfortunately, the method applied in this study (i.e., with a single aeolian deposition measurement at the end of each study season) was not adequate to determine wind speed thresholds for efficient material deposition in the Ebba Valley. In contrast to wind, mean aeolian deposition was significantly related to air temperature. This strong relationship obtained in our study seems to contradict the experimental findings that have shown that the wind's ability to carry more material is greater at lower air temperatures (McKenna Neuman, 2004). This may be because on Spitsbergen, air temperature differences between individual summer seasons were on a much smaller range than during the

laboratory experiments (McKenna Neuman, 2004). Therefore, temperature differences may not have had a significant impact on air density. However, higher temperatures had a significant effect on Ebba glacier regime and its melting. This, in turn, resulted in higher discharge of the Ebba river carrying large amounts of sediments, especially in the first part of the summer season during which the snow cover was melting. Later in the season, when river flow is low, this material has a chance to be deposited on the riverbanks, from which it can be incorporated into aeolian activity within the Ebba Valley. In fact, the strongest positive relationships between mean aeolian deposition and air temperature occurred in test sites located close to the river and especially in its upper part. Thus, we infer this strong positive relationship between air temperature and aeolian deposition as rather an indirect relationship. Moreover, higher air temperatures increase evaporation and dryness of the surface sediments that further can be effectively incorporated into aeolian processes within the valley. In densely vegetated parts of the valley, this dependence was weaker or absent, which suggests that presence of vegetation clearly limits the accessibility of source material. Relationship between glaciofluvial and aeolian activity was previously discussed by Bullard and Austin (2011) and Dijkmans and Tørnqvist (1991) and led to similar conclusions. Crusius et al. (2011) indicated that exposure of river sediments and favourable wind directions may be more important in aeolian activity than air humidity, which may further explain the lack of statistically significant dependences between mean aeolian deposition and air humidity in the study area.

The significant positive relationship revealed in this study between air temperature and mean aeolian deposition has the potential to expand our understanding of linkages between climate and aeolian processes, and hence our understanding of periglacial valley responses to climate change. This is of particular importance in the light of currently observed temperature increases and projected warming of the Arctic (IPCC, 2021). Long-term observations in Greenland have shown already an intensification of dust events (Saros et al., 2019). Therefore, future studies should not overlook the interactions between sediment supply, availability and aeolian deposition in the High Arctic. Especially, since these processes are extremely important for soil cover formation (van der Meij et al., 2016), and further, for plant succession and tundra habitat formation in periglacial conditions (Borysiak et al., 2020). The supply of fresh aeolian material is also important for albedo and glacier mass balance (Bergstrom et al., 2020).

5.2. Past aeolian deposition rates

The uncertainty of long-term aeolian deposition rates depends on the uncertainty of the chronology used to calculate the rates. Bayesian age models are a suitable tool to assess and constrain the uncertainty of the chronology and the resulting deposition rates (Bronk Ramsey, 2008; Trachsel and Telford, 2017; van der Meij et al., 2019). The applied deposition model combined datings from different methods and helped to constrain the distributions of AMS ^{14}C ages. Nonetheless, the uncertainty of rates calculated with these ages was still quite high due to the partly overlapping chronologies (Table 7, Fig. 8). The uncertainty of these rates was further reduced by only considering the deposition rates from ages sampled using the Markov Chain Monte Carlo approach that were found in the correct chronologic and stratigraphic order, which prevented the calculation of negative rates. Leaving out negative rates caused a minor positive bias in the average rates for partly overlapping samples, but provided a more realistic representation of deposition rates, where both the uncertainty of the given age and sampling depth are considered.

The modelled deposition dates (1165–1233 CE) indicate the possibility that the beginning of the formation of niveo-aeolian covers in the study area occurred several dozen years earlier than in Greenland (1220–1280 cal AD) (Christiansen, 1998). This initiation was coeval with the end of the Medieval Warm Period and the advance of glaciers on Spitsbergen (Rachlewicz et al., 2007; Farnsworth et al., 2020), as well as the cooling of the climate (with an air temperature reduction at least 0.6–2.0°C) (Martín-Moreno and Allende-Álvarez, 2016). The Little Ice Age lasted on Svalbard from the 14th to the 19th centuries. However, Humlum et al. (2005) found that significant growth of some of Spitsbergen's glaciers had started already>1100 calibrated years BP. Christiansen (1998) suggested that on Greenland the start of the accumulation was connected with increased nivation activity. Greenland settings showed also increased deposition in the period 1500/1580–1690 CE with the highest niveo-aeolian sedimentation ranging from 0.26 to 0.63 cm per year. The analyses of aeolian activity for Western Greenland carried out on a larger time scales showed, inter alia, the intensification of aeolian deposition after 550 cal yr BP, what was associated with local changes in proglacial floodplain development (Willemse et al., 2003). Results obtained for the Ebba Valley demonstrate rather constant and slow deposition rates for the entire Little Ice Age until the modern times, with values around 0.05 cm per year. This may indicate only a small amount of source material available in the valley as well as minor snow accumulation or topographically unfavorable conditions for nivation. Data obtained by D'Andrea et al. (2012) suggest somewhat higher winter snow precipitation in the LIA period. The same study indicates that summer temperatures on Svalbard reached their lowest values (2 °C) in the 10th century and between the years 1100 and 1300 CE. After the year 1600 CE the temperature began to rise. Especially warm summers were reported for the period 1750–1780 CE (D'Andrea et al., 2012), which could have influenced the beginning of the formation of aeolian covers in the Ebba Valley (1740 ± 30 CE, compare with dating results for site D2). This may also be related to contemporary observations of aeolian deposition indicating a significant impact of higher air temperatures for material accumulation.

Both niveo-aeolian deposition rates and the emergence of aeolian landforms seem to suggest the high importance of source material availability in the studied valley. The greatest importance may be attached here to the noted increase in air temperature, which is especially important, particularly in light of on-going and projected climate change in the High Arctic, that might increase both intensity and efficiency of aeolian processes in the periglacial ecosystems.

5.3. Comparison of the contemporary and past aeolian deposition rates

Our estimates on past and contemporary aeolian deposition were calculated with the assumption that 1 m^3 of sand weighs 1,520 kg. The mean aeolian deposition rate of 560 $g \cdot m^{-2}$ per summer season observed in the years 2012–2018 for the Ebba Valley should therefore accumulate a 0.04 cm thick layer of aeolian material, which is comparable with the lowest niveo-aeolian deposition values recorded in the past for the study area. Our results for the mean aeolian deposition in the windward slope test site, which was located at the same location as the D1 dating site yielded potentially a deposition rate of 0.07 cm per summer season, which is significantly lower than the deposition values calculated for the past 60–40 years via AMS ^{14}C dating (i.e., 0.3 cm per year). It should be remembered, however, that this sand cover was to a greater extent affected by the niveo-aeolian activity through its specific geomorphic setting and close proximity to the slope. Comparable results were obtained in the sandy surface test site where the D2 dating site was located. Estimated past deposition values of 0.20–0.25 cm per year were still higher than the contemporary mean aeolian deposition rates (i.e., 0.15 cm per summer season). However extreme values calculated for the sandy surface site in 2015 with 74.4 $g \cdot m^{-2}$ per summer season would yield a 0.49 cm layer of material during the summer, which is twice as high as past deposition rates estimated for this location.

6. Conclusions

Quantification of aeolian processes in High Arctic is rarely carried out across multiple years. We believe that our results of summer aeolian deposition rates obtained for seven study periods, supplemented by past

aeolian and niveo-aeolian deposition rates estimation, will provide a valuable contribution to the current knowledge on periglacial geo-ecosystem functioning and its temporal changes. Specifically, it was possible to estimate that mean aeolian deposition in the Ebba Valley equals 5.6 $g{\cdot}m^{-2}{\cdot}day^{-1}$, thus the valley can be covered with ca. 500–600 $g{\cdot}m^{-2}$ of aeolian material every year. The amount of mean aeolian deposition was positively related to air temperature and was higher at the test sites located close to glacifluvial source material. Also, it was showed that mean aeolian deposition might be locally limited by the presence of vegetation cover. Contemporary aeolian processes in this part of central Spitsbergen seem to incorporate rather local material deposited in the valley by glaciofluvial streams. Material transported over long distances is likely to be deposited in Petunia Bay waters, and should be quantified in the future. Also, future studies should aim to estimate total annual rates of aeolian deposition, in relation to both air temperature and soil moisture. Wind properties should also be incorporated in such studies, especially when daily and weekly aeolian deposition rates are estimated.

Modelled past niveo-aeolian and aeolian rates noted since the 11th century showed that ongoing climate change, especially warming, impacts aeolian activity. The increase in aeolian deposition rates ranging from 0.05 to 0.3 cm per year since the beginning of the 1960s is a significant indicator of an environmental change, taking place in the study area. We might expect, that further increase in air temperature projected for the Arctic might increase future aeolian deposition rates. This will have a significant effect on the functioning and succession of vegetation cover, changes in glacier albedo, supply of fine sediment to the fjord system, as well as the life of people and animals in general.

Data availability

The data that support the findings of this study are available from the corresponding author upon request.

CRediT authorship contribution statement

Krzysztof G. Rymer: Conceptualization, Formal analysis, Funding acquisition, Investigation, Methodology, Writing – original draft, Writing – review & editing. **Grzegorz Rachlewicz:** Investigation, Supervision, Writing – review & editing. **Agata Buchwal:** Formal analysis, Writing – review & editing. **Arnaud J.A.M. Temme:** Investigation, Writing – review & editing. **Tony Reimann:** Investigation, Writing – review & editing. **W. Marijn van der Meij:** Formal analysis, Methodology, Writing – review & editing.

Declaration of Competing Interest

The authors declare that they have no known competing financial interests or personal relationships that could have appeared to influence the work reported in this paper.

Acknowledgments

The study was completed at AMUPS and was funded by the National Science Centre (Grant No. 2014/15/N/ST10/00825). Our research benefits from a long-term effort, therefore, we would like to thank all members of AMUPS expeditions involved in logistics and fieldwork on Svalbard in the years 2012-2018, with special thanks to T. Kurczaba. AMS ^{14}C dates were calibrated using OxCal software, version 4.4 (Bronk Ramsey, 2009). We would also like to thank Gerard Heuvelink for his help with calculations of multimodal age distributions of calibrated ^{14}C ages. Sieve data were analysed using Gradistat 9.1 software developed by Simon Blott at the University of London. In particular, we wish to acknowledge J. Małecki for sharing his Sven glacier meteorological data (Project funded by the National Science Centre, Grant No. N N306 062940). Weather data for both Pyramiden and Longyearbyen were obtained from the Seklima database run by the Norwegian Meteorological Institute. An orthophotomap was shared by the Norwegian Polar Institute (TopoSvalbard WMTS service). The participation of G. Rachlewicz in fieldwork was financed by the National Science Centre (Grant No. 2011/03/B/ST10/06172). We gratefully thank the two anonymous reviewers for their valuable comments.

Appendix A. Supplementary data

Supplementary data to this article can be found online at https://doi.org/10.1016/j.catena.2021.105974.

References

Aitken, M.J., 1998. An introduction to optical dating: the dating of Quaternary sediments by the use of photon-stimulated luminescence. Oxford University Press, Oxford, p. 280.

Åkerman, J., 1980. Studies on periglacial geomorphology in West Spitsbergen (PhD. thesis). Lunds Universitets Geografiska Inst. Ser. Avh. LXXXIX, 297 pp.

Åkerman, J., 1983. Notes concerning the vegetation on deflation surfaces, Knapp Linné, Spitsbergen. Polar Research 1, 161–169.

Arnalds, O., 2010. Dust sources and deposition of aeolian materials in Iceland. Icelandic Agricultural Sciences 23, 3–21.

Baranowski, S., Pękala, K., 1982. Nival-eolian processes in the tundra area in the nunatak zone of the Hans and Werenskiold Glaciers (SW Spitsbergen). Results of investigations of the Polish Scientific Spitsbergen Expeditions, 4. Acta Universitatis Wratislaviensis 525, 11–27.

Bateman, M.D., 2013. Aeolian processes in periglacial environments. In: Shroder, J. (Editor in Chief), Giardino, R., Harbor, J. (Eds.), Treatise on Geomorphology. Academic Press, San Diego, vol. 8, Glacial and Periglacial Geomorphology, pp. 416–429.

Bergstrom, A., Gooseff, M., Myers, M., Doran, P.T., The seasonal evolution of albedo across glaciers and the surrounding landscape of the Taylor Valley, Antarctica. The Cryosphere, 14, 769–788 (doi: 10.5194/tc-14-769-2020).

Beylich, A.A., Dickson, J.C., Zwoliński, Z., 2016. Source-To-Sink Fluxes in Undisturbed Cold Environments. Cambridge Univ, Press, p. 419.

Blott, S.J., Pye, K., 2001. GRADISTAT: A grain size distribution and statistics package for the analysis of unconsolidated sediments. Earth Surface Processes and Landforms 26 (11), 1237–1248. https://doi.org/10.1002/esp.261.

Borysiak, J., Pleskot, K., Rachlewicz, G., 2020. Dryas aeolian landforms in Arctic deflationary tundra, central Spitsbergen. Polish Polar Research 41 (1), 41–68. https://doi.org/10.24425/ppr.2020.132569.

Bronk Ramsey, C., 1995. Radiocarbon calibration and analysis of stratigraphy: the OxCal program. Radiocarbon 37, 425–430. https://doi.org/10.2458/rc.v37i2.1690.

Bronk Ramsey, C., 2008. Deposition models for chronological records. Quaternary Science Reviews 27 (1–2), 42–60. https://doi.org/10.1016/j.quascirev.2007.01.019.

Bronk Ramsey, C., 2009. Bayesian analysis of radiocarbon dates. Radiocarbon 51 (1), 337–360. https://doi.org/10.1017/S0033822200033865.

Brookfield, M.E., 2011. Aeolian processes and features in cool climates. In: Martini, I.P, French, H.M., Pérez Alberti, A. (Eds.), Ice-marginal and Periglacial Processes and Sediments, Geological Society, London, 241–258 (doi:10.1144/SP354.16).

Buchwal, A., Rachlewicz, G., Fonti, P., Cherubini, P., Gärtner, H., 2013. Temperature modulates intra-plant growth of Salix Polaris from a high Arctic site (Svalbard). Polar Biology 36 (9), 1305–1318. https://doi.org/10.1007/s00300-013-1349-x.

Bullard, J.E., 2012. Contemporary glacigenic inputs to the dust cycle. Earth Surface Processes and Landforms 38, 71–89. https://doi.org/10.1002/esp.3315.

Bullard, J.E., Austin, M.J., 2011. Dust generation on a proglacial floodplain, West Greenland. Aeolian Research 3, 43–54. https://doi.org/10.1016/j.aeolia.2011.01.002.

Christiansen, H.H., 1998. "Little Ice Age" nivation activity in northeast Greenland. The Holocene 8 (6), 719–728. https://doi.org/10.1191/095968398666994797.

Crusius, J., Schroth, A.W., Gassó, S., Moy, C.M., Levy, R.C., Gatica, M., 2011. Glacial flour dust storms in the Gulf of Alaska: hydrologic and meteorological controls and their importance as a source of bioavailable iron. Geophysical Research Letters 38, L06602. https://doi.org/10.1029/2010GL046573.

Cunningham, A.C., Wallinga, J., 2010. Selection of integration time intervals for quartz OSL decay curves. Quaternary Geochronology 5, 657–666. https://doi.org/10.1016/j.quageo.2010.08.004.

Czeppe, Z., 1966. Przebieg głównych procesów morfogenetycznych w południowozachodnim Spitsbergenie. Zeszyty Naukowe UJ, Prace Geograficzne 13, 96–102 in Polish.

Czeppe, Z., 1968. The annual rhythm of morphogenetic processes in Spitsbergen. Geographia Polonica 14, 57–65.

D'Andrea, W.J., Vaillencourt, D.A., Balascio, N.L., Werner, A., Roof, S.R., Retelle, M., Bradley, R.S., 2012. Mild Little Ice Age and unprecedented recent warmth in an 1800 year lake sediment record from Svalbard. Geology 40 (11), 1007–1010. https://doi.org/10.1130/G33365.1.

Dahlke, S., Hughes, N.E., Wagner, P.M., Gerland, S., Wawrzyniak, T., Ivanov, B., Maturilli, M., 2020. The observed recent surface air temperature development across Svalbard and concurring footprints in local sea ice cover. International Journal of Climatology 40, 5246–5265. https://doi.org/10.1002/joc.6517.

Dallmann, W.K., Pipejohn, K., Blomeier, D., 2004. Geological Map of Billefjorden, Central Spitsbergen, Svalbard with geological excursion guide 1:50 000. Norsk Polarinstitutt Tematkart 36.

Dijkmans, J.W.A., Tørnqvist, T.E., 1991. Modern periglacial eolian deposits and landforms in the Søndre Strømfjord area, West Greenland and their palaeoenvironmental implications. Meddelelser om Grønland, Geoscience 25, 3–39.
Farnsworth, W.R., Allaart, L., Ingólfsson, Ó., Alexanderson, H., Forwick, M., Noormets, R., Retelle, M., Schomacker, A., 2020. Holocene glacial history of Svalbard: Status, perspectives and challenges. Earth-Science Reviews 208, 103249. https://doi.org/10.1016/j.earscirev.2020.103249.
Folk, R.L., 1954. The distinction between grain size and mineral composition in sedimentary-rock nomenclature. Journal of Geology 62, 344–359.
Folk, R.L., Ward, W.C., 1957. Brazos River bar: a study in the significance of grain size parameters. Journal of Sedimentary Petrology 27, 3–26.
Galbraith, R.F., Roberts, R.G., Laslett, G.M., Yoshida, H., Olley, J.M., 1999. Optical dating of single and multiple grains of quartz from Jinmium rock shelter, northern Australia: part I, experimental design and statistical models. Archaeometry 41, 339–364. https://doi.org/10.1111/j.1475-4754.1999.tb00987.x.
Gębica, P., Szczęsny, R., 1988. Symptoms of aeolian accumulation in western Sorkapp Land. Spitsbergen. Polish Polar Research 9 (4), 447–460.
Goossens, D., Offer, Z.Y., 2000. Wind tunnel and field calibration of six aeolian dust samplers. Atmospheric Environment 34, 1043–1057. https://doi.org/10.1016/S1352-2310(99)00376-3.
Goslar, T., Czernik, J., Goslar, E., 2004. Low-energy 14C AMS in Poznan radiocarbon Laboratory, Poland. Nuclear Instruments and Methods in Physics Research Section B: Beam Interactions with Materials and Atoms 223–224, 5–11. https://doi.org/10.1016/j.nimb.2004.04.005.
Grove, J.M., 2004. Little Ice Ages: Ancient and Modern, (2 volumes). Routledge, London, 718 pp.
Hall, D.J., Upton, S.L., 1988. A wind tunnel study of the particle collection efficiency of an inverted Frisbee used as a dust deposition gauge. Atmospheric Environment 22 (7), 1383–1394. https://doi.org/10.1016/0004-6981(88)90163-1.
Hua, Q., Barbetti, M., Rakowski, A.J., 2013. Atmospheric Radiocarbon for the Period 1950–2010. Radiocarbon 55 (4), 2059–2072. https://doi.org/10.2458/azu_js_rc.v55i2.16177.
Humlum, O., Elberling, B., Hormes, A., Fjordheim, K., Hansen, O.H., Heinemeier, J., 2005. Late-Holocene glacier growth in Svalbard, documented by subglacial relict vegetation and living soil microbes. The Holocene 15 (3), 396–407. https://doi.org/10.1191/0959683605hl817rp.
Ipcc, 2021. Summary for Policymakers. In: Masson-Delmotte, V., Zhai, P., Pirani, A., Connors, S.L., Péan, C., Berger, S., Caud, N., Chen, Y., Goldfarb, L., Gomis, M.I., Huang, M., Leitzell, K., Lonnoy, E., Matthews, J.B.R., Maycock, T.K., Waterfield, T., Yelekçi, O., Yu, R., Zhou, B. (Eds.), Climate Change 2021: The Physical Science Basis. Contribution of Working Group I to the Sixth Assessment Report of the Intergovernmental Panel on Climate Change. Cambridge University Press. In Press.
Ivanov, B.V., Prokhorova, U.V., Sviashchennikov, P.N., 2020. Analysis of continentality and anomality of Svalbard climate according to observations of surface air temperature in the second half of the XX century. IOP Conf. Series: Earth and Environmental Science, 606, 012021 (doi:10.1088/1755-1315/606/1/012021).
Karczewski, A. (ed.), Borówka, M., Gonera, P., Kasprzak, L., Kłysz, P., Kostrzewski, A., Lindner, L., Marks, L., Rygielski, W., Stankowski, W., Wojciechowski, A., Wysokiński, L., 1990. Petuniabukta, Billefjorden, Spitsbergen. Geomorphology. 1 : 40 000. Adam Mickiewicz University, Poznań.
Kavan, J., Láska, K., Nawrot, A., Wawrzyniak, T., 2020. High Latitude Dust Transport Altitude Pattern Revealed from Deposition on Snow. Svalbard. Atmosphere 11, 1318. https://doi.org/10.3390/atmos11121318.
Kida, J., 1981. Badania procesów i form eolicznych na Ziemi Wedel-Jarlsberga (Spitsbergen). In: VII Sympozjum Polarne w Sosnowcu, Materiały cz. II, IG UŚl., Katowice, 36-37 (in Polish).
Kida, J., 1986. Eolian Processes in the Werenskiold, Nann and Torell glacier forefields (Wedel-Jarlsberg Land, SW Spitsbergen). Results of Investigation of the Polish Scientific Spitsbergen Expeditions, 6. Acta Universitatis Wratislaviensis 966, 25–43.
Kida, J., 1995. Procesy eoliczne na wybrzeżach SW Spitsbergenu. In: Pereyma, J., Piasecki, J., XXII Sympozjum Polarne, Wrocław – Książ, 27-28 października 1995, 41-47 (in Polish).
Klimešová, J., Doležal, J., Prach, K., Košnar, J., 2012. Clonal growth forms in Arctic plants and their habitat preferences: a study from Petuniabukta, Spitsbergen. Polish Polar Research 33, 421–442. https://doi.org/10.2478/v10183−012−0019−y.
Kłysz, P., Lindner, L., Marks, L., Wysokiński, L., 1989. Late Pleistocene and Holocene relief remodeling in the Ebbadalen-Nordenskiöldbreen region in Olav V Land, central Spitsbergen. Polish Polar Research 10 (3), 277–301.
Maher, B.A., 2011. The magnetic properties of Quaternary aeolian dusts and sediments, and their palaeoclimatic significance. Aeolian Research 3 (2), 87–144. https://doi.org/10.1016/j.aeolia.2011.01.005.
Małecki, J., 2015. Glacio–meteorology of Ebbabreen, Dickson Land, central Svalbard, during 2008–2010 melt seasons. Polish Polar Research 36, 145–161.
Małecki, J., 2019. Meteorology and summer net radiation of an Arctic alpine glacier: Svenbreen. Svalbard. International Journal of Meteorology 39 (10), 4107–4124. https://doi.org/10.1002/joc.6062.
Mann, M., 2002. Little Ice Age. In: McCracken, M.C., Perry, J.S. (Eds.), The Earth system: physical and chemical dimensions of global environmental change. Encyclopedia of Global Environmental Change, 504-509.
Martín-Moreno, R., Allende-Álvarez, F., 2016. Little Ice Age glacier extension and retreat in Spitsbergen Island (High Arctic, Svalbard Archipelago). Cuadernos de Investigación Geográfica 42, 383–398. https://doi.org/10.18172/cig.2919.
Maybeck, P., 1979. Stochastic models, estimation and control. Academic Press, New York.
McKenna Neuman, C., 1993. A review of aeolian transport processes in cold environments. Progress in Physical Geography 17 (2), 137–155. https://doi.org/10.1177/030913339301700203.
McKenna Neuman, C., 2004. Effects of temperature and humidity upon the transport of sedimentary particles by wind. Sedimentology 51, 1–17. https://doi.org/10.1046/j.1365-3091.2003.00604.x.
Migała, K., Sobik, M., 1984. Deflation and nival eolian phenomena observed under conditions of congelation in the forefield of the Werenskiold Glacier (SW Spitsbergen). Zeitschrift fur Gletscherkunde und Glazialgeologie 20, 197–206.
Murray, A.S., Wintle, A.G., 2003. The single aliquot regenerative dose protocol: potential for improvements in reliability. Radiation Measurements 37, 377–381. https://doi.org/10.1016/S1350-4487(03)00053-2.
Pękala, K., 1980. Morphogenetic processes and cover deposits of nunataks in the Hornsund area (SW Spitsbergen). Polish Polar Research 1 (2–3), 9–44.
Piotrowski, A., 1983. Results of investigations over a magnitude of aeolian transport in the western part of Oscar II Land (NW Spitsbergen) during summer 1979. Acta Universitatis Nicolai Copernici, Geografia, XVII 56, 63–67.
Pleskot, K., 2015. Sedimentological characteristics of debris flow deposits within ice−cored moraine of Ebbabreen, central Spitsbergen. Polish Polar Research 36 (2), 125–144. https://doi.org/10.1515/popore−2015−0006.
Prescott, J.R., Hutton, J.T., 1994. Cosmic ray contributions to dose rates for luminescence and ESR dating: large depths and long-term time variations. Radiation Measurements 23, 497–500. https://doi.org/10.1016/1350-4487(94)90086-8.
Przybylak, R., Araźny, A., Gluza, A., Hojan, M., Migała, K., Sikora, S., Siwek, K., Zwoliński, Z., 2006. Porównanie warunków meteorologicznych na zachodnim wybrzeżu Spitsbergenu w sezonie letnim 2005 r. Problemy Klimatologii Polarnej 16, 125–138 in Polish.
Przybylak, R., Araźny, A., Nordli, Ø., Finkelnburg, R., Kejna, M., Budzik, T., Migała, K., Sikora, S., Puczko, D., Rymer, K., Rachlewicz, G., 2014. Spatial distribution of air temperature on Svalbard during 1 year with campaign measurements. International Journal of Climatology 34, 3702–3719. https://doi.org/10.1002/joc.3937.
Rachlewicz, G., 2003. Warunki meteorologiczne w Zatoce Petunia (Spitsbergen środkowy) w sezonach letnich 2000 i 2001. Problemy Klimatologii Polarnej 13, 127–138 in Polish.
Rachlewicz, G., 2009. Contemporary sediment fluxes and relief changes in high Arctic glacierized valley systems (Billefjorden, Central Spitsbergen). Wydawnictwo Naukowe UAM, Poznań.
Rachlewicz, G., Styszyńska, 2007. Porównanie przebiegu temperatury powietrza w Petuniabukta i Svalbard-Lufthavn (Isfjord, Spitsbergen) w latach 2001-2003. Problemy Klimatologii Polarnej, 17, 121-134 (in Polish).
Rachlewicz, G., Szczuciński, E., M.,, 2007. Post-"Little Ice Age" retreat rates of glaciers around Billefjorden in central Spitsbergen, Svalbard. Polish Polar Research 28, 159–186.
Rachlewicz, G., Szczuciński, W., 2008. Changes in thermal structure of permafrost active layer in a dry polar climate, Petuniabukta, Svalbard. Polish Polar Research 29, 261–278.
Reimer, P.J., Bard, E., Bayliss, A., Beck, J.W., Blackwell, P.G., Bronk Ramsey, C., Grootes, P.M., Guilderson, T.P., Haflidason, H., Hajdas, I., Hatt'e, C., Heaton, T.J., Hoffmann, D.L., Hogg, A.G., Hughen, K.A., Kaiser, K.F., Kromer, B., Manning, S.W., Niu, M., Reimer, R.W., Richards, D.A., Scott, E.M., Southon, J.R., Staff, R.A., Turney, C.S.M., van der Plicht, J., 2013. IntCal13 and Marine13 Radiocarbon Age Calibration Curves 0–50,000 Years cal BP. Radiocarbon 55 (4), 1869–1887. https://doi.org/10.2458/azu_js_rc.55.16947.
Reimer, P., Austin, W., Bard, E., Bayliss, A., Blackwell, P., Bronk Ramsey, C., Butzin, M., Cheng, H., Edwards, R., Friedrich, M., Grootes, P., Guilderson, T., Hajdas, I., Heaton, T., Hogg, A., Hughen, K., Kromer, B., Manning, S., Muscheler, R., Palmer, J., Pearson, C., van der Plicht, J., Reimer, R., Richards, D., Scott, E., Southon, J., Turney, C., Wacker, L., Adolphi, F., Büntgen, U., Capano, M., Fahrni, S., Fogtmann-Schulz, A., Friedrich, R., Köhler, P., Kudsk, S., Miyake, F., Olsen, J., Reinig, F., Sakamoto, M., Sookdeo, A., Talamo, S., 2020. The IntCal20 Northern Hemisphere radiocarbon age calibration curve (0–55 cal kBP). Radiocarbon 62 (1), 821–863. https://doi.org/10.1017/RDC.2020.46.
Rymer, K., Rachlewicz, G., 2014. Thermal dynamics of the permafrost active layer in Ebba valley (Central Spitsbergen) in the years 2009–2012. International Journal of Applied and Natural Sciences 3, 79–86.
Saros, J.E., Anderson, N.J., Juggins, S., McGowan, S., Yde, J.C., Telling, J., Bullard, J.E., Yallop, M.L., Heathcote, A.J., Burpee, B.T., Fowler, R.A., Barry, C.D., Northington, R. M., Osburn, C.L., Pla-Rabes, S., Mernild, S.H., Whiteford, E.J., Andrews, M.G., Kerby, J.T., Post, E., 2019. Arctic climate shifts drive rapid ecosystem responses across the West Greenland landscape. Environmental Research Letters 14, 074027. https://doi.org/10.1088/1748-9326/ab2928.
Seppälä, M., 2004. Wind as a Geomorphic Agent in Cold Climates. Cambridge University Press.
Svendsen, J.I., Mangerud, J., 1997. Holocene glacial and climatic variations on Spitsbergen, Svalbard. The Holocene 7, 45–57. https://doi.org/10.1177/095968369700700105.
Szczypek, T., 1982. Działalność eoliczna w rejonie Zatoki Gas (południowy Spitsbergen). Wyprawy polarne Uniwersytetu Śląskiego 1977–1980, t. I. Prace Naukowe U. Śl. 543, 87–108 in Polish.
Trachsel, M., Telford, R.J., 2017. All age–depth models are wrong, but are getting better. The Holocene 27 (6), 860–869. https://doi.org/10.1177/0959683616675939.
Troll, C., 1948. Der subnivale oder periglaziale Zyklus der Denudation. Erdkunde 2, 1–21 in German.
Willemse, N., Koster, E., Hoogakker, B., Van Tatenhove, F., 2003. A continuous record of Holocene eolian activity in West Greenland. Quaternary Research 59 (3), 322–334. https://doi.org/10.1016/S0033-5894(03)00037-1.

Wojtanowicz, J., 1976. Occurrence and intensity of the recent deflation and accumulation of aeolian dust. Biul. Inst. Geol. 297, 93–99.
van der Meij, W.M., Temme, A.J.A.M., de Kleijn, C.M.F.J.J., Reimann, T., Heuvelink, G.B. M., Zwoliński, Z., Rachlewicz, G., Rymer, K., Sommer, M., 2016. Arctic soil development on a series of marine terraces on Central Spitsbergen, Svalbard: a combined geochronology, fieldwork and modelling approach. SOIL 2, 221–240. https://doi.org/10.5194/soil-2-221-2016.
van der Meij, W.M., Reimann, T., Vornehm, V.K., Temme, A.J.A.M., Wallinga, J., Van Beek, R., Sommer, M., 2019. Reconstructing rates and patterns of colluvial soil redistribution in agrarian (hummocky) landscapes. Earth Surface Processes and Landforms 44 (12), 2408–2422. https://doi.org/10.1002/esp.4671.

Supplementary materials for:

Contemporary and past aeolian deposition rates in periglacial conditions (Ebba Valley, central Spitsbergen)

Krzysztof G. Rymer[a,*], Grzegorz Rachlewicz[a], Agata Buchwal[a], Arnaud J. A. M. Temme[b], Tony Reimann[c], W. Marijn van der Meij[c]

[a] Institute of Geoecology and Geoinformation, Adam Mickiewicz University in Poznań, ul. Bogumiła Krygowskiego 10, 61-680 Poznań, Poland

[b] Department of Geography and Geospatial Sciences, Kansas State University, 920 N17th Street, Manhattan, KS 66506, USA

[c] Institute of Geography, University of Cologne, Zülpicher Str. 45, 50674 Köln, Germany

* Corresponding author.

E-mail address: krym@amu.edu.pl (K. G. Rymer)

List of symbols

A	entrainment coefficient
C	empirical coefficient
d	particle diameter (m)
D	diameter of a standard 0.00025 sand particle (m)
g	gravitational acceleration (m s^{-2})
k	von Karman constant
Q	mass transport rate (kg m^{-1} s^{-1})
ρ	air density (kg m^{-3})

σ	grain density (kg m^{-3})
u_*	friction velocity (m s^{-1})
u_{*t}	threshold friction velocity (m s^{-1})
u_z	wind speed at high z (m s^{-1})
z	height above the ground surface (m)
z_0	roughness length (m)

Mass transport rates in summer seasons 2013-2018

Temporal changes of wind carrying capacity in the years 2013-2018 in the Ebba Valley were analysed based on the Bagnold formula (Bagnold, 1941),

$$Q = C\sqrt{\frac{d}{D}}\frac{\rho}{g}u_*^3$$

where *C* was the empirical coefficient assumed as 2.8 (for sand with wide range of grain sizes), *d* was the typical particle diameter of the sediment found in the aeolian traps (0.00022 m), *D* was the grain diameter of a standard 0.00025 m sand, ρ was the air density, *g* was gravitational acceleration, and u_* was the friction velocity.

Mean daily friction velocity (u_*) was determined based on the Prandtl equation and von Karman's constant (k = 0.4) (McKenna Neuman, 2004), with the usage of mean daily wind speed data (u_z) collected in the Ebba Valley at 2 m height (z),

$$\frac{k\,u_z}{u_*} = ln\left(\frac{z}{z_0}\right)$$

Roughness length (z_0) was assumed as 0.007 m.

Mean daily threshold friction velocity (u_{*t}) was determined based on Bagnold equation,

$$u_{*t} = A\sqrt{\frac{\sigma-\rho}{\rho}gd}$$

with the assumptions of the grain density (σ) as 2 650 kg m^{-3} and particle diameter (d) as 0.00022 m.

Mean daily air density (ρ) was calculated based on the Pyramiden meteorological dataset. The *A* coefficient was calculated based on the empirical relationship ($A = -0.0028\ Q + 0.1452$) estimated by Li et al. (2014).

Theoretical values of mean daily mass transport rates based on the Bagnold formula were calculated to estimate possible seasonal wind carrying capacity changes in the Ebba Valley (Fig. S1). Only days on which the friction velocity has exceeded the threshold friction velocity were taken into account. Share of the number of such days in the total number of days in the study period ranged from 6-12% (years 2013 and 2018, respectively) to 41-50% (years 2015 and 2016, respectively). Thus, the conditions favourable to the development of aeolian processes occurred only on some days in most of the measuring seasons. Generally, higher potential mass transport rates, exceeding 0.02 $kg \cdot m^{-1} \cdot s^{-1}$, were observed usually in the August. Only at the beginning of 2015, higher Q-values were calculated for the very beginning of the measuring season. Also in 2015 there were several days with high mean daily mass transport rates and very low soil volumetric water content values at the same time (Fig. S2). However, most days when friction velocity has exceeded the threshold friction velocity was characterized by typical (0.16-0.18 $m^3 \cdot m^{-3}$) soil volumetric water content values.

The calculated mean seasonal mass transport rates values for the 2013-2018 study periods ranged from 0.001 (in the 2013) to 0.008 (in the 2015) $kg \cdot m^{-1} \cdot s^{-1}$. The highest daily Q values (0.057 and 0.059 $kg \cdot m^{-1} \cdot s^{-1}$) were noticeable in the year 2015.

Theoretical calculations of the mean daily mass transport rates showed that the 2015 study period was characterized by relatively high Q-values at the very beginning of the season when the availability of the easily accessible material for transport was potentially higher (Fig. S1). Simultaneously in the same year days with calculated high mean daily mass transport rates and extremely very low soil volumetric water content values were noticed (Fig. S2). These two factors could have influenced greatly the higher mean aeolian deposition rates observed in the Ebba Valley in the 2015 study period. On the other hand in the years when the higher mean daily mass transport rates were calculated for the end of the study period the mean aeolian deposition rates were noticeably lower.

No statistically significant relationships were found between mean aeolian deposition and calculated mean mass transport rates, as well as with percentage of days when friction velocity has exceeded the threshold friction velocity.

Bagnold, R.A., 1941. The Physics of Blown Sand and Desert Dunes. Methuen, London, 265 pp.

Li, B., Ellis, J.T., Sherman, D.J., 2014. Estimating the Impact Threshold for Wind-Blown Sand. In: Green, A.N. and Cooper, J.A.G. (eds.), Proceedings 13th International Coastal Symposium (Durban, South Africa), Journal of Coastal Research, Special Issue No. 70, 627-632 (doi: 10.2112/SI70-106.1).

McKenna Neuman, C., 2004. Effects of temperature and humidity upon the transport of sedimentary particles by wind. Sedimentology, 51, 1–17 (doi:10.1046/j.1365-3091.2003.00604.x).

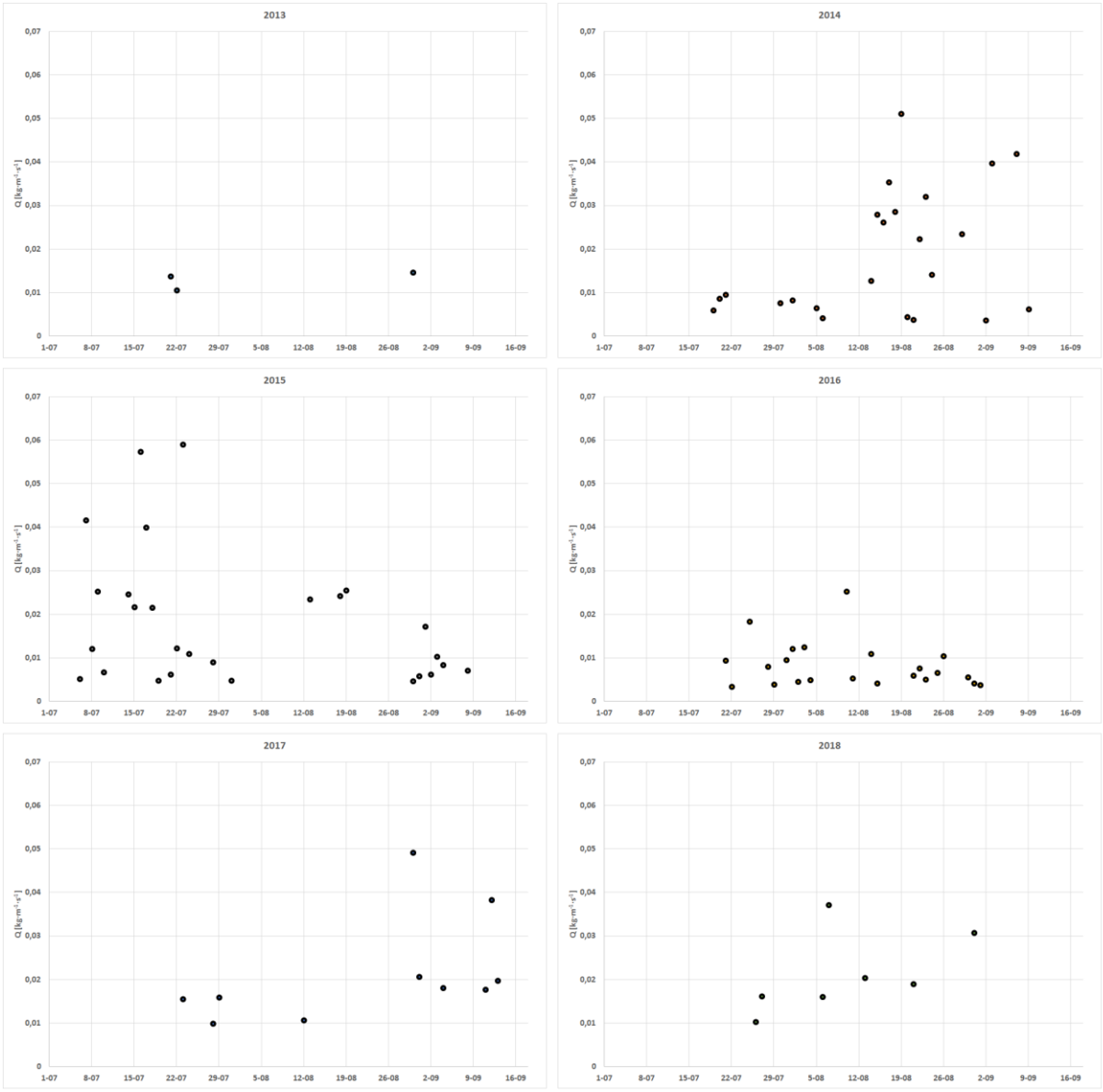

Fig. S1. Mean daily aeolian mass transport rates (Q) in the Ebba Valley calculated for the 2013-2018 study periods.

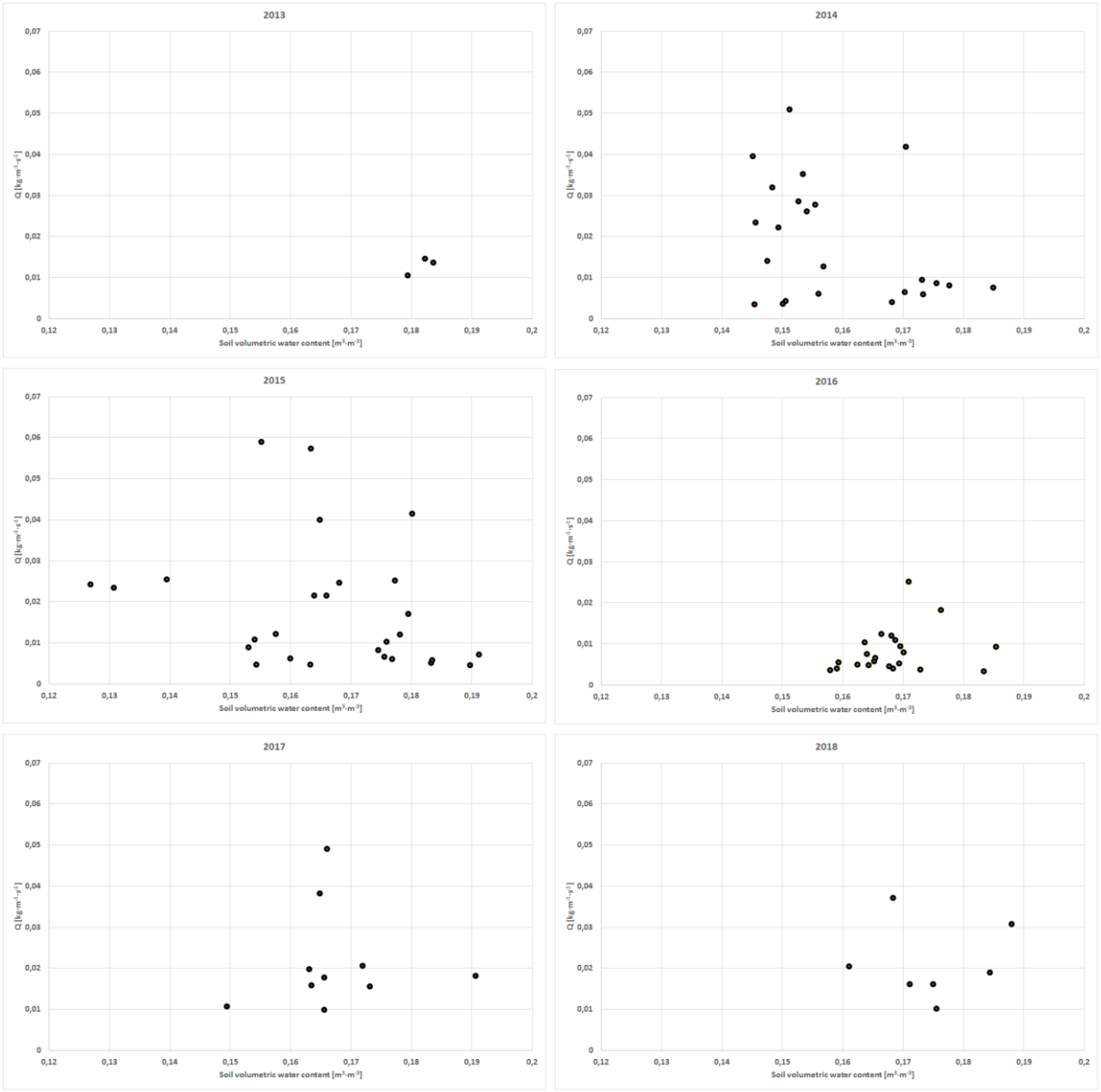

Fig. S2. Mean daily aeolian mass transport rates (Q) in the Ebba Valley calculated for the 2013-2018 study periods in relation to the mean daily soil volumetric water content.

8. Załącznik nr 2

Artykuł nr 2

Rymer K.G., 2024: Intraseasonal changes in aeolian deposition rates in Ebba Valley, central Spitsbergen. Landform Analysis, 43: 41-46. DOI: 10.12657/landfana-043-004

Landform Analysis 43: 41–46
doi: 10.12657/landfana-043-004
Received: 2024.09.12; Accepted: 2024.10.11

Intraseasonal changes in aeolian deposition rates in Ebba Valley, central Spitsbergen

Krzysztof Grzegorz Rymer

Institute of Geoecology and Geoinformation, Adam Mickiewicz University in Poznań, Poland, krym@amu.edu.pl

Abstract: This study investigates seasonal variations in aeolian deposition within the Ebba Valley, focusing on a single summer season 2022. Measurements revealed that aeolian deposition rates were low at the start of the season, ranging from 0.3 to 0.6 g·m^{-2} per day, but peaked at 25.4 g·m^{-2} per day towards the end of the season. The findings suggest that late summer conditions, with stronger winds and higher precipitation, including lower river water levels and the availability of fresh fluvioglacial material, may enhance aeolian deposition. Understanding these dynamics is crucial for modelling aeolian processes in the context of ongoing climate change.

Keywords: aeolian deposition, aeolian trap, periglacial conditions, Svalbard, Arctic

Introduction

Subsequent research seasons in the polar areas are characterized by an increasing intensity of above-average processes and phenomena, which are related to the observed climate change (Koenigk et al. 2020). However, in addition to tracking long-term trends, it is extremely important, to further investigate the nature and variability of processes and phenomena in the environment also in shorter periods like within a single season.

Arctic ecosystems are still not yet well recognized, both quantitatively and qualitatively, and all new data constitutes an important addition to the existing knowledge and models (Beylich et al. 2016). Despite the existence of several fundamental works devoted to the subject of aeolian processes (see McKenna Neuman 1993, Seppälä 2004, Brookfield 2011, Bullard 2012, and Bateman 2013) usually most of the research was only realised on a small number of test sites for the limited time in the past (Maher 2011).

In central Spitsbergen, a comprehensive geological and geographical study of the Ebba Valley area (see Fig. 1) was conducted for over 30 years, but the aeolian issue was raised extremely rarely for this particular region. Taking into account the current state of knowledge and specific climatic conditions, this valley was chosen as the test site for the measurements carried out and presented in the current study. It should be mentioned that in the Ebba Valley measurements of the efficiency of transport and accumulation of aeolian material were conducted during the summer of 2002 (Paluszkiewicz 2003). It was shown that deflation and accumulation mainly pertain to the silt fraction. The largest aeolian transport efficiency was observed when the wind reached velocities exceeding 5–6 m·s^{-1}. The most important influence on the intensity of aeolian processes was generated by air and soil humidity, terrain morphology, and vegetation cover. Due to the lack of constant and strong winds in the summer of 2002, the efficiency of transport and aeolian accumulation was relatively small. Studies of aeolian processes in the Ebba Valley were also conducted in the summer of 2005. However, this research was limited to the identification of the accumulation and erosion of landforms of aeolian origin (Górska-Zabielska 2007). Moreover, the aeolian deposition component was estimated and included as an important factor of soil formation in the Ebba Valley (van der Meij et al. 2016). The influence of wind activity on vegetation cover was also analysed by Borysiak et al. (2020). Kavan et al. (2020) estimated the total sediment (dust) concentration in snow samples for 2.66–24.56 g·m^{-2} per snow season in the area of Petunia Bay. Aeolian deposition for summer seasons 2012–2018 was measured in Ebba Valley by Rymer et al. (2022) and estimated for 2.1 to 12.3 g·m^{-2} per day.

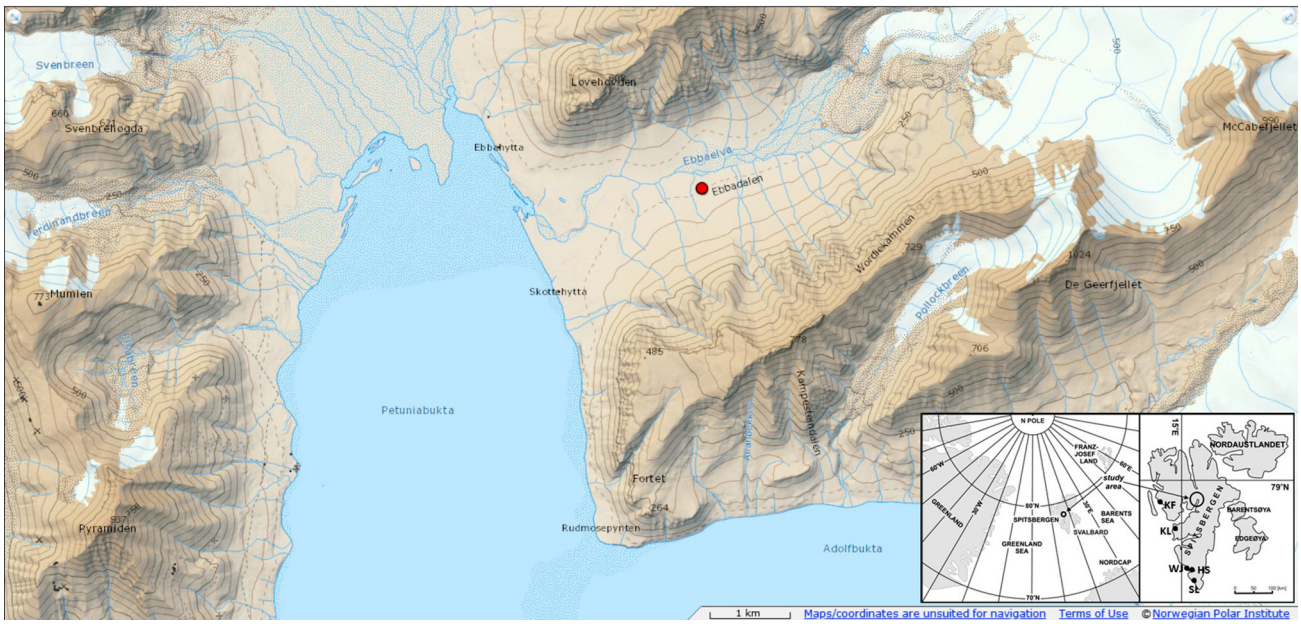

Fig. 1. Map of the study area with aeolian deposition test site (red dot) location within the Ebba Valley. Inner map shows the location of the study area (black arrows and circle) in the central Spitsbergen, High Arctic. Map source: Norwegian Polar Institute

The main goal of the study was to quantify aeolian deposition rates in periglacial conditions of the postglacial valley over a seasonal scale (across one summer season), and to investigate possible relationships between aeolian deposition and meteorological condition changes over the summer season, i.e. in July and August.

Study area

Ebbadalen (eng. Ebba Valley) is located in the central part of Spitsbergen, the largest island of the Svalbard Archipelago (Fig. 1). This postglacial valley is surrounded by steep mountain ranges, with clearly marked glacial features (Rachlewicz 2009, Rymer et al. 2022). *Ebbadalen* geologically is built of pre-Devonian metamorphic rocks overlapped by sedimentary formations, primarily from the Carboniferous period. Those layers include sequences of shales, sandstones, limestone, and anhydrite (Harland 1997, Dallmann et al. 2002). The geological stratification in many places is much more complex due to tectonic activity in this area in the past. The valley basis is composed of glaciofluvial and morainic forms generated by retreating glaciers and proglacial streams. Typical features in the mouth section of the valley are a series of raised marine terraces. Terraces are elevated up to 30 m a.s.l. and their TL age was determined from around 13.3 to 1.3 ka (Kłysz et al. 1989, Rachlewicz 2009, van der Meij et al. 2016). The terraces were also dated using AMS radiocarbon dating of *Astarte borealis* shells and their ^{14}C ages varied from 9.9 to ca. 3 ka (Long et al. 2012).

The environment of Ebba Valley is typical for high Arctic areas and is characterized by a cold climate, with mean annual temperature usually below −6.0°C. Positive temperatures are observed between May and October and the warmest months are July and August when the temperature rises to 5–6°C of the daily average (Rachlewicz and Szczuciński 2008, Rymer and Rachlewicz 2014). The inner-archipelago location is responsible for the quasi-continental individuality of the whole area. Usually, it is slightly warmer during summer and much dryer than in southern and western parts of Spitsbergen with total precipitation not reaching 200 mm per year (Rachlewicz and Styszyńska 2007, Przybylak et al. 2014). Due to observed climate change recent data shows warming trends, which cause melting seasons to be longer. Increased rainfall rather than snowfall from spring to autumn is also more common (Førland et al. 2011, Sobota et al. 2020). Snow cover is usually not thick and is present in the area during winter and early spring months (Przybylak et al. 2006). Southern and north-eastern winds dominate, but the strongest gusts are most often observed from the north and north-west, conditioned by the morphology of surrounding mountain chains (Rachlewicz 2003, Przybylak et al. 2006, Małecki 2015).

The very sparse vegetation adapts to Arctic conditions and consists mostly of mosses, lichens, and shrubby species. This fragile tundra ecosystem is colonizing areas uncovered by glaciers retreat, to reach the best conditions for development on terraces in

the valley mouths (Stawska 2017). Individual vegetation types were described in this area by Prach et al. (2012) and Johansen et al. (2012). Tundra plants are quite often shaped by aeolian activity and grow on the aeolian sediments (Borysiak et al. 2020). The limited vegetation is an important archive and marker of ecological responses to changing climate (Elvebakk 2005, Buchwal et al. 2013).

Methods

The measurements were taken at a single test site located in the central part of the Ebba Valley (Fig. 1). Previous studies have shown that this site recorded aeolian deposition values close to the average deposition calculated for the entire valley based on a comparison of nine test sites (Rymer et al. 2022). In order to measure the amount of aeolian deposition, measurement equipment (three traps) was set out three times during the summer season in 2022 for a period between 11 and 17 days (traps A, B, and C). Additionally, three traps were set out for 41 days during the whole measuring season (traps X, Y, and Z). All traps were placed approximately 1–1.5 meters from each other. The measurement periods and the number of days are listed in Table 1. To compare and standardise the obtained results, they were divided by the number of days.

The traps were arranged by using 195 mm diameter plastic trays filled with glass marbles (*phi* = 15 mm). After the measurement was completed, the trays and glass marbles were washed with filtered water to isolate the collected material. It was then dried and weighed. The original method was first proposed to measure vertical dust flux (Hall and Upton 1988). However, further research proved that this type of trap can be used to measure aeolian sediment concentration and deposition (Goossens and Offer 2000). The details and modifications to the method implemented during measurements in Ebba Valley have been widely described by Rymer et al. (2022).

Meteorological data for Pyramiden (daily average temperature and daily average wind speed) and Longyearbyen (daily precipitation) meteorological stations (located respectively 10 and 60 km southwest from the study area) were acquired via the Seklima database (NMI 2024).

Table 1. Time periods for aeolian deposition measurements during summer season 2022

Traps	Start date	End date	Number of days
X, Y, Z	16.07.2022	26.08.2022	41
A1, B1, C1	16.07.2022	29.07.2022	13
A2, B2, C2	29.07.2022	9.08.2022	11
A3, B3, C3	9.08.2022	26.08.2022	17

Results

The day the measurements started fell on the period of the highest temperatures in the summer season of 2022. Since then, there has been a systematic decline in average daily temperatures (Fig. 2. and Table 2). The situation was slightly different in the case of average wind speed, where wind speeds exceeding an average of 5 $m \cdot s^{-1}$ were observed only towards the end of the measurement season. The above statement excludes two days in the second half of July when average wind speeds were close to 5 $m \cdot s^{-1}$. The intensity of rainfall also increased towards the end of the measurement period.

The obtained amount of aeolian deposition varied between 0.05–0.10 g (during the shortest period of 11 days in the middle of the season) and 11.50–14.85 g (during the period of 17 days at the end of

Table 2. Selected weather variables measured at the Pyramiden and Longyearbyen weather stations for the summer season 2022

Period	Average temperature	Total precipitation	Average wind speed
	[°C]	[mm]	[m s^{-1}]
16–29.07.2022	10.1	3.2	2.18
29.07–9.08.2022	9.0	9.5	1.20
9–26.08.2022	7.0	32.7	2.62

Table 3. Aeolian deposition rates in Ebba Valley in summer season 2022

Trap	Period	Aeolian deposition measured in the trap	Mean aeolian deposition measured in the traps	Standardized aeolian deposition
		[g]		[$g \cdot m^{-2}$ day^{-1}]
X	16.07–26.08.2022	13.35		
Y	16.07–26.08.2022	10.75	11.20	9.1
Z	16.07–26.08.2022	9.50		
A1	16–29.07.2022	0.20		
B1	16–29.07.2022	0.35	0.25	0.6
C1	16–29.07.2022	0.20		
A2	29.07–9.08.2022	0.05		
B2	29.07–9.08.2022	0.10	0.08	0.3
C2	29.07–9.08.2022	0.10		
A3	9–26.08.2022	12.45		
B3	9–26.08.2022	11.50	12.93	25.4
C3	9–26.08.2022	14.85		

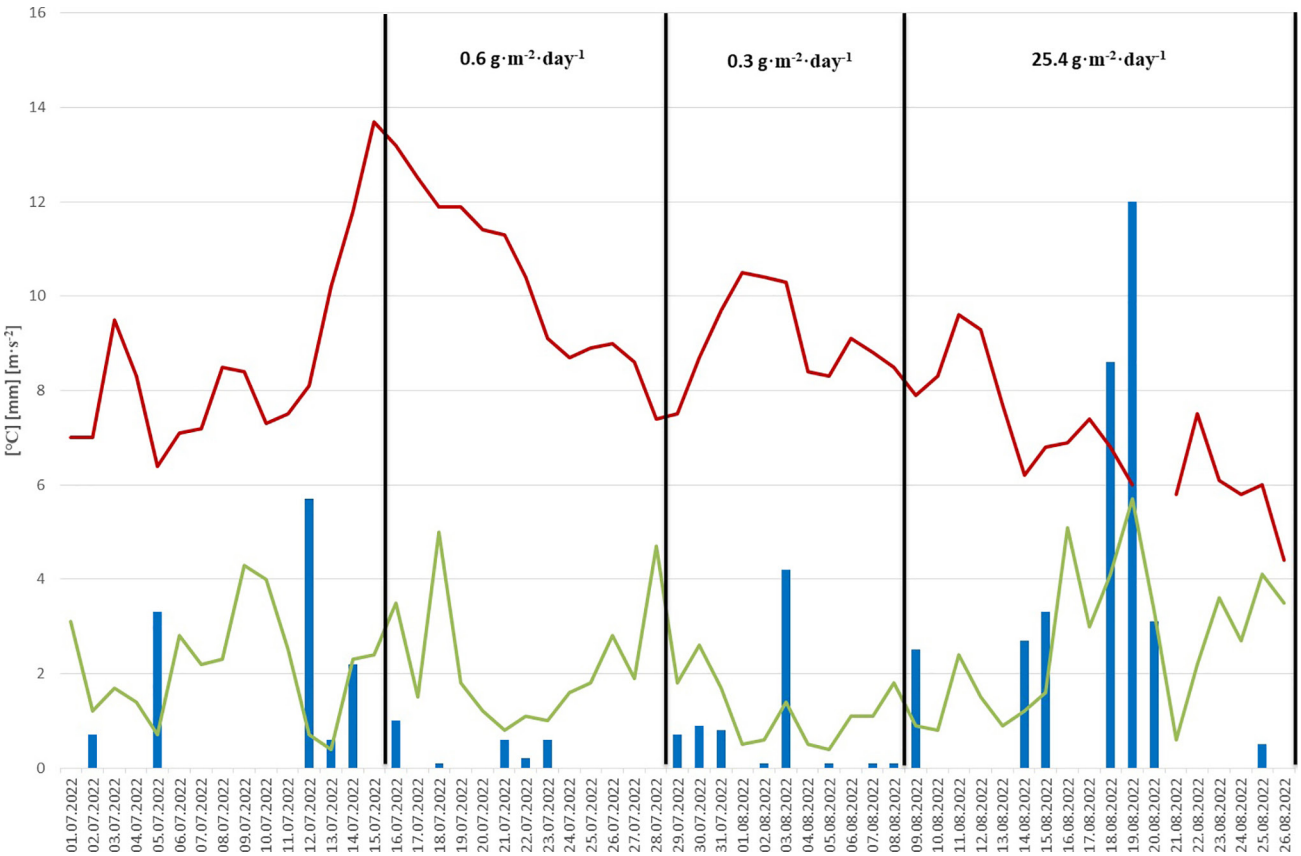

Fig. 2. Selected weather variables measured at the Pyramiden (temperature and wind speed) and Longyearbyen (precipitation) weather stations for the aeolian deposition measurement periods during summer season 2022. Red colour indicates average daily air temperature. Green colour indicates average daily wind speed. Blue bars indicate daily precipitation totals

the season). After the standardization, this resulted in values in the range from 0.3 g·m^{-2} per day (in the middle of the season), through 0.6 g·m^{-2} per day (at the beginning of the measurements) to 25.4 g·m^{-2} per day (at the end of the season). The mean standardized aeolian deposition during the whole summer season of 2022 reached 9.1 g·m^{-2} per day (Table 3). Previous research showed that the deposited material mainly consisted of moderately sorted fine sands (Rymer et al. 2022).

Discussion

Although the research conducted in the summer season of 2022 was relatively shorter than the measurements conducted in the years 2012–2018 (compare Rymer et al. 2022), the obtained value of mean standardized aeolian deposition (9.1 g·m^{-2} per day) was in a similar range to the results from previous years for this test site (2.0–16.4 g·m^{-2} per day). However, this value was slightly higher than the multi-year average (3.2 g·m^{-2} per day higher than the 2012–2018 average). The selected measurement period in 2022 was also characterized by a significantly higher average air temperature than in previous years (by 1–2°C). Therefore, at this stage of work, a broader comparison with the model proposed by Rymer et al. (2022) was omitted. It is therefore necessary to collect further data that will allow for the identification of critical values in terms of weather conditions, especially in times of climate change.

However, it should be noticed that values of aeolian deposition during the season were not equal and much higher results were obtained at the end of the season. This could have been due to the occurrence of stronger winds. The occurrence of more rainfall certainly also had an impact on the greater capacity of the traps (but also of the ground surface) to absorb all material transported by the wind during that period. On the other hand, rainfall is one of the factors limiting the uplift and movement of aeolian material (Jackson and Nordstrom 1998). A trap drainage system should certainly be used in further research, which would result in greater accuracy of the measurements. Although no statistically important correlations were found between meteorological conditions and values of the aeolian deposition (Table 4), high r Pearson values may suggest some

Table 4. Correlation between different weather variables and aeolian deposition rates during measurement periods in Ebba Valley in summer season 2022

Parameter	Precipitation	Temperature	Wind speed
r Pearson	0.98	−0.93	0.75
p value	0.13451	0.23591	0.46233

kind of combination of relations between the precipitation, air temperature, and aeolian deposition.

The drop-in air temperature at the end of the season contributes to the drop in water levels of proglacial rivers. This results in the increased presence and availability of fresh glaciofluvial material, which can then be blown by the wind around the valley. The existence of the relationship between glaciofluvial and aeolian activities was previously discussed by Dijkmans and Tørnqvist (1991), Bullard and Austin (2011), as well as, Rymer et al. (2022). Similar regularities have been also found by Gilbert et al. (2018) and Rasmussen et al. (2023).

Conclusions

The undertaken research was one of the first aimed at a more detailed quantitative assessment of the amount of aeolian deposition within one summer season on Svalbard. Although the year 2022 was different in terms of weather conditions from the previous years, the measured seasonal values are similar to those obtained for the study area in the past. Differences in aeolian deposition rates through the season are significant. For most of the summer, the daily values of aeolian deposition reach 0.3–0.6 $g \cdot m^{-2}$. Then, at the end of the season, they can even reach up to 25.4 $g \cdot m^{-2}$ per day.

The results indicate that the processes of deposition of wind-borne material are intensifying only at the end of the summer season, mainly due to stronger winds and lower air temperatures. The lower air temperatures cause the water level in rivers to drop, which in turn exposes the sediment carried by the river. Then the fresh glaciofluvial material can be transported by the wind and deposited at the bottom of the valley.

Acknowledgements

The study was conducted at Adam Mickiewicz Polar Station "Petuniabukta" (AMUPS). The author would like to thank all the AMUPS expedition members involved in logistics and fieldwork on Svalbard in the year 2022, with special thanks to Mateusz Drożdżyński. The author is grateful to Professor Grzegorz Rachlewicz for his valuable comments on the manuscript. Weather data for both Pyramiden and Longyearbyen were obtained from the Seklima database run by the Norwegian Meteorological Institute. The map was provided by the Norwegian Polar Institute (TopoSvalbard WMTS service). The author would also like to thank the reviewers for their valuable comments that contributed to improving the article.

References

Bateman M.D., 2013. Aeolian processes in periglacial environments. In: R.Giardino, J.Harbor (eds), Treatise on Geomorphology (8) Glacial and Periglacial Geomorphology, Academic Press, San Diego: 416–429.

Beylich A.A., Dickson J.C., Zwoliński Zb., 2016. Source-To-Sink Fluxes in Undisturbed Cold Environments. Cambridge University Press.

Borysiak J., Pleskot K., Rachlewicz G., 2020. Dryas aeolian landforms in Arctic deflationary tundra, central Spitsbergen. Polish Polar Research 41(1): 41–68.

Buchwal A., Rachlewicz G., Fonti P., Cherubini P., Gaertner H., 2013. Temperature modulates intra-plant growth of Salix polaris from a high Arctic site (Svalbard). Polar Biology 36(9): 1305–1318.

Bullard J.E., 2012. Contemporary glacigenic inputs to the dust cycle. Earth Surface Processes and Landforms 38: 71–89. DOI 10.1002/esp.3315.

Bullard J.E., Austin M.J., 2011. Dust generation on a proglacial floodplain, West Greenland. Aeolian Research 3: 43–54. DOI 10.1016/j.aeolia.2011.01.002.

Brookfield M.E., 2011. Aeolian processes and features in cool climates. In: I.P.Martini, H.M.French, A. Pérez Alberti (eds), Ice-marginal and Periglacial Processes and Sediments. Geological Society, London: 241–258. DOI 10.1144/SP354.16.

Dallmann W. K., Hjelle A., Ohta Y., Salvigsen O., Balashov Y. A., Maher Jr. H. D., 2002. Geological map of Svalbard 1: 100,000, sheet B9G Adventdalen. Norwegian Polar Institute.

Dijkmans J.W.A., Tørnqvist T.E., 1991. Modern periglacial eolian deposits and landforms in the Søndre Strømfjord area, West Greenland and their palaeoenvironmental implications. Meddelelser om Grønland. Geoscience 25: 3–39.

Elvebakk A., 2005. A vegetation map of Svalbard on the scale 1: 3.5 mill. Phytocoenologia 35(4): 951–967.

Førland E.J., Benestad R., Hanssen-Bauer I., Haugen J.E., Skaugen T.E., 2011. Temperature and precipitation development at Svalbard 1900–2100. Advances in Meteorology 893790: 1–14. DOI 10.1155/2011/893790.

Gilbert G.L., O'Neill H.B., Nemec W., Thiel C., Christiansen H.H., Buylaert J.-P., 2018. Late Quaternary sedimentation and permafrost development in a Svalbard fjord-valley, Norwegian high Arctic. Sedimentology 65: 2531–2558. DOI 10.1111/sed.12476.

Goossens D., Offer Z.Y., 2000. Wind tunnel and field calibration of six aeolian dust samplers. Atmospheric Environment 34: 1043–1057. DOI 10.1016/S1352-2310(99)00376-3.

Górska-Zabielska M., 2007. Formy eoliczne na przedpolu lodowca Ebba, środkowy Spitsbergen. In: E.Smolska, D.Giriat (eds), Rekonstrukcja dynamiki i procesów geomorfologicznych – formy rzeźby i osady. Uniwersytet Warszawski, Wydział Geografii i Studiów Regionalnych, Komitet Badań Czwartorzędu Polskiej Akademii Nauk: 199–204.

Hall D.J., Upton S.L., 1988. A wind tunnel study of the particle collection efficiency of an inverted Frisbee used as a dust deposition gauge. Atmospheric Environment 22(7): 1383–1394. DOI 10.1016/0004-6981(88)90163-1.

Harland W.B., 1997. The geology of Svalbard. Geological Society of London.

Jackson N.L., Nordstrom K.F., 1998. Aeolian transport of sediment on a beach during and after rainfall, Wildwood, NJ, USA. Geomorphology 22(2): 151–157. DOI 10.1016/S0169-555X(97)00065-2.

Johansen B.E., Karlsen S.R., Tømmervik H., 2012. Vegetation mapping of Svalbard utilising Landsat TM/ETM+ data. Polar Record 48(1): 47–63.

Kavan J., Láska K., Nawrot A., Wawrzyniak T., 2020. High Latitude Dust Transport Altitude Pattern Revealed from Deposition on Snow. Svalbard. Atmosphere 11: 1318. DOI 10.3390/atmos11121318.

Kłysz P., Lindner L., Marks L., Wysokiński L., 1989. Late Pleistocene and Holocene relief remodeling in the Ebbadalen-Nordenskiöldbreen region in Olav V Land, central Spitsbergen. Polish Polar Research 10(3): 277–301.

Koenigk T., Key J., Vihma T., 2020. Climate change in the Arctic. In: A.Kokhanovsky, C.Tomasi (eds), Physics and chemistry of Arctic atmosphere. Springer Polar Sciences: 673–705.

Long A.J., Strzelecki M.C., Lloyd J.M., Bryant C.L, 2012. Dating High Arctic Holocene relative sea level changes using juvenile articulated marine shells in raised beaches. Quaternary Science Reviews 48: 61–66.

Maher B.A., 2011. The magnetic properties of Quaternary aeolian dusts and sediments, and their palaeoclimatic significance. Aeolian Research 3(2): 87–144. DOI 10.1016/j.aeolia.2011.01.005.

Małecki J., 2015. Glacio–meteorology of Ebbabreen, Dickson Land, central Svalbard, during 2008–2010 melt seasons. Polish Polar Research 36(2): 145–161. DOI 10.1515/popore-2015-0010.

McKenna Neuman C., 1993. A review of aeolian transport processes in cold environments. Progress in Physical Geography 17(2): 137–155. DOI 10.1177/030913339301700203.

NMI [Norwegian Meteorological Institute], 2024. Norsk Klimaservicesenter, Online: seklima.met.no/ (access 2024.10.10)

Paluszkiewicz R., 2003. Zróżnicowanie natężenia transportu eolicznego w warunkach polarnych jako efekt zmienności czynników meteorologicznych na przykładzie doliny Ebby (Petuniabukta, Billefjorden, Spitsbergen Środkowy). In: M.A.Olech (ed), XXIX Międzynarodowe Sympozjum Polarne. Funkcjonowanie ekosystemów polarnych na tle globalnych zmian środowiska. Instytut Botaniki Uniwersytetu Jagiellońskiego, Kraków: 235-237.

Prach K., Klimešová J., Košnar J., Redčenko O., Hais M., 2012. Variability of contemporary vegetation around Petuniabukta, central Spitsbergen. Polish Polar Research 33(4): 383–394.

Przybylak R., Araźny A., Gluza A., Hojan M., Migała K., Sikora S., Siwek K., Zwoliński Zb., 2006. Porównanie warunków meteorologicznych na zachodnim wybrzeżu Spitsbergenu w sezonie letnim 2005 r. Problemy Klimatologii Polarnej 16: 125–138.

Przybylak R., Araźny A., Nordli Ø., Finkelnburg R., Kejna M., Budzik T., Migała K., Sikora S., Puczko D., Rymer K., Rachlewicz G., 2014. Spatial distribution of air temperature on Svalbard during 1 year with campaign measurements. International Journal of Climatology 34: 3702–3719.

Rachlewicz G., 2003. Warunki meteorologiczne w Zatoce Petunia (Spitsbergen środkowy) w sezonach letnich 2000 i 2001. Problemy Klimatologii Polarnej 13: 127–138.

Rachlewicz G., 2009. Contemporary sediment fluxes and relief changes in high Arctic glacierized valley systems (Billefjorden, Central Spitsbergen). Wydawnictwo Naukowe UAM, Poznań.

Rachlewicz G., Styszyńska A., 2007. Porównanie przebiegu temperatury powietrza w Petuniabukta i Svalbard-Lufthavn (Isfjord, Spitsbergen) w latach 2001–2003. Problemy Klimatologii Polarnej 17: 121–134.

Rachlewicz G., Szczuciński W., 2008. Changes in thermal structure of permafrost active layer in a dry polar climate, Petuniabukta, Svalbard. Polish Polar Research 29: 261–278.

Rasmussen C.F., Christiansen H.H., Buylaert J.-P., Cunningham A., Schneider R., Knudsen M.F., Stevens T., 2023. High-resolution OSL dating of loess in Adventdalen, Svalbard: Late Holocene dust activity and permafrost development. Quaternary Science Reviews 310: 108137. DOI 10.1016/j.quascirev.2023.108137.

Rymer K., Rachlewicz G., 2014. Thermal dynamics of the permafrost active layer in Ebba Valley (Central Spitsbergen) in the years 2009–2012. International Journal of Applied and Natural Sciences 3: 79–86.

Rymer K.G., Rachlewicz G., Buchwal A., Temme A.J.A.M., Reimann T., van der Meij W.M., 2022. Contemporary and past aeolian deposition rates in periglacial conditions (Ebba Valley, central Spitsbergen). Catena 211. DOI 10.1016/j.catena.2021.105974.

Seppälä M., 2004. Wind as a Geomorphic Agent in Cold Climates. Cambridge University Press.

Sobota I., Weckwerth P., Grajewski T., 2020. Rain-on-snow (ROS) events and their relation to snowpack and ice layer changes on small glaciers in Svalbard, the high Arctic. Journal of Hydrology 590: 125279.

Stawska M., 2017. Impacts of geomorphic disturbances on plant colonization in Ebba Valley, central Spitsbergen, Svalbard. Quaestiones Geographicae 36(1): 51–64.

van der Meij W.M., Temme A.J.A.M., de Kleijn C.M.F.J.J., Reimann T., Heuvelink G.B.M., Zwoliński Zb., Rachlewicz G., Rymer K., Sommer M., 2016. Arctic soil development on a series of marine terraces on Central Spitsbergen, Svalbard: a combined geochronology, fieldwork and modelling approach. SOIL 2: 221–240.

9. Załącznik nr 3

Artykuł nr 3

Rymer K.G., Wachecka-Kotkowska L., 2024: Sources of the aeolian material in periglacial conditions based on quartz grain analysis, Ebba Valley, Svalbard. Quaestiones Geographicae, 43(4): 17–29. DOI: 10.14746/quageo-2024-0034

SOURCES OF THE AEOLIAN MATERIAL IN PERIGLACIAL CONDITIONS BASED ON QUARTZ GRAIN ANALYSIS, EBBA VALLEY, SVALBARD

KRZYSZTOF GRZEGORZ RYMER [1], LUCYNA WACHECKA-KOTKOWSKA [2]

[1] Cryosphere Research Unit, Institute of Geoecology and Geoinformation, Adam Mickiewicz University, Poznań, Poland
[2] Department of Geology and Geomorphology, Faculty of Geographical Sciences, University of Łódź, Łódź, Poland

Manuscript received: August 21, 2024
Revised version: October 12, 2024

RYMER K.G., WACHECKA-KOTKOWSKA L., 2024. Sources of the aeolian material in periglacial conditions based on quartz grain analysis, Ebba Valley, Svalbard. *Quaestiones Geographicae* 43(4), Bogucki Wydawnictwo Naukowe, Poznań, pp. 17–29. 4 figs, 5 tables.

ABSTRACT: The research conducted in this study is an attempt to quantitatively and qualitatively supplement the still insufficient knowledge on aeolian processes under polar conditions, where some of the most visible and dynamic climate changes are occurring. This study presents the results of rounding and matting analysis of quartz grains collected from aeolian deposition traps located in the Ebba Valley, Svalbard. The results are based on four summer field campaigns (2015–2018). Quartz grains with a diameter of 0.8–1.0 mm were selected and subjected to further analysis under a microscope, which allowed them to be divided into six individual classes. The nature of the grains can largely indicate the environmental conditions in which the material was transported. The collected material was dominated by grains with a low degree of roundness, which may indicate relatively short fluvial or aeolian transport. The small amounts of typically matted quartz grains may indicate low environmental dynamics and short transport, as well as the fact that large amounts of the material are blown from the valley interior to the nearby bay and fjord. This study highlights the importance of a fresh sediment supply from two main sources (i.e., moraines and rivers) and their subsequent aeolian redistribution, particularly in a wind-channelled valley environment. These findings underscore the complex interactions between aeolian processes and environmental conditions in cold regions. Climate change may significantly affect the magnitude of aeolian processes. Further research is needed to refine these correlations and enhance the understanding of sedimentary dynamics in polar settings.

KEYWORDS: aeolian processes, polar desert, sedimentary environments, meteorological variables, statistical analysis, Arctic

Corresponding author: Krzysztof Grzegorz Rymer; krym@amu.edu.pl

Introduction

Studying the characteristics of the environment via the rounding and matting analysis of quartz grains is a common research method, especially at moderate latitudes (Woronko, Bujak 2018). A method originally proposed by Cailleux (1942) has been applied, especially in the context of distinguishing sedimentary environments (Wachecka-Kotkowska 2004, 2015). With the advancement of analytical techniques, foundational knowledge on sedimentary rock origins and

https://doi.org/10.14746/quageo-2024-0034
ISSN 2082-2103, eISSN 2081-6383

processes, as well as discussions on the petrography and sedimentology of sand and sandstone, with an emphasis on quartz grains, has developed (e.g., Blatt et al. 1980, Pettijohn et al. 1987). Different quartz grain textures, their implications for sedimentary processes, and methods as well as various case studies for sedimentary rock and environmental analyses have also been presented (e.g., Blott, Pye 2001, Mahaney 2002, Boggs 2009, Lyu et al. 2019). Different environments (fluvial, glacial, and aeolian) contribute to variations in grain mineralogy and texture. Therefore, the possibility of separating grains formed in the aquatic environment from those shaped by the wind is particularly useful not only in the study of aeolian processes but it also allows for a broad analysis of the processes taking place in the geoecosystems (cf. Folk 1980, Pye, Tsoar 2009, Wachecka-Kotkowska et al. 2014, Woronko et al. 2015, Zieliński et al. 2015).

Despite the growing interest in sedimentary systems in cold regions (Zhang et al. 2022), information about aeolian processes in the Arctic and Antarctic regions is currently incomplete, which is due to the low availability of these areas and problems in obtaining reliable quantitative data under polar conditions and in various seasons (Müller et al. 2016). Studies have been sparsely distributed and have selectively covered different aspects of aeolian activity, including erosion and sediment transport, deposition and landform development, and seasonal and climatic influences, as well as ecological and environmental implications (e.g., Borysiak et al. 2020). However, data regarding aeolian processes are crucial for better understanding the functioning of polar geoecosystems, which are important markers of environmental changes occurring at global and local scales (Beylich et al. 2016).

The current knowledge on wind activity in periglacial environments was collected by Seppälä (2004) and Brookfield (2011). Recently, Rymer et al. (2022) summarised the work on aeolian processes occurring under polar conditions in recent decades. Notably, in recent years, interest in aeolian processes in polar environments has increased (see Kavan et al. 2020), as has interest in the nature of transported sediments (Kalińska-Nartiša et al. 2017, Kalińska 2019, Kalińska et al. 2019).

Owing to the lack of detailed research on the aeolian activity in this part of the Arctic, this work was intended to further develop and interpret the previously obtained research material (aeolian deposits collected in traps), with a particular emphasis on a detailed analysis of the nature and character of aeolian sediments (quartz grains 0.8–1.0 mm in size). Therefore, a quantitative and qualitative analysis of quartz grains collected from the aeolian material deposited in traps was performed. The obtained data were subjected to further statistical analysis. This study aimed to determine the main source of the deposited aeolian material as well as to determine the degree of aeolisation (acquisition of typically aeolian features by quartz grains) of the material transported by wind inside a relatively small postglacial valley under periglacial conditions. Additionally, the possible influences of meteorological variables on grain type distributions were investigated.

Study area

Ebba Valley (nor. Ebbadalen) is located in the central part of Spitsbergen, the largest island in the Svalbard Archipelago (Fig. 1). The central part of the valley with aeolian deposits is located at approximately 78°42' N latitude and 16°39' E longitude. This postglacial valley is flanked by steep mountain ranges, with prominent glacial features etched into the landscape (Rachlewicz 2009, Rymer et al. 2022). Geologically, Ebbadalen features an array of pre-Devonian metamorphic rock outcrops associated with overlapping sedimentary formations, primarily from the Carboniferous, including sequences of shale, sandstone, limestone, and anhydrite layers, which record a history of ancient tropical environments, marine transgressions, and orogenic cycles (Harland 1997, Dallmann et al. 2002). In many places, geological stratification is much more complicated because of the presence of tectonic faults in the area. The weathering of rock outcrops is one of the sources of the material supplied to the valley floor. However, there is no current data on the volume of this material supply and the impact of climate change on the intensification of these processes. The bottom of the valley is composed of morainic and glaciofluvial forms generated by the decaying Ebba and Bertram glaciers and their proglacial streams, eroding a series of six raised marine terraces in the mouth section of the valley

(Fig. 2). The terraces are elevated to 30 m a.s.l., and their thermoluminescence ages vary from 13.3 ka to 1.3 ka (Kłysz et al. 1989, Rachlewicz 2009, van der Meij et al. 2016). The terraces were also dated by AMS radiocarbon dating of *Astarte borealis* shells, and their ^{14}C ages varied from 9.9 to ca. 3 ka (Long et al. 2012).

The high Arctic environment of Ebbadalen is characterised by a cold climate, with a mean annual temperature slightly below −6.0°C, positive temperatures usually occur between May and October and are warmest in July and August, when they rise to 5–6°C on a daily average (Rachlewicz, Szczuciński 2008, Rymer, Rachlewicz 2014). The inner-fiord location results in the quasi-continental individuality of the area, which is slightly warmer during summer and much drier than the southern and western parts of Spitsbergen, with precipitation not exceeding 200 mm annually (Rachlewicz, Styszyńska 2007, Przybylak et al. 2014). Recent studies have shown significant warming trends, lengthening melt seasons, and increasing rainfall rather than snowfall from spring to autumn (Førland et al. 2011, Sobota et al. 2020). These changes and their consequences may be of key importance for the intensity of aeolian processes, but further work is necessary to determine the nature and direction of changes. Typically, thick snow cover does not occur there during the winter (Przybylak et al. 2006). The wind structure is dominated by southern and north-eastern directions; whereas, the strongest gusts are observed from the north and northwest and are affected by the morphology of the surrounding mountain chains (Rachlewicz 2003, Przybylak et al. 2006, Małecki 2015). A typical feature of areas in the immediate vicinity of glacier-covered areas is the occurrence of katabatic winds, which may ultimately lead to the wind blowing aeolian material out of valley.

Ebbadalen supports various Arctic flora adapted to extreme conditions. The sparse vegetation

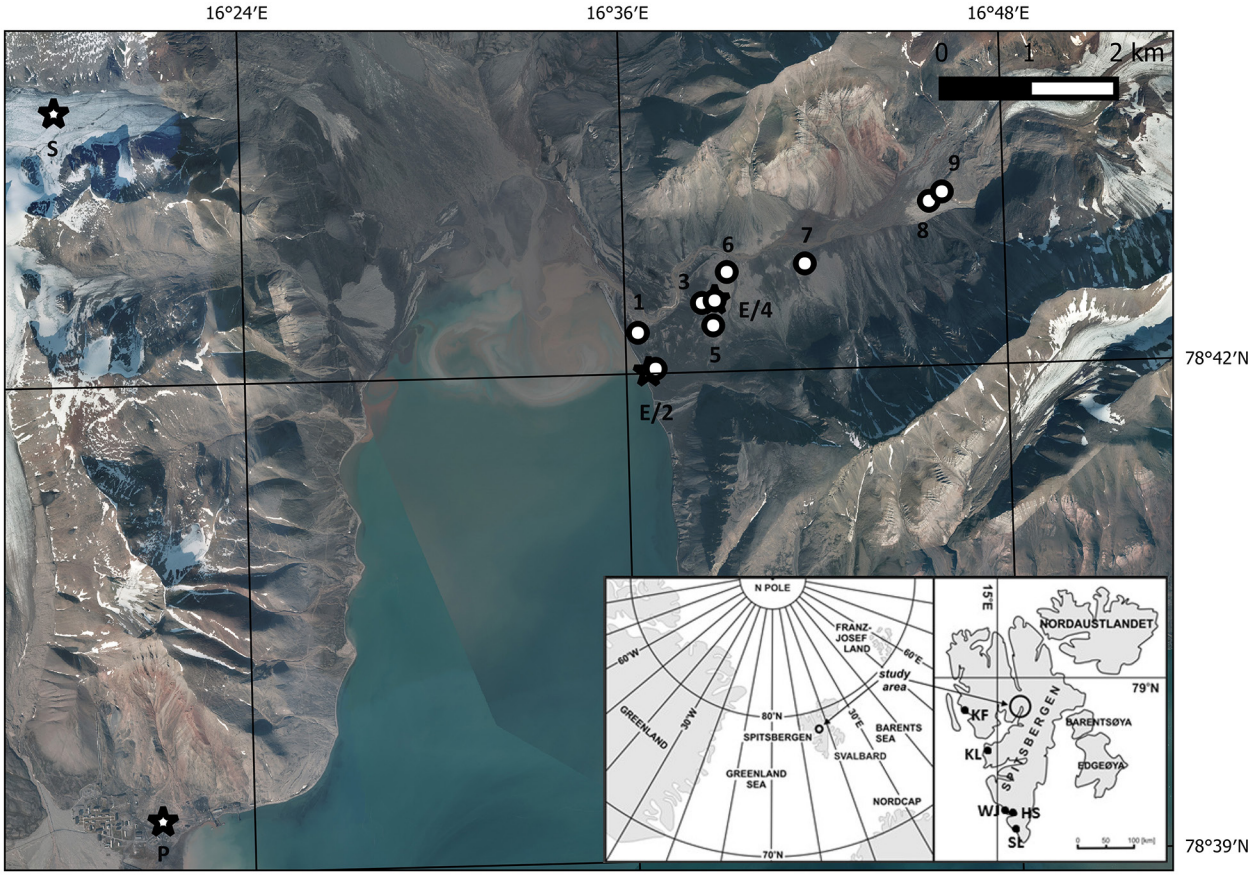

Fig. 1. Orthophotomap of the study area with nine aeolian deposition test sites (1–9) located within the Ebba Valley. Weather stations (E – Ebba Valley, S – Sven Glacier, and P – Pyramiden city) are marked with black stars. Orthophotomap source – Norwegian Polar Institute. Inner map shows the location of the study area (black arrows and circle) in the central Spitsbergen, High Arctic.

includes mosses, lichens, and shrubby species that form a fragile tundra ecosystem, colonising bare surfaces uncovered by glacial retreat and reaching climax on terraces in the valley mouths (Stawska 2017). Studies leading to the determination of individual types of vegetation have been carried out in this area, among others, by Prach et al. (2012) and Johansen et al. (2012). Plant communities provide a unique environment for trapping aeolian sediment (Borysiak et al. 2020). The area's biodiversity, although limited, is important for understanding ecological responses to a changing climate (Elvebakk 2005, Buchwal et al. 2013). The occurrence of vegetation is one of the important factors limiting the occurrence of aeolian processes (Seppälä 2004).

Within the Ebba Valley, there are no typical large forms resulting from the aeolian activity (such as dunes, ripple marks, or eologlyptoliths). In the field, only one larger cover composed of sandy sediments with a thickness not exceeding approximately 60 cm can be observed. In some places, mainly on slopes and local depressions, small niveo-aeolian covers can be found (see the locations of the sandy surface and windward slope test sites in the next section).

Materials and methods

Samples of summer aeolian deposition were collected using plastic trays (195 mm or 210 mm diameter) filled with glass marbles or pre-rinsed local beach gravel sediments from nine test sites located in the Ebba Valley. Test sites were chosen to reflect different geomorphological and vegetation settings along the Ebbadalen axis (Fig. 1): wet (1) and dry (2) tundra sites located closest to the fjord with dense tundra vegetation; leeward slope (3), top (4), and windward slope (5) sites located on the highest marine terrace with less or sparse tundra vegetation; a sandy surface (6) site covered only with individual tufts of grass; and three test sites with almost no vegetation located in the central part of the valley (7), as well as the upper part of the valley: sandur (8) and moraine (9). Test sites 3–5 were located around an old marine terrace with a height of approximately 40–45 m a.s.l., which is a minor terrain obstacle in the valley axis.

The measurement season for logistical and technical reasons usually starts in mid-July and ends at the beginning of September or mid-September. The length of the measuring season

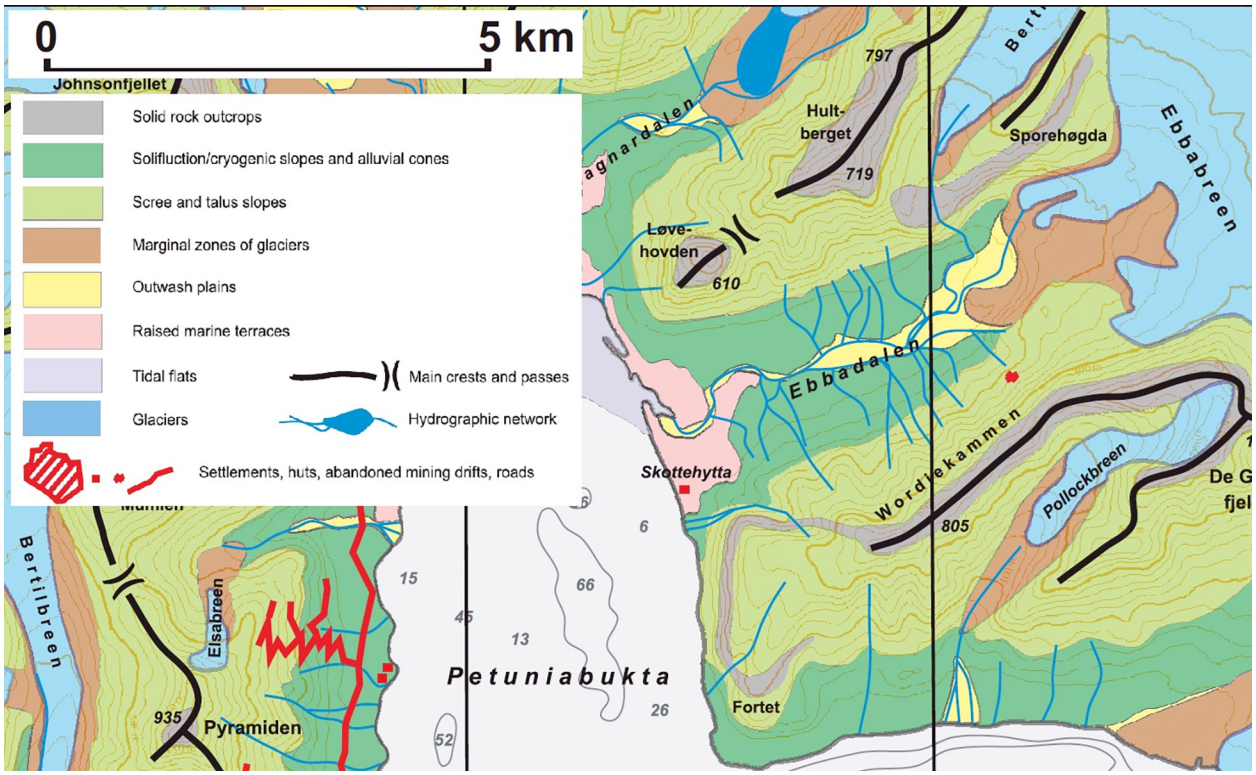

Fig. 2. Geomorphological sketch of the study area (Ebba Valley, Svalbard). Modified after the original figure by Rachlewicz (2009).

varied across the years (from 44 days to 64 days). Certainly, shorter measurement seasons resulted in less representative data, but further work is necessary to assess the resulting errors (especially when comparable measurement periods are used, which is, however, extremely difficult under polar conditions).

Although the measurements of aeolian deposition started in 2012, only samples from 2015 to 2018 were selected for this analysis to ensure greater representativeness, which involved placing three traps at each test site (for technical reasons, there were only two traps at a sandy surface test site in 2015 and at the central part test site in 2016).

The traps, together with gravel or glass marbles, were then washed with water to separate the collected material, dried, and subjected to further analyses. Previous studies have not shown significant differences between the uses of different materials in traps (despite the greater roughness of the gravel material). However, the use of glass marbles facilitated the subsequent recovery of the deposited material (Rymer et al. 2022). An additional source of errors could be the accumulation of rainwater in the traps. In future studies, it would be advisable to use a system that allows for the drainage of rainwater from traps.

The aeolian material obtained during the measurements was sieved to isolate grains with a diameter of 0.8–1.0 mm, which is typical for this type of analysis (Goździk 1980, 1995, Mycielska-Dowgiałło, Woronko 1998). Only quartz grains were then selected for further analyses. HCl was not used because of the lack of grain contamination with carbonates.

The quartz grains were then classified, using binocular microscope, into six groups based on the method of rounding and matting according to Krumbein (1941) and the classification of the degree of rounding and a modified method of matting of the surface of the quartz grains according to Cailleux (1942), together with modifications proposed by Goździk (1980, 1995) and Mycielska-Dowgiałło and Woronko (1998): angular (NU), matte rounded (RM), shiny rounded (EL), transitional matte (EM–RM), transitional shiny (EM–EL), and broken grains (C). The collected aeolian deposition samples allowed for the analysis of 1974 quartz grains from 106 samples in terms of rounding and matting.

Spearman's rank correlation coefficient between the characteristics of the quartz grains and the meteorological variables (average wind speed at three weather stations, average air temperature, total precipitation, and average air humidity during the sampling period) was estimated in the stats library using R software (Version. 4.2; R Development Core Team). The assumptions were checked visually (histogram plots) and tested with formal methods (Shapiro–Wilk test). Before analysis, all the data were log-transformed (ln) to approximate the data to a normal distribution.

Meteorological data (average air temperature and average air humidity) for the Ebba Valley were collected via ONSET HOBO devices, located close to the highest marine terrace test site (E/4, Fig. 1). The wind speed and direction (at a height of 2 m) were recorded at the same location at 15 min intervals (in 2016, 2017, and 2018). Unfortunately, some of the recording devices left in the area were occasionally damaged. Therefore, wind speed and direction data from the automatic weather station (recorded at one-hour intervals) located near the dry tundra test site (E/2, Fig. 1) were used to fill the data gaps for 2015. Owing to sensor failure in 2015, the recording of wind direction only started on August 17. Additionally, wind speed data from stations installed on Sven Glacier (S, Fig. 1; see Małecki 2019) and Pyramiden (P, Fig. 1) were also used. Both of these weather stations were located approximately 10 km from the centre of the Ebba Valley. Moreover, the total precipitation data were collected from the Longyearbyen meteorological station, which is located approximately 60 km southwest of the study area. The Norwegian Meteorological Institute collected data from the Pyramiden and Longyearbyen stations. The meteorological data were previously presented by Rymer et al. (2022).

Results

A full summary of the data is attached to the publication (Appendix 1). The greatest amounts of grains were recorded in 2015 and 2018 (Table 1), mainly because of relatively greater deposition in the indicated measurement seasons (according to Rymer et al. (2022), the mean seasonal aeolian

Table 1. Total number of quartz grains collected in the Ebba Valley in 2015–2018 divided into grain rounding and matting classes according to Cailleux (1942) with modification by Goździk (1995) and Mycielska-Dowgiałło and Woronko (1998).

Year	Class						
	C	EL	EM–EL	RM	EM–RM	NU	Total
2015	83	45	213	55	215	126	737
2016	55	29	125	37	73	67	386
2017	40	8	64	27	59	14	212
2018	47	88	197	110	177	20	639

deposition was almost 7 times greater in 2015 and more than 5 times greater in 2018 than the mean aeolian deposition rates measured in 2017). The differences in the number of quartz grains caught in traps between the individual seasons were relatively significant. The total number of grains in 2015 was almost 3.5 times greater than that in 2017. In total, the number of EL grains in 2017 was the lowest (only eight grains). The largest number of one type of grain was recorded in 2015 (the number of EM–RM grains reached 215).

In 2016–2018, transitional shiny (EM–EL) grains dominated, reaching 30.2–32.4% of the values (Table 2 and Fig. 3). Transitional matte (EM–RM) grains constitute 29.2% of the total grains only in 2015. In total, both transitional classes (EM–EL and EM–RM) exceeded more than half of the analysed grains in all years. Moreover, the share of angular (NU) grains in 2018 and shiny rounded (EL) grains in 2017 was the smallest, at 3.1% and 3.8%, respectively. The lowest percentage differences within the class were observed for the EM–EL class (3.5% between 2015 and 2016). On the contrary, the highest seasonal variability in the percentage share was observed for the NU class (14.3% between 2016 and 2018). This means that the percentage of grains belonging to the NU class was more than 5.6 times greater in 2016 than in 2018. In the case of the remaining classes, the seasonal differences oscillated approximately 10%.

Table 2. Percentage of quartz grains collected in the Ebba Valley in 2015–2018 divided into grain rounding and matting classes according to Cailleux (1942) with modification by Goździk (1995) and Mycielska-Dowgiałło and Woronko (1998).

Year	Class					
	C	EL	EM–EL	RM	EM–RM	NU
2015	11.3	6.1	28.9	7.5	29.2	17.1
2016	14.2	7.5	32.4	9.6	18.9	17.4
2017	18.9	3.8	30.2	12.7	27.8	6.6
2018	7.4	13.8	30.8	17.2	27.7	3.1

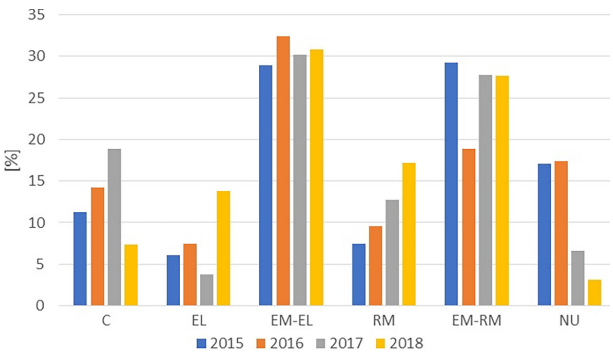

Fig. 3. Percentage of quartz grains in the Ebba Valley in 2015–2018 divided into grain rounding and matting classes according to Cailleux (1942) with modification by Goździk (1995) and Mycielska-Dowgiałło and Woronko (1998).

The greatest number of quartz grains over the four research seasons was recorded on the sandy surface (645) and windward slope (530) test sites (Table 3). The total number of quartz grains at these two sites alone was almost 60% of the total grains analysed. In the case of the windward slope test site, the amount of deposition was approximately 2 times greater than the average. At both of the abovementioned test sites, transitional grains were dominant. Almost 1/3 of the grains collected at the sandy surface test site were the EM–EL class. On the contrary, three test sites with relatively high plant coverage (wet tundra, dry tundra, and leeward slope) together accounted for only 3% of all the analysed grains. The remaining test sites with a significantly lower share of vegetation were characterized by an average

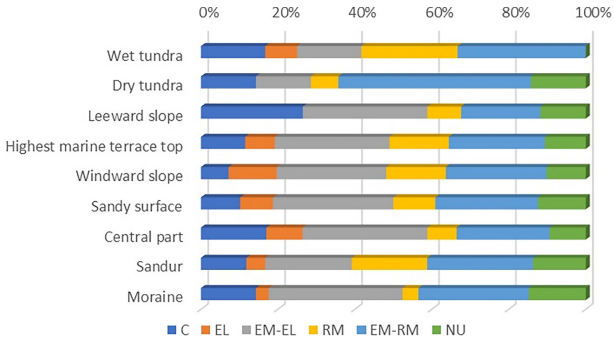

Fig. 4. Percentage of quartz grains in the years 2015–2018 collected in Ebba Valley divided into grain rounding and matting classes according to Cailleux (1942) with modification by Goździk (1995) and Mycielska-Dowgiałło and Woronko (1998) at nine test sites.

number of collected quartz grains ranging from 102 to 277 grains for the entire 4-year period.

The mentioned tundra sites were also characterised by greater dominance of certain grain types: 50% of the grains at the dry tundra test site were assigned to the EM–RM class, no grains belonging to the EL class were found at the dry tundra and leeward slope test sites, and no grains were assigned to the NU class at the wet tundra test site (Table 4 and Fig. 4.). This could have been influenced by the greater randomness of grains reaching the aeolian traps, which resulted from the significantly lower aeolian deposition at these test sites (according to Rymer et al. (2022), the mean values of aeolian deposition at the dry and wet tundra test sites were more than 50 times lower than the average for the entire valley). Considering the remaining test sites (where the sample size was larger and amounted to at least 100 grains), there was a significant proportion of grains in the EM–EL class (28.5–34.8%), except for the sandur test site, where the share of grains belonging to the EM–RM class was greater (27.5%) than that of the other classes. At most test sites, the share of grains in the EM–RM class was slightly lower but still higher (24.2–28.7%) than the share of EM–EL grains. Most often, the smallest proportion of grains belonged to classes that fully defined the depositional environment (i.e., EL and RM). The percentage of quartz grains belonging to the NU and C classes, apart from a few exemptions, was usually approximately a dozen at most test sites throughout the 4-year period. The relatively small (10.9%) percentage of typically aeolian RM quartz grains collected at the sandy surface test site is surprising, as the

Table 3. Total number of quartz grains collected in the Ebba Valley in 2015–2018 divided into grain rounding and matting classes according to Cailleux (1942) with modification by Goździk (1995) and Mycielska-Dowgiałło and Woronko (1998) at nine test sites.

Test site name	Class						
	C	EL	EM–EL	RM	EM–RM	NU	Total
The mouth of the valley with dense vegetation							
1. Wet tundra	4	2	4	6	8	0	24
2. Dry tundra	2	0	2	1	7	2	14
The middle part of the valley floor with little or no vegetation							
3. Leeward slope	9	0	11	3	7	4	34
4. Highest marine terrace top	12	8	31	16	26	11	104
5. Windward slope	38	66	151	82	139	54	530
6. Sandy surface	66	55	202	70	172	80	645
7. Central part of the valley	47	26	90	21	67	26	277
The upper part of the valley without vegetation cover							
8. Sandur	12	5	23	20	28	14	102
9. Moraine	35	8	85	10	70	36	244

Table 4. Percentage of quartz grains collected in the Ebba Valley in 2015–2018 divided into grain rounding and matting classes according to Cailleux (1942) with modification by Goździk (1995) and Mycielska-Dowgiałło and Woronko (1998) at nine test sites.

Test site name	Class					
	C	EL	EM–EL	RM	EM–RM	NU
The mouth of the valley with dense vegetation						
1. Wet tundra	16.7	8.3	16.7	25.0	33.3	0.0
2. Dry tundra	14.3	0.0	14.3	7.1	50.0	14.3
The middle part of the valley floor with little or no vegetation						
3. Leeward slope	26.5	0.0	32.4	8.8	20.6	11.8
4. Highest marine terrace top	11.5	7.7	29.8	15.4	25.0	10.6
5. Windward slope	7.2	12.5	28.5	15.5	26.2	10.2
6. Sandy surface	10.2	8.5	31.3	10.9	26.7	12.4
7. Central part of the valley	17.0	9.4	32.5	7.6	24.2	9.4
The upper part of the valley without vegetation cover						
8. Sandur	11.8	4.9	22.5	19.6	27.5	13.7
9. Moraine	14.3	3.3	34.8	4.1	28.7	14.8

expected values were higher for this type of surface and local landform, assuming a mainly local nature of aeolian transport in this area.

Discussion

Owing to the unique nature of the obtained data, it is extremely difficult to find comparative studies, especially in polar areas. In most cases, the analysis of quartz grains is carried out based on the samples collected from sediments and concerns to ancient aeolian and fluvioglacial palaeoenvironments. The samples collected from these sediments cover a longer period of time than just a few months of the year. There have been many studies on the 'European Sand Belt', that is, the area of Europe where periglacial conditions were present in the past (see Kalińska 2019, Kalińska et al. 2019, Łopuch, Jary 2023, Łopuch et al. 2023). Kalińska and Nartišs (2014) observed similar percentages of RM and EM–RM quartz grains in many profiles located in central Poland, Latvia, Estonia, and Finland compared with those collected in traps at test sites located in the Ebba Valley. However, the share of EL and EM–EL grains was significantly lower in those palaeoenvironments than in the current periglacial conditions observed on Spitsbergen.

For the weathered sediments of north-western Spitsbergen, Kowalkowski and Kocoń (1991) observed a small number of quartz grains, exhibiting features acquired through transport in an aeolian environment. In the modern glacial and proglacial environments of southwestern Greenland, Kalińska-Nartiša et al. (2017) estimated the share of non-abraded fresh grains with sharp edges and shiny surfaces to be 78% of the sample collected from aeolian cover on a hillslope. Interestingly, samples collected close to the glacial margin presented greater numbers of moderately rounded grains with both shiny and matte surfaces (up to 27%). The proportions of moderately rounded grains were even greater in the part of the area farther from the glacier. The percentage of moderately rounded grains with shiny surfaces reached 34–37% at some locations, and the percentage of moderately rounded grains with matte surfaces was even greater (up to 46%). A comparison of the results obtained in this study with the modern example from Greenland may therefore indicate that the occurrence of incompletely rounded grains is typical for contemporary periglacial environments (such as small postglacial valleys). The decrease in the degree of grain rounding in contemporary environments compared with the Last Glacial Maximum period was also noted by Warrier et al. (2016) for East Antarctica. Owing to the formation process (mutual impact while suspended in the air), RM grains require high transport dynamics over a longer time to fully form.

The statistically significant Spearman's rank correlation coefficient (r_s) results between the number of quartz grains in different classes and the meteorological variables were relatively low (r_s up to 0.49). This was possibly due to the small amount of data associated with only four measurement seasons. However, on this basis, certain conclusions can be drawn regarding the regularities concerning the sources of the material and the influence of meteorological conditions on

Table 5. Spearman's rank correlation coefficient between different quartz grain types collected in the Ebba Valley and different meteorological variables. The red colour indicates a positive correlation. The blue colour indicates a negative correlation.

Parameter	C	EL	EM–EL	RM	EM–RM	NU
Average wind speed Ebba Valley	−0.01 p = 0.92	−0.02 p = 0.87	−0.03 p = 0.75	−0,14 p = 0.19	−0.05 p = 0.63	0.49 p < 0.01
Average wind speed Pyramiden	0.08 p = 0.43	−0.31 p < 0.01	−0.22 p = 0.04	−0.08 p = 0.47	0 p = 0.99	−0.01 p = 0.92
Average wind speed Sven Glacier	−0.04 p = 0.71	−0.1 p = 0.34	0.04 p = 0.73	−0.18 p = 0.08	−0.13 p = 0.23	0.45 p < 0.01
Average temperature Ebba Valley	−0.07 p = 0.52	0.31 p < 0.01	0.21 p = 0.05	0.03 p = 0.76	0.01 p = 0.91	0.23 p = 0.03
Total precipitation Longyearbyen	−0.08 p = 0.43	0.31 p < 0.01	0.22 p = 0.04	0.08 p = 0.47	0 p = 0.99	0.01 p = 0.92
Average air humidity Ebba Valley	−0.08 p = 0.46	0.08 p = 0.47	0.11 p = 0.3	0.05 p = 0.66	−0.07 p = 0.5	−0.26 p = 0.01

the functioning of aeolian processes in the Ebba Valley (Table 5). The strongest positive relationships (r_s = 0.49–0.45) were observed between the occurrence of NU grains and average wind speed in the Ebba Valley and on the Sven Glacier. These grains are commonly associated with frost weathering and are most often found in moraine deposits (Mycielska-Dowgiałło, Woronko 1998). Considering the dominant directions of the strongest winds (especially in the Ebba Valley), this may mean that stronger winds from the north and east (i.e., along the valley axis) influence the appearance of a greater amount of the fresh material of the glacial origin (NU grains). Therefore, the moraine areas (and possibly weathered material on the slopes) were the first significant source of the material transported by wind within the valley. On the contrary, stronger winds from the south and west (typical for the Pyramiden station) were negatively related to the supply of EL and EM–EL grains, which are usually related to aquatic transport. Most likely, the occurrence of these winds limited the delivery and transport of the material brought to the valley by the river. The importance of the river as one of the main sources of the material available for wind transport was also evidenced by the occurrence of positive relationships between the presence of EL and EM–EL grains and the average air temperature and total precipitation. Both of these variables significantly influence river discharge (Rachlewicz 2009) and, consequently, the amount of the material carried by it and delivered to the valley. Interestingly, a positive correlation was also detected between the average air temperature and the appearance of NU grains. Perhaps in the warmest periods, the water flow in the river was so intense that there was greater erosion of moraine zones, and fresh NU grains were thus transported short distances across the river (so that they had no opportunity to acquire the characteristics of the aquatic environment). However, sediments carried by rivers usually become available for aeolian transport only at the end of the summer season when the water level decreases and the sediments dry out (Rasmussen et al. 2023). Moreover, there was a noticeable negative relationship between the occurrence of fresh angular NU grains and the average air humidity. Higher air humidity may result in greater wind transport capabilities and, consequently, greater intensity of processing of the material carried by the wind (Csavina et al. 2014). This issue, however, certainly requires further analysis and broader research.

Conclusions

On the basis of new data, it was possible to establish certain relationships between the occurrence of grains belonging to certain classes and other environmental variables (meteorological and geomorphological). It is therefore important to carry out further analyses, especially in years when the aeolian deposition values are the highest, as well as to conduct measurements in similar time periods.

Two main sources of origin for the aeolian material deposited in the traps were identified. One was the fresh angular material (NU grains) derived from moraines, where there is strong crumbling of the material. This non-abraded material is distributed over short distances within the valley by the wind (in line with the valley axis) and possibly processed into other types of transitional grains, the percentage of which was usually the highest. The second was the fluvioglacial material (EL and EM–EL grains) originating from river alluvia. The amount of this material supply is most often dependent on the river level and therefore on the amount of carried sediment. This level, in turn, depends on the temperature and amount of precipitation in a given year. This material supply can be limited by stronger winds that are off-axis with the valley axis. Both aeolian and fluvial transports are usually not long, which translates into the largest share of grains belonging to the EM–EL and EM–RM classes. These grains may also have their features acquired in the original sedimentary environments – glacial and fluvioglacial.

The relatively small number of grains belonging to the RM class, that is, those with typical aeolian characteristics, may indicate very short transport or low environmental dynamics in this type of periglacial valley. Most of the material (grains) before reaching its final form is possibly blown away and deposited in nearby bay and fjord. This may be confirmed by the relatively high share of RM grains near the bay at the dry tundra site. The second reason for such a small

aeolisation is the short period of study for the abrasion of the material in the valley. The summer season is too short for the surface of a single grain to be sufficiently rounded and matted and for its classification as an RM grain. In this case, there is no question of accidental addition of grains that are already matted. To prove greater aeolisation, studies should be performed over longer periods, especially concerning autumn.

Owing to its orientation and morphology (the valley floor is surrounded by high formations in close proximity to a glacier), Ebba Valley acts as a wind tunnel where newly deposited sediments under periglacial conditions undergo the initial phase of aeolisation.

Under climate change conditions, the dynamics of the environment may change significantly. The proportions of the supply of the aeolian material from moraines and weathering to those supplied by the river may also change. The second material source may gain importance because of the increasing rainfall and temperatures in the Arctic. These changes may significantly affect the functioning of periglacial geoecosystems at both local and regional scales.

Acknowledgments

The study was conducted at Adam Mickiewicz Polar Station 'Petuniabukta' (AMUPS) and was funded by the National Science Centre (Grant No. 2014/15/N/ST10/00825). We would like to thank Alfred Stach, Michał Rybak, and Agata Buchwał for their help with statistical analysis, as well as Grzegorz Rachlewicz for his valuable comments on the manuscript, and Tomasz Kurczaba for the help in fieldwork. We are particularly grateful to Jakub Małecki for sharing his meteorological data from Sven glacier (Project funded by the National Science Centre, Grant No. N N306 062940). We also gratefully thank four anonymous reviewers for their valuable comments.

Author's contribution

KGR: conceptualization, formal analysis, funding acquisition, investigation, methodology, writing – original draft, writing – review & editing, visualization. LW-K: formal analysis, investigation, writing – review & editing, visualization.

References

Beylich A.A., Dickson J.C., Zwolinski Z., 2016. *Source-to-sink fluxes in undisturbed cold environments*. Cambridge University Press, Cambridge.

Blatt H., Middleton G., Murray R., 1980. *Origin of sedimentary rocks*. Prentice-Hall, Englewood Cliffs.

Blott S.J., Pye K., 2001. Grain size distribution and statistics of unconsolidated sediments. *Earth Surface Processes and Landforms* 26: 1237–1248. DOI 10.1002/esp.261.

Boggs S., 2009. *Petrology of sedimentary rocks*. Cambridge University Press, Cambridge. DOI 10.1017/CBO9780511626487.

Borysiak J., Pleskot K., Rachlewicz G., 2020. Dryas aeolian landforms in Arctic deflationary tundra, central Spitsbergen. *Polish Polar Research* 41(1): 41–68. DOI 10.24425/ppr.2020.132569.

Brookfield M.E., 2011. Aeolian processes and features in cool climates, In: Martini I.P., French H.M., Pérez Alberti A. (eds), *Ice-marginal and periglacial processes and sediments*. Geological Society, London: 241–258. DOI 10.1144/SP354.16.

Buchwal A., Rachlewicz G., Fonti P., Cherubini P., Gaertner H., 2013. Temperature modulates intra-plant growth of Salix Polaris from a high Arctic site (Svalbard). *Polar Biology* 36(9): 1305–1318. DOI 10.1007/s00300-013-1349-x.

Cailleux A., 1942. Les action eoliennes periglaciaires en Europe. *Mémoires de la Société géologique de France* 41: 1–176.

Csavina J., Field J., Félix O., Corral-Avitia A.Y., Sáez A.E., Betterton E.A., 2014. Effect of wind speed and relative humidity on atmospheric dust concentrations in semi-arid climates. *Science of the Total Environment* 487: 82–90. DOI 10.1016/j.scitotenv.2014.03.138.

Dallmann W.K., Hjelle A., Ohta Y., Salvigsen O., Balashov Y.A., Maher H.D. Jr., 2002. *Geological map of Svalbard 1: 100,000, sheet B9G Adventdalen*. Norwegian Polar Institute.

Elvebakk A., 2005. A vegetation map of Svalbard on the scale 1: 3.5 million. *Phytocoenologia* 35(4): 951–967. DOI 10.1127/0340-269X/2005/0035-0951.

Folk R.L., 1980. *Petrology of sedimentary rocks*. Hemphill Publishing Company, Austin.

Førland E.J., Benestad R., Hanssen-Bauer I., Haugen J.E., Skaugen T.E., 2011. Temperature and precipitation development at Svalbard 1900-2100. *Advances in Meteorology* 2011(893790): 14. DOI 10.1155/2011/893790.

Goździk J., 1980. Zastosowanie morfoskopii i graniformametrii do badań osadów w kopalni węgla brunatnego "Bełchatów". *Studia Regionalne* IV(IX): 101–104.

Goździk J.S., 1995. Wybrane metody kształtu ziarn piasków do celów paleogeograficznych i stratygraficznych, In: Mycielska-Dowgiałło E., Rutkowski J. (eds), *Badania osadów czwartorzędowych. Wybrane metody i interpretacja wyników*. WGiSR, UW, Warszawa: 115–132.

Harland W.B., 1997. *The geology of Svalbard*. Geological Society of London, London.

Johansen B.E., Karlsen S.R., Tømmervik H., 2012. Vegetation mapping of Svalbard utilising Landsat TM/ETM+ data. *Polar Record* 48(1): 47–63. DOI 10.1017/S0032247411000647.

Kalińska E., 2019. Understanding a continuous inland aeolian deposition: a closer look into a chronological and sedimentary record of the north-eastern European Sand Belt. *Bulletin of Geography. Physical Geography Series* 16(1): 31−43. DOI 10.2478/bgeo-2019-0003.

Kalińska E., Hang T., Jõeleht A., Olo S., Nartišs M., Adamiec G., 2019. Macro- and micro-scale study and chronology of Late Weichselian aeolian sediment in Estonia, north-eastern European Sand Belt. *International Journal of Earth Science* 108(6): 2021–2035. DOI 10.1007/s00531-019-01746-2.

Kalińska E., Nartišs M., 2014. Pleistocene and Holocene aeolian sediments of different location and geological history: a new insight from rounding and frosting of quartz grains. *Quaternary International* 328-329: 311–322. DOI 10.1016/j.quaint.2013.08.038.

Kalińska-Nartiša E., Lamsters K., Karušs J., Krievans M., Rečs A., Meija R., 2017. Quartz grain features in modern glacial and proglacial environments: a microscopic study from the Russell Glacier, southwest Greenland. *Polish Polar Research* 38(3): 265–289. DOI 10.1515/popore-2017-0018.

Kavan J., Laska K., Nawrot A., Wawrzyniak T., 2020. High latitude dust transport altitude pattern revealed from deposition on snow, Svalbard. *Atmosphere* 11: 1318. DOI 10.3390/atmos11121318.

Kłysz P., Lindner L., Marks L., Wysokiński L., 1989. Late Pleistocene and Holocene relief remodeling in the Ebbadalen-Nordenskiöldbreen region in Olav V Land, central Spitsbergen. *Polish Polar Research* 10(3): 277–301.

Kowalkowski A., Kocoń J., 1991. Procesy wietrzenia na Spitsbergenie na podstawie badań w skaningowym mikroskopie elektronowym, In: Kostrzewski A. (ed), *Geneza, litologia i stratygrafia utworów czwartorzędowych. Geografia 50*. Wydawnictwo Naukowe Uniwersytetu im. Adama Mickiewicza, Poznań: 77–104.

Krumbein W.C., 1941. Measurement and geological significance of shape and roundness of sedimentary particles. *Journal of Sedimentary Petrology* 11(2): 64–72. DOI 10.1306/D42690F3-2B26-11D7-8648000102C1865D.

Long A.J., Strzelecki M.C., Lloyd J.M., Bryant C.L., 2012. Dating High Arctic Holocene relative sea level changes using juvenile articulated marine shells in raised beaches. *Quaternary Science Reviews* 48: 61–66. DOI 10.1016/j.quascirev.2012.06.009.

Łopuch M., Jary Z., 2023. Sand sources and migration of the dune fields in the central European Sand Belt – a pattern analysis approach. *Geomorphology* 439: 108856. DOI 10.1016/j.geomorph.2023.108856.

Łopuch M., Sokołowski R.J., Jary Z., 2023. Factors controlling the development of cold-climate dune fields within the central part of the European Sand Belt – insights from morphometry. *Geomorphology* 420: 108514. DOI 10.1016/j.geomorph.2022.108514.

Lyu Q., Shunshe L., Yulong G., Jinhua F., Xiaobing N., Shengbin F., Shixiang L., 2019. A new method of lithologic identification and distribution characteristics of fine – grained sediments: a case study in southwest of Ordos Basin, China. *Open Geosciences* 11: 17–28. DOI 10.1515/geo-2019-0002.

Mahaney W.C., 2002. *Atlas of sand grain surface textures and applications*. Oxford University Press, Oxford.

Małecki J., 2015. Glacio–meteorology of Ebbabreen, Dickson Land, central Svalbard, during 2008–2010 melt seasons. *Polish Polar Research* 36: 145–161. DOI 10.1515/popore-2015-0010.

Małecki J., 2019. Meteorology and summer net radiation of an Arctic alpine glacier: Svenbreen, Svalbard. *International Journal of Meteorology* 39(10): 4107–4124. DOI 10.1002/joc.6062.

Müller M., Thiel C., Kühn P., 2016. Holocene palaeosols and aeolian activities in the Umimmalissuaq valley, West Greenland. *The Holocene* 26(7): 1149–1161. DOI 10.1177/0959683616632885.

Mycielska-Dowgiałło E., Woronko B., 1998. Analiza obtoczenia i zmatowienia powierzchni ziarn kwarcowych frakcji piaszczystej i jej wartość interpretacyjna. *Przegląd Geologiczny* 46(12): 1275–1281.

Pettijohn F.J., Potter P.E., Siever R., 1987. *Sand and Sandstone*. Springer-Verlag, New York.

Prach K., Klimešová J., Košnar J., Redčenko O., Hais M., 2012. Variability of contemporary vegetation around Petuniabukta, central Spitsbergen. *Polish Polar Research* 33(4): 383–394. DOI 10.2478/v10183-012-0026-z.

Przybylak R., Araźny A., Gluza A., Hojan M., Migała K., Sikora S., Siwek K., Zwoliński Z., 2006. Porównanie warunków meteorologicznych na zachodnim wybrzeżu Spitsbergenu w sezonie letnim 2005 r. *Problemy Klimatologii Polarnej* 16: 125–138.

Przybylak R., Araźny A., Nordli Ø, Finkelnburg R., Kejna M., Budzik T., Migała K., Sikora S., Puczko D., Rymer K., Rachlewicz G., 2014. Spatial distribution of air temperature on Svalbard during 1 year with campaign measurements. *International Journal of Climatology* 34: 3702–3719. DOI 10.1002/joc.3937.

Pye K., Tsoar H., 2009. *Aeolian Sand and Sand Dunes*. Springer, Berlin.

Rachlewicz G., 2003. Warunki meteorologiczne w Zatoce Petunia (Spitsbergen środkowy) w sezonach letnich 2000 i 2001. *Problemy Klimatologii Polarnej* 13: 127–138.

Rachlewicz G., 2009. *Contemporary sediment fluxes and relief changes in high Arctic glacierized valley systems (Billefjorden, Central Spitsbergen)*. Wydawnictwo Naukowe UAM, Poznań.

Rachlewicz G., Styszyńska A., 2007. Porównanie przebiegu temperatury powietrza w Petuniabukta i Svalbard-Lufthavn (Isfjord, Spitsbergen) w latach 2001-2003. *Problemy Klimatologii Polarnej* 17: 121–134.

Rachlewicz G., Szczuciński W., 2008. Changes in thermal structure of permafrost active layer in a dry polar climate, Petuniabukta, Svalbard. *Polish Polar Research* 29: 261–278.

Rasmussen C.F., Christiansen H.H., Buylaert J.-P., Cunningham A., Schneider R., Knudsen M.F., Stevens T., 2023. High-resolution OSL dating of loess in Adventdalen, Svalbard: Late Holocene dust activity and permafrost development. *Quaternary Science Reviews* 310: 108137. DOI 10.1016/j.quascirev.2023.108137.

Rymer K., Rachlewicz G., 2014. Thermal dynamics of the permafrost active layer in Ebba valley (Central Spitsbergen) in the years 2009–2012. *International Journal of Applied and Natural Sciences* 3: 79–86.

Rymer K.G., Rachlewicz G., Buchwal A., Temme A.J.A.M., Reimann T., van der Meij W.M., 2022. Contemporary and past aeolian deposition rates in periglacial conditions (Ebba Valley, central Spitsbergen). *CATENA* 211: 105974. DOI 10.1016/j.catena.2021.105974.

Seppälä M., 2004. *Wind as a geomorphic agent in cold climates*. Cambridge University Press, Cambridge.

Sobota I., Weckwerth P., Grajewski T., 2020. Rain-on-snow (ROS) events and their relation to snowpack and ice layer changes on small glaciers in Svalbard, the high Arctic. *Journal of Hydrology* 590: 125279. DOI 10.1016/j.jhydrol.2020.125279.

Stawska M., 2017. Impacts of geomorphic disturbances on plant colonization in Ebba Valley, central Spitsbergen,

Svalbard. *Quaestiones Geographicae* 36(1): 51–64. DOI 10.1515/quageo-2017-0004.

van der Meij W.M., Temme A.J.A.M., de Kleijn C.M.F.J.J., Reimann T., Heuvelink G.B.M., Zwoliński Z., Rachlewicz G., Rymer K., Sommer M., 2016. Arctic soil development on a series of marine terraces on Central Spitsbergen, Svalbard: a combined geochronology, fieldwork and modelling approach. *SOIL* 2: 221–240. DOI 10.5194/soil-2-221-2016.

Wachecka-Kotkowska L., 2004. Ewolucja doliny Luciąży – uwarunkowania klimatyczne a lokalne (in Polish, summary in English: evolution of the Luciąża River valley – local and climatic conditions). *Acta Geographica Lodziensia* 86: 161.

Wachecka-Kotkowska L., 2015. Rozwój rzeźby obszaru między Piotrkowem Trybunalskim, Radomskiem a Przedborzem w czwartorzędzie (in Polish, summary in English: Relief development of the area between Piotrków Trybunalski, Radomsko and Przedbórz in the Quaternary). Wydawnictwo Uniwersytetu Łódzkiego, Łódź. 126.

Wachecka-Kotkowska L., Krzyszkowski D., Król E., Klaczak K., 2014. Middle Weichselian Pleniglacial fluvial erosion and sedimentation in the Krasówka river valley, Szczerców field, Bełchatów open cast mine, central Poland. *Annales Societatis Geologorum Poloniae* 84(4): 323–340.

Warrier A.K., Pednekar H., Mahesh B.S., Mohan R., Gazi S., 2016. Sediment grain size and surface textural observations of quartz grains in late quaternary lacustrine sediments from Schirmacher Oasis, East Antarctica: Paleoenvironmental significance. *Polar Science* 10(1): 89–100. DOI 10.1016/j.polar.2015.12.005.

Woronko B., Bujak Ł, 2018. Quaternary aeolian activity of Eastern Europe (a Poland case study). *Quaternary International* 478: 75–96. DOI 10.1016/j.quaint.2017.03.058.

Woronko B., Zieliński P., Sokołowski R.J., 2015. Climate evolution during the Pleniglacial and Late Glacial as recorded in quartz grain morphoscopy of fluvial to aeolian successions of the European Sand Belt. *Geologos* 21(2): 89–103. DOI 10.1515/logos-2015-0005.

Zhang T., Li D., East A.E., Walling D.E., Lane S., Overeem I., Beylich A.A., Koppes M., Lu X., 2022. Warming-driven erosion and sediment transport in cold regions. *Nature Reviews Earth & Environment* 3: 832–851. DOI 10.1038/s43017-022-00362-0.

Zieliński P., Sokołowski R.J., Woronko B., Jankowski M., Fedorowicz S., 2015. The depositional conditions of the fluvio-aeolian succession during the last climate minimum based on the examples from Poland and NW Ukraine. *Quaternary International* 386: 30–41. DOI 10.1016/j.quaint.2014.08.013.

Appendix 1. Full summary of quartz grains numbers collected in the Ebba Valley in 2015-2018 divided into grain rounding and matting classes according to Cailleux (1942) with modification by Goździk (1995) and Mycielska-Dowgiałło and Woronko (1998) at nine test.

2015	Trap 1						Trap 2						Trap 3					
	C	EL	EM-EL	RM	EM-RM	NU	C	EL	EM-EL	RM	EM-RM	NU	C	EL	EM-EL	RM	EM-RM	NU
Wet tundra	0	0	0	0	0	0	0	0	0	0	0	0	0	0	0	0	0	0
Dry tundra	0	0	0	0	0	0	0	0	0	0	0	0	0	0	0	0	0	0
Leeward slope	0	0	0	1	0	0	0	0	0	0	0	0	0	0	0	0	0	0
Highest marine terrace top	1	1	6	4	4	3	2	0	2	3	5	1	3	1	5	1	3	0
Windward slope	3	10	13	21	30	7	2	9	8	5	15	5	5	0	7	0	6	5
Sandy surface	26	0	68	5	65	57	9	2	13	0	10	4						
Central part	10	3	30	3	27	3	2	8	10	3	6	5	3	4	7	3	5	4
Sandur	3	2	4	2	4	2	1	2	5	1	4	4	0	0	3	2	0	1
Moraine	10	1	18	1	21	13	3	2	6	0	8	9	0	0	8	0	2	3
2016	Trap 1						Trap 2						Trap 3					
	C	EL	EM-EL	RM	EM-RM	NU	C	EL	EM-EL	RM	EM-RM	NU	C	EL	EM-EL	RM	EM-RM	NU
Wet tundra	2	0	3	2	2	0	0	0	0	0	1	0	0	0	0	0	0	0
Dry tundra	0	0	1	0	0	1	0	0	1	0	1	0	0	0	0	0	0	0
Leeward slope	4	0	4	0	2	3	0	0	0	0	1	1	1	0	0	0	0	0
Highest marine terrace top	0	1	0	1	0	0	0	0	1	1	2	0	0	0	4	3	1	0
Windward slope	7	6	21	9	13	6	7	3	11	0	6	11	4	1	22	0	5	15
Sandy surface	1	3	3	2	3	1	6	4	10	7	8	6	4	9	19	10	12	3
Central part	6	0	7	2	5	8	5	2	5	0	3	0						
Sandur	1	0	1	0	0	1	0	0	0	0	0	0	0	0	1	0	0	1
Moraine	0	0	0	0	1	3	5	0	7	0	3	5	2	0	4	0	4	2
2017	Trap 1						Trap 2						Trap 3					
	C	EL	EM-EL	RM	EM-RM	NU	C	EL	EM-EL	RM	EM-RM	NU	C	EL	EM-EL	RM	EM-RM	NU
Wet tundra	1	0	0	0	2	0	0	0	0	1	0	0	0	0	0	0	1	0
Dry tundra	0	0	0	0	2	1	2	0	0	1	2	0	0	0	0	0	1	0
Leeward slope	2	0	1	1	1	0	0	0	0	1	0	0	2	0	1	0	0	0
Highest marine terrace top	0	0	1	0	2	3	1	1	3	0	1	0	1	0	0	0	3	0
Windward slope	1	1	3	2	2	0	1	2	7	3	6	2	1	0	11	4	4	0
Sandy surface	2	0	1	1	1	0	0	1	0	1	0	0	5	0	4	2	2	2
Central part	4	1	7	0	2	1	5	0	3	1	3	0	3	0	5	2	4	0
Sandur	1	0	1	0	2	2	1	1	2	3	2	1	0	0	1	1	4	1
Moraine	3	0	5	0	5	0	0	1	6	1	5	1	4	0	2	2	2	0
2018	Trap 1						Trap 2						Trap 3					
	C	EL	EM-EL	RM	EM-RM	NU	C	EL	EM-EL	RM	EM-RM	NU	C	EL	EM-EL	RM	EM-RM	NU
Wet tundra	1	0	1	0	0	0	0	0	0	0	0	0	0	2	0	3	2	0
Dry tundra	0	0	0	0	0	0	0	0	0	0	1	0	0	0	0	0	0	0
Leeward slope	0	0	0	0	0	0	0	0	1	0	0	0	0	0	4	0	3	0
Highest marine terrace top	2	3	5	2	4	4	1	0	1	0	0	0	1	1	3	1	1	0
Windward slope	2	14	14	4	10	0	1	11	16	10	8	1	4	9	18	24	34	2
Sandy surface	3	12	32	5	22	1	5	18	41	10	16	4	5	6	11	27	33	2
Central part	2	3	3	2	4	1	3	3	4	3	4	4	4	2	9	2	4	0
Sandur	3	0	1	2	3	0	1	0	2	4	4	1	1	0	2	5	5	0
Moraine	2	0	8	1	6	0	3	4	6	2	7	0	3	0	15	3	6	0